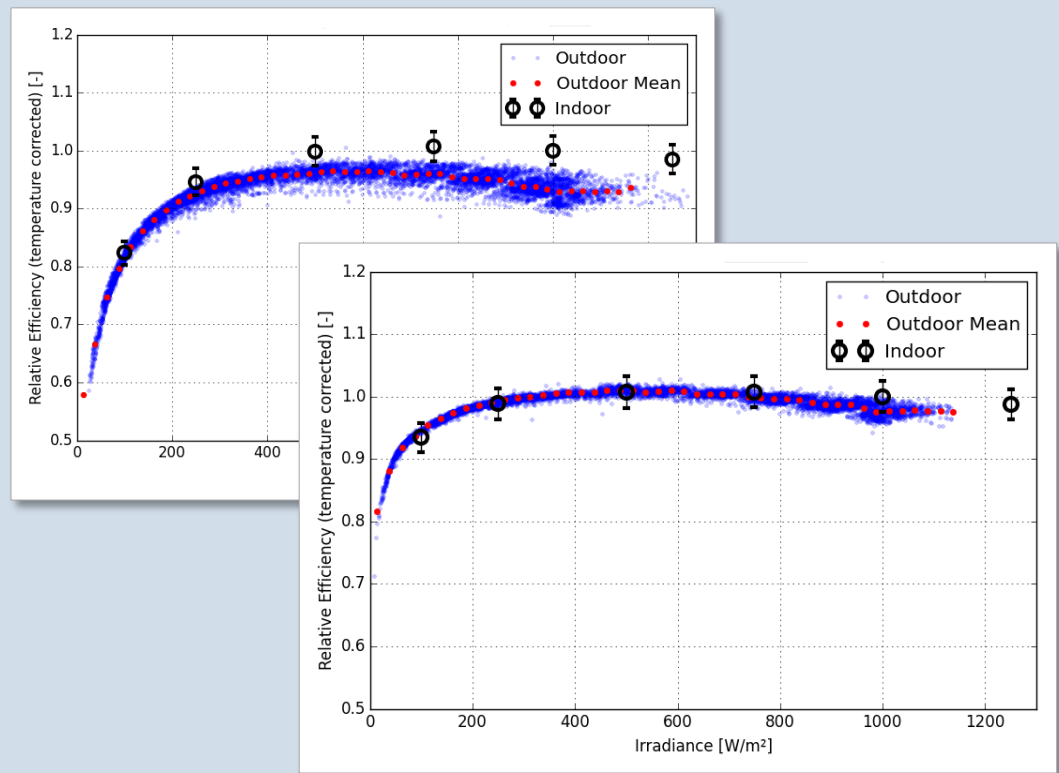




Uncertainties in PV System Yield Predictions and Assessments



PVPS

PHOTOVOLTAIC
POWER SYSTEMS
PROGRAMME

Report IEA-PVPS T13-12:2018

INTERNATIONAL ENERGY AGENCY
PHOTOVOLTAIC POWER SYSTEMS PROGRAMME

**Uncertainties in PV System
Yield Predictions and Assessments**

IEA PVPS Task 13, Subtasks 2.3 & 3.1
Report IEA-PVPS T13-12:2018
April 2018

ISBN 978-3-906042-51-0

Primary Authors:

Christian Reise, Björn Müller
Fraunhofer ISE, Freiburg, Germany

David Moser, Giorgio Belluardo, Philip Ingenhoven
Eurac Research, Institute for Renewable Energy, Bolzano, Italy

Contributing Authors:

Anton Driesse
PV Performance Labs, Canada

Guillaume Razongles
Institut National de l'Energie Solaire (INES), France

Mauricio Richter
3E s.a., Belgium

Table of contents

Foreword	5
Acknowledgements	6
List of abbreviations	7
Executive summary	9
1 Introduction	11
2 Measurements & uncertainties	13
2.1 Irradiation sensors and related measurement uncertainties	13
2.1.1 Exemplary data	13
2.1.2 Reducing measurement uncertainties	16
2.2 Laboratory (indoor) characterization of PV modules	19
2.2.1 Sample selection	20
2.2.2 Measurement uncertainties at STC	21
2.2.3 Non-STC conditions	23
2.2.4 Comparison of indoor and outdoor power rating	24
2.3 System testing	29
2.4 Degradation and uncertainties related to long-term stability	30
2.4.1 Uncertainty of the estimation of the performance metric	30
2.4.2 Overall uncertainty of the performance loss ratio	32
3 Modelling & uncertainties	36
3.1 Long-term energy yield predictions	36
3.2 Estimation of overall uncertainty in modelling	37
3.3 Uncertainties associated with irradiation data	38
3.3.1 Comparing different data sources of satellite-derived irradiation time series	38
3.3.2 Long-term trends of global horizontal irradiation	42
3.4 Conversion to tilted plane	44
3.5 Soiling	46
3.6 Module efficiency	48
3.6.1 Angle of incidence effects	49
3.6.2 Spectral effects	49
3.6.3 Irradiance level	51
3.6.4 Temperature	52

4	Effects of uncertainty	54
4.1	Uncertainty in module energy rating.....	54
4.1.1	Module characteristics	55
4.1.2	Meteorological data	55
4.1.3	Module performance ratio and uncertainty	57
4.1.4	Energy rating under consideration of uncertainty.....	59
4.2	A framework to calculate yield prediction uncertainties	60
4.2.1	Introduction.....	60
4.2.2	Definitions	61
4.2.3	Uncertainty sources.....	61
4.2.4	Uncertainty propagation	62
4.2.5	Results	63
4.2.6	Conclusion	64
	References.....	67

Foreword

The International Energy Agency (IEA), founded in November 1974, is an autonomous body within the framework of the Organization for Economic Co-operation and Development (OECD) which carries out a comprehensive programme of energy co-operation among its member countries. The European Union also participates in the work of the IEA. Collaboration in research, development and demonstration of new technologies has been an important part of the Agency's Programme.

The IEA Photovoltaic Power Systems Programme (PVPS) is one of the collaborative R&D Agreements established within the IEA. Since 1993, the PVPS participants have been conducting a variety of joint projects in the application of photovoltaic conversion of solar energy into electricity.

The mission of the IEA PVPS Technology Collaboration Programme is: To enhance the international collaborative efforts which facilitate the role of photovoltaic solar energy as a cornerstone in the transition to sustainable energy systems. The underlying assumption is that the market for PV systems is rapidly expanding to significant penetrations in grid-connected markets in an increasing number of countries, connected to both the distribution network and the central transmission network.

This strong market expansion requires the availability of and access to reliable information on the performance and sustainability of PV systems, technical and design guidelines, planning methods, financing, etc., to be shared with the various actors. In particular, the high penetration of PV into main grids requires the development of new grid and PV inverter management strategies, greater focus on solar forecasting and storage, as well as investigations of the economic and technological impact on the whole energy system. New PV business models need to be developed, as the decentralised character of photovoltaics shifts the responsibility for energy generation more into the hands of private owners, municipalities, cities and regions.

IEA PVPS Task 13 engages in focusing the international collaboration in improving the reliability of photovoltaic systems and subsystems by collecting, analysing and disseminating information on their technical performance and failures, providing a basis for their technical assessment, and developing practical recommendations for improving their electrical and economic output.

The current members of the IEA PVPS Task 13 include Australia, Austria, Belgium, Chile, China, Denmark, Finland, France, Germany, Israel, Italy, Japan, Malaysia, Netherlands, Norway, Solar-Power Europe, South Africa, Spain, Sweden, Switzerland, Thailand and the United States of America.

This report focusses on uncertainties in PV system yield predictions and assessments, which may influence business decisions on long term investments into PV power plants. A first section covers the uncertainties related to the most important measurands in PV solar energy, i.e. solar irradiation, PV module properties, and PV system performance. Then, the uncertainties of several of the modelling steps for gains and losses in a PV system, both needed for yield predictions and for system performance assessment. Finally, the results achieved are combined in two application cases. The first one is the PV module energy rating, the second application case is the long term yield prediction of PV power plants.

The editors of this document are Christian Reise and Boris Farnung, Fraunhofer ISE, Freiburg, Germany.

The report expresses, as nearly as possible, the international consensus of opinion of the Task 13 experts on the subject dealt with. Further information on the activities and results of the Task can be found at: <http://www.iea-pvps.org>.

Acknowledgements

This report was merged from two different draft documents, featuring Daniela Dirnberger and Nils H. Reich as principal authors. Although both experts left the PVPS Task 13 expert group a long time before this report was finished, several of their text fractions are still present with this report.

Many thanks go to Roger French of Case Western Reserve University, Cleveland OH, for his proof reading as a native speaker of the English language.

Parts of the German contribution to this work have been funded by German Federal Ministry for Economic Affairs and Energy (BMWi) under Contract No. 0325786-B.

Parts of the contribution of EURAC Research to this work have been funded by the Südtiroler Stiftung Sparkasse.

List of abbreviations

AC	Alternating current
AM	Air mass
AOI	Angle of incidence
APE	Average photon energy
ASTM	American Section of the International Association for Testing Materials
BIPM	Bureau International des Poids et Mesures
BMWi	Bundesministerium für Wirtschaft und Energie (German Federal Ministry for Economic Affairs and Energy)
BSRN	Baseline Surface Radiation Network
CAMS	Copernicus Atmosphere Monitoring Service
CdTe	Cadmium telluride
CEA	Commissariat à l'Énergie Atomique et aux Énergies Alternatives (French Alternative Energies and Atomic Energy Commission)
CIGS	Copper indium gallium selenide
CM SAF	Satellite Application Facility on Climate Monitoring
CMIP	Climate Model Intercomparison Project
CPP	Cloud Physical Properties
CZTS	Copper zinc tin sulfide
DC	Direct current
DWD	Deutscher Wetterdienst (German meteorological office)
EC	European Commission
GHI	Global horizontal irradiation
GHOR	Global horizontal irradiation
GPOA	Global irradiation in plane of array
GUM	Guide to the expression of uncertainty in measurement
HIT	Heterojunction with intrinsic thin layer
IAM	Incidence angle modifier
IEA	International Energy Agency
IEC	International Electrotechnical Commission
IEEE	Institute of Electrical and Electronics Engineers
INES	Institut National de l'Énergie Solaire (French National Solar Energy Institute)
IPCC	Intergovernmental Panel on Climate Change
ISE	Fraunhofer Institute for Solar Energy Systems ISE
ISO	International Organization for Standardization
JCGM	Joint Committee for Guides in Metrology
JRC	Joint Research Centre
KNMI	Koninklijk Nederlands Meteorologisch Instituut (Royal Netherlands Meteorological Institute)
KPI	Key performance indicator
LID	Light-induced degradation
LTYP	Long term yield prediction
MM	Mismatch
MPP	Maximum power point
MPR	Module performance ratio
MSG	Meteosat second generation
NOAA	National Oceanic and Atmospheric Administration
NOCT	Nominal operating cell temperature
NREL	National Renewable Energy Laboratory
OECD	Organisation for Economic Co-operation and Development

PLR	Performance loss rate
PR	Performance ratio
PSP	Precision spectral pyranometer
PV	Photovoltaic
PVPS	Photovoltaic Power Systems Programme
RMI	Royal Meteorological Institute of Belgium
RMSE	Root mean square error
SDE	Standard deviation error
SHCP	Solar Heating and Cooling Programme
SIT	Standard irradiance and temperature
SR	Spectral response
STC	Standard test conditions
TMY	Typical meteorological year
UTC	Coordinated universal time
WCRP	World Climate Research Programme
WMO	World Meteorological Organization

Executive summary

Long term yield predictions (LTYP) are a prerequisite for business decisions on long term investments into photovoltaic (PV) power plants. The preparation of a LTYP report typically relies on numerical modelling and prediction of the expected electrical yield, based on experience with previous PV power plants, laboratory measurements and more or less the whole knowledge gained in the PV community over the past years and decades. However, though PV system modelling has been performed for decades, not much effort has been spent on a comprehensive investigation of the uncertainties related to this task. This report tries to collect some insights into the field of uncertainties of several technical aspects of PV system yield prediction and assessment.

The first main section lists typical measurements, dealing either with a PV system component's properties or with PV system performance. It covers the uncertainties related to the most important measurands in PV solar energy:

- the solar resource
- PV module properties
- system output and performance—including long term effects

Uncertainty in irradiance measurements is in part related to the instruments, and in part to the measurement practices. While existing handbooks and guidelines may help to reduce operational issues, the uncertainties related to the instruments themselves are more difficult to minimize or reduce. However, if a certain non-ideal behaviour of an instrument is systematic and known, then a systematic correction can be applied to reduce or remove its influence on the measurement. In some cases manufacturers already supply information about temperature dependency and/or non-linearity. In the current PVSENSOR project, a wide range of instruments were characterized, and many systematic errors were identified and quantified. With such knowledge of instrument operating conditions it will be possible to quantify each systematic source of measurement error.

STC power measurement of PV modules and the estimation of its uncertainties is a topic that gained attention in recent years and saw remarkable improvements. For a full uncertainty assessment, it is important that stability issues are considered in addition to pure measurement uncertainty. There are laboratories with a profound knowledge on their uncertainty budget, typically those with the smallest overall uncertainties (down to $\pm 1.6\%$), laboratories where the reference cell or reference module calibration dominates the uncertainty budget, and laboratories where apparently uncertainties were not analysed in detail.

System testing looks at the performance of the complete conversion chain of a PV system. The determination of the observed performance ratio PR is rather easy, including an assessment of its uncertainty. The determination of the expected PR (as a quality requirement) is the major issue, as the PR depends on the system design and changes with the system's operating conditions. Despite this potential weakness, a PR test can form a valuable tool during the commissioning of a PV system.

The second major section of this report investigates several of the modelling steps for gains and losses in a PV system, again along a similar list:

- the solar resource—including long term trends
- PV module properties
- system output and performance

Irradiation data derived from satellite images are increasingly used as input for long-term yield estimations and as reference yield for monitoring and business reporting. Several authors have evaluated the quality of satellite-based irradiance data in the past, typical normalized root mean

square errors for satellite-based irradiation reported in literature are situated between 4% to 8% for monthly and 2% to 6% for annual irradiation values.

Solar irradiation at the Earth's surface is not stable over time for all locations on earth but may undergo significant long-term variations for particular regions, which is referred to as "global dimming and brightening". Consequently, also related uncertainties may not be considered to be negligible. In the presence of long-term trends, the question for solar resource assessments is no longer "what is the 'true' climatological value?", but "what is the best predictor for the next 20 years?". A suitable estimator should be a recent time period, that is long enough to filter the influence of single years with high anomalies, but which is short enough, to minimize the influence of past trends. Using irradiance data for the 10 most recent years is proposed as a good compromise to fulfil these conditions.

The DC energy yield of a PV module depends on module characteristics as well as operating conditions. With respect to uncertainties, the different influencing effects (irradiance level, angle of incidence, operating temperature, etc.) are typically represented by one individual factor per effect. The influences are assumed to be independent. Furthermore, these factors are often used in integrated form, e.g. over one year. The calculation of the influencing factors and the uncertainty estimation in detail is described and discussed in the main text.

Following the investigation of uncertainties in measurements (Section 2) and in modelling (Section 3), the combination of the knowledge gained is demonstrated in Section 4 for two application cases.

One example deals with the uncertainty of PV module energy rating, i.e. the question, whether the expected differences in performance between two module types are bigger than the associated error margins. The results show that significant energy rating is possible already today, at least if a module reference data set is available, and the difference from a reference energy yield is evaluated for the rating. Energy rating can already be useful for a number of reasons, but its full opportunities will only come to life after the IEC 61853 standard is finalized. The work presented here can be helpful in this process and includes a method suitable for being used as part of the standard.

As a second case, a framework for the calculation of uncertainty for a complete long term yield prediction is presented. As the simplified error propagation approach of the first example is not suitable for a complex LTYP, a Monte-Carlo simulation is used here instead.

The aim is to develop a method to handle all sources of uncertainties influencing lifetime energy yield predictions and to present the information needed to feed financial models with time dependent yield estimates and exceedance probabilities as desired by investors or stakeholders. The proposed method is based on a Monte-Carlo simulation which uses Gaussian or triangular distributions for individual modelling steps, including the solar resource data and long term changes of system behaviour. The parameters may be adjusted to individual sites and system layouts. A comparison of expected uncertainty and observed variability showed a good agreement.

This method can be seen as a part of a common framework that can assess the impact of technical risks on the economic performance of a PV project. The proposed approach is an effort to standardize the procedure of uncertainty calculation of predicted energy yields of PV systems in order to properly estimate financial investment risk.

1 Introduction

Large scale photovoltaic systems, often referred to as PV power plants, are long term investments. The return on investment depends on a variety of meteorological, technical and contractual parameters. The solar resource, the system design, the components' quality, and the operation and maintenance (O&M) schedule all may influence the energy yield and the financial result within the expected lifetime, a time frame of 20 to 30 years.

Long term yield predictions (LTYP) are a prerequisite for business decisions on long term investments into PV power plants. The preparation of a LTYP report typically relies on numerical modelling and prediction of the expected electrical yield, based on experience with previous PV power plants, laboratory measurements and more or less the body of knowledge gained in the PV community over the past years or decades.

For a proper O&M concept, the continuous assessment of electrical yield (or system performance, looking at yield in relation to solar input) is one of the main tasks. An analytical performance assessment gives a chance to understand system operation and to develop or improve the numerical models used for the yield predictions. Thus, numerical modelling forms a feedback loop from system design to system operation and vice versa. As a complementary task, the components' characterization also plays its role in both domains. Modelling tools need measured input data, so measurements and modelling are quite well entangled.

However, even since PV system modelling has been performed for decades, not too much effort has been spent on a comprehensive investigation of the uncertainties related to this task. This report tries to collect some insights into the field of uncertainties of several technical aspects of PV system yield prediction and assessment.

The greater image beyond technical data and electrical yield figures, i.e. the economic aspects of modelling financial risk of PV projects, are described in detail in another Technical Report of PVPS Task 13 entitled "Technical Assumptions Used in PV Financial Models – Review of Current Practices and Recommendations" [1].

In this report, we are looking on the technical or engineering side only, with emphasis on:

- Uncertainties related to component characterization
- Uncertainties related to long term (electrical) yield predictions (LTYP)
- Uncertainties related to PV performance assessment

As mentioned, measurements and modelling (prediction) of PV component or system behaviour are closely related, and their respective uncertainties are related similarly. Therefore, we take a look from two sides onto several of the mechanisms which influence a PV system's electrical yield. For example, the low light behaviour may be measured in a laboratory or even extracted from outdoor operational data. Measurement uncertainties exist in both cases. Within a LTYP, this low light behaviour needs to be modelled for all irradiance conditions seen in a typical year. Again, uncertainties in the model's reproduction of reality (i.e. the measured behaviour) come into effect.

For that reason, this report starts with two major sections dealing with measurements and with modelling. In Figure 1, these sections 2 and 3 are placed on both sides of a typical Sankey diagram, which acts as a symbol for the chain of gains and losses seen within a PV power plant. On the left hand side, typical measurements are listed, dealing either with component's properties or with PV system performance. On the right hand side, a large number of the various gain and loss modelling steps are listed. According to this division, sections 2 and 3 are about to present the

major tasks in measurement as well as in modelling, and, at the same time, to discuss their uncertainties.

In the third main section, the results of the previous steps are combined in two application cases. The first one is the PV module energy rating, an approach to rank a product by its expected “standard energy delivery” instead of its power under standard test conditions. Naturally, also this ranking is affected by uncertainties, but even the knowledge of the magnitude of uncertainties might be turned into additional information on a module’s data sheet.

The second application case is the long term yield prediction itself. A LTYP can clearly benefit from an integral view of input data, models, parameters and related uncertainties, especially when compared to existing approaches which sometimes only add an error margin to the final result.

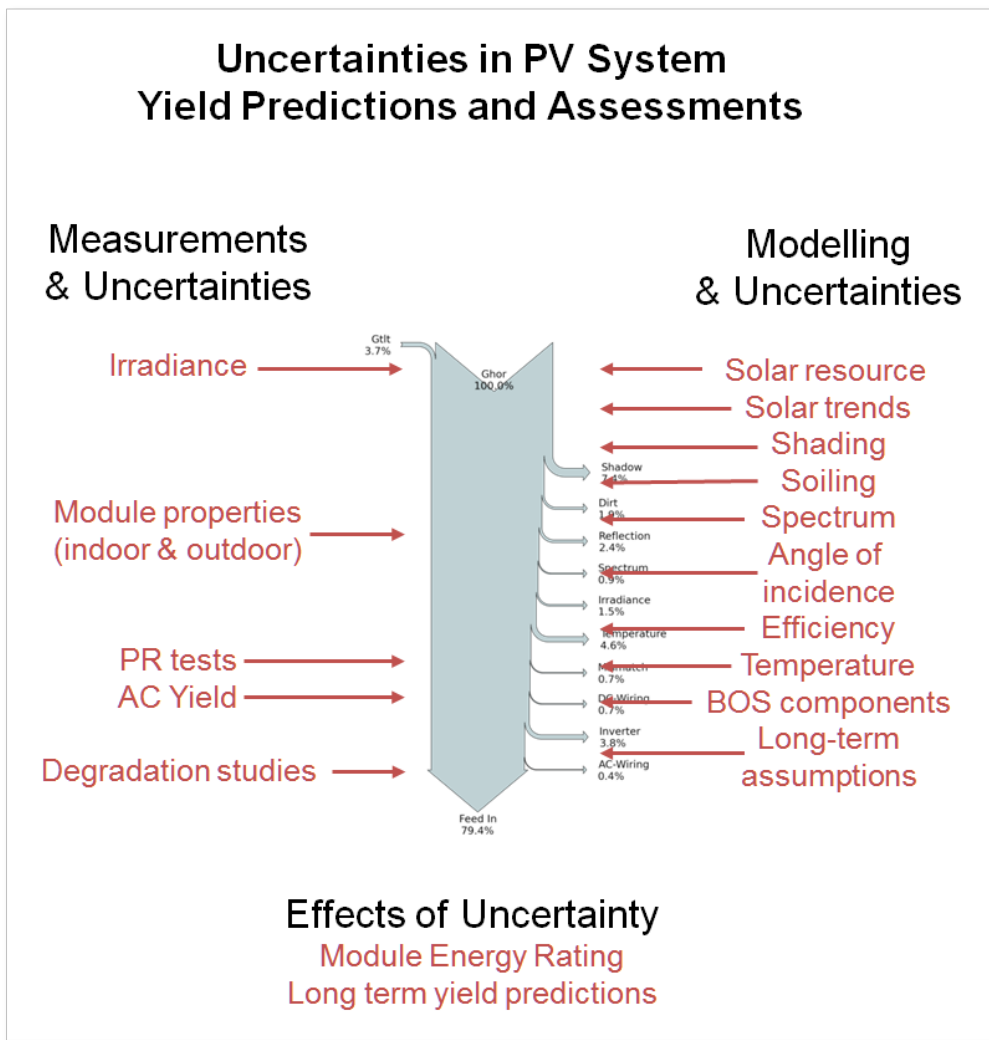


Figure 1: Structure of this report.

2 Measurements & uncertainties

Uncertainty assessment of component or system performance is based in measurements and analysis under certain fixed conditions as well as on extrapolation (called modelling) of component or system behaviour to other operating conditions. Therefore, the uncertainties of the measurements are included in all consecutive steps of assessment or modelling.

For that reason, this section covers the uncertainties related to the most important measurands in PV solar energy:

- the solar resource
- module properties
- system output and performance—including long term effects

2.1 Irradiation sensors and related measurement uncertainties

Solar irradiance must be quantified for energy performance calculations, whether they be calculations of expected future yields or for evaluations of past yields. Uncertainty in solar irradiance quantities is most often discussed in the context of long-term future yields where it is dominated by the difficulty of predicting future weather and climate conditions. Nevertheless, past irradiance measurements are relied on for these predictions, and the uncertainty associated with those past measurements also contributes substantially to the overall uncertainty—at least in the case of long-term predictions.

Uncertainty in both measured and projected irradiance quantities is a function of the time period under consideration. In fact, this time period should always be stated along with the uncertainty figure because integrated irradiance quantities for a specific year, month, day or hour will all have different uncertainties. In the case of projected quantities, shorter periods are dominated more by weather variability; whereas for measurements, different instrument characteristics come into play for different periods. For example, over the course of a year, instrument instability could be a significant factor, whereas over the course of a particular day this would be insignificant. Similarly, over the course of a day instrument non-linearity errors may cancel out, but over the course of a particular hour they are more likely to lead to a bias in the measurements. This situation is reflected in the WMO classification of pyranometers, where the required achievable uncertainties for hourly totals are up to twice the values for daily totals [2].

Uncertainty in irradiance measurements is in part related to the instruments, and in part to the measurement practices. As an example of the latter, measurements made with an instrument that was never cleaned, or that was mounted on an unstable platform, will carry a much higher uncertainty. Best practices to minimize these factors are described in multiple sources [2][3][4].

2.1.1 Exemplary data

The uncertainties related to the instruments themselves are more difficult to minimize or reduce, particularly after a specific instrument type has been purchased and installed. An ideal instrument would produce a signal proportional to the measurand—the solar irradiance incident on the sensor receiving surface—and the signal would not be affected by any other factors. In real instruments, however, that signal proportionality may change with irradiance (non-linearity), sensor body temperature, sky temperature, wind speed, irradiance angle of incidence, instrument mounting angle, time (response time and long-term stability), and spectrum. Furthermore, there may be interactions between these factors. Figure 2 illustrates four different non-ideal characteristics measured on different instrument classes in the context of the PVSENSOR project [5].

When little is known about the instrument characteristics, other than perhaps a threshold value for their contribution to measurement error, then little more can be done than assign a single uncertainty value to all measurements taken with a particular instrument. It is clear though, that not every irradiance measurement has the same total uncertainty, and the analysis of individual sources of uncertainty that contribute to this total uncertainty has received considerable attention [6][7][8]. Table 1 lists many of the sources of uncertainty that are applicable to thermopile pyranometers; many of them are directly related to the known non-ideal instrument behaviour.

Much of the research on uncertainty analysis will feed directly into the new ASTM “Standard Guide for Evaluating Uncertainty in Calibration and Field Measurements of Broadband Irradiance with Pyranometers and Pyrheliometers”, which is under development in collaboration with instrument manufacturers. The procedures to be described there will permit the calculation of uncertainties specific to time, location and instrument, which can then be applied to individual readings or series of reading of arbitrary duration. Figure 3 shows a result of this procedure applied to a year of hourly GHI measurements taken with a ventilated Eppley PSP and a ventilated Kipp & Zonen CM22 at NREL in Golden Colorado. Such individual measurement uncertainties can be propagated into PV system simulations or performance analysis procedures in order to produce a very high-resolution picture of the system yield uncertainties.

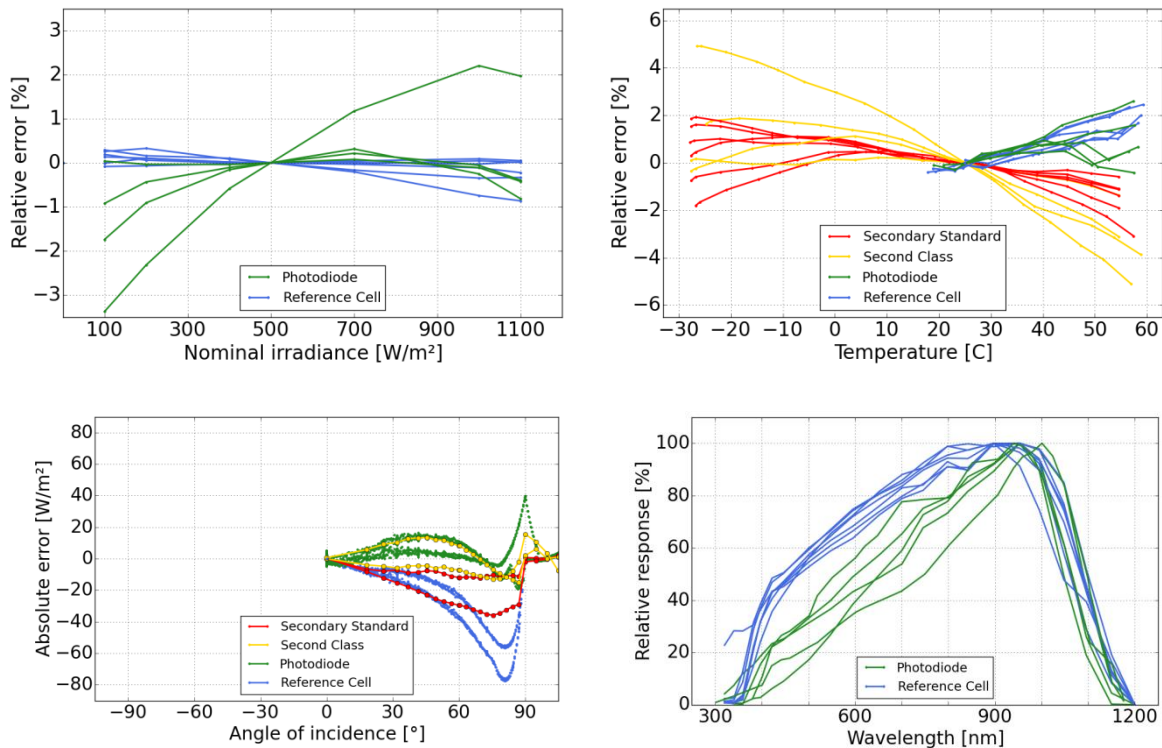


Figure 2: Examples of four non-ideal instrument characteristics: influence of non-linearity (a), temperature (b), angle-of-incidence (c) and spectrum (d).

Table 1: Examples of sources of measurement uncertainty for a pyranometer [8].

Uncertainty component	Quantity	Statistical Distribution	Uncertainty Type	Standard Uncertainty	Expanded Uncertainty
Calibration	R	Normal	Type B	$u/2 = 1.38\%$	2.76% (calibration done at 45°)
Zenith Response	R	Rectangular	Type B	$u/\sqrt{3} = 1.15\%$	2% (calibration done at 45°)
Spectral Response	R	Rectangular	Type B	$u/\sqrt{3} = 0.58\%$	1% (calibration done at 45°)
Nonlinearity	R	Rectangular	Type B	$u/\sqrt{3} = 0.29\%$	0.5%
Temperature Response	R	Rectangular	Type B	$u/\sqrt{3} = 0.29\%$	1%
Aging per Year	R	Rectangular	Type B	$u/\sqrt{3} = 0.58\%$	1%
Data logger Accuracy	V	Rectangular	Type B	$u/\sqrt{3} = 5.77\mu V$	$10 \mu V$
Maintenance	R	Rectangular	Type B	$u/\sqrt{3} = 0.17\%$	0.3%

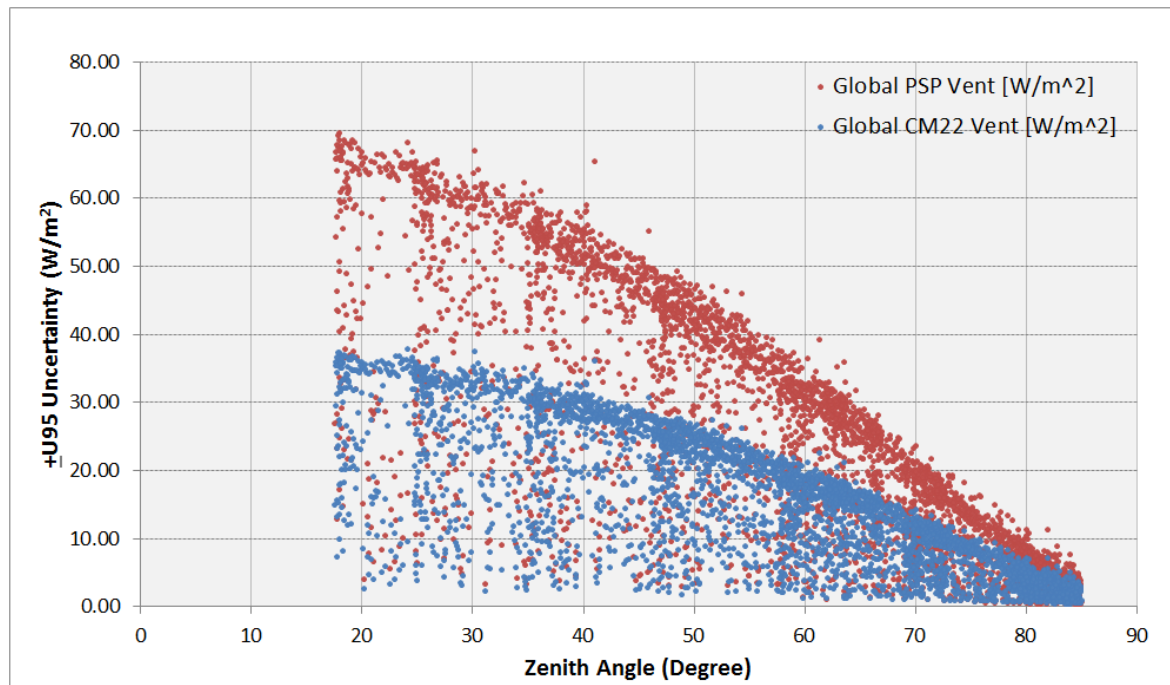


Figure 3: Absolute uncertainty for hourly GHI sums over a one-year period measured with a ventilated Eppley PSP or Kipp & Zonen CM22.

Source: http://www.nrel.gov/midc/radiometer_uncert.xlsx

2.1.2 Reducing measurement uncertainties

It has long been known that additional information can be used to reduce irradiance measurement uncertainties. The 1981 IEA Conference on Pyranometer Measurements had the goal to “determine ways to improve the measurement accuracies of pyranometers currently available by developing a more complete understanding of the instruments' performance characteristics” [9] and in 1996 the IEA Solar Heating and Cooling Programme Task 9 studied “Improved Measurements of Solar Irradiance by Means of Detailed Pyranometer Characterization” [10]. The PVSENSOR project that was started in 2014 continues with this approach, looking not only at pyranometers, but also commercial photodiode pyranometers and silicon reference cells [5].

The basic premise is that if one or more of these secondary characteristics are systematic, then a systematic correction can be applied to reduce or remove its influence on the measurement. In some cases manufacturers already supply information about temperature dependency and/or non-linearity so that the user may apply corrections, but because of the additional effort required by the manufacturer to perform these characterizations, it usually offered only for the most expensive instruments. In the PVSENSOR project, a wide range of instruments were characterized, and many systematic errors were identified and quantified. Thus, with knowledge of instrument operating conditions it is possible to quantify each systematic source of measurement error. Based on the instrument characteristics gathered in the PVSENSOR project, Figure 4 and Figure 5 demonstrate how such errors evolve over the course of a day and year respectively. It is also seen that relative errors (%) often give a different impression than absolute errors (W/m^2) about where the biggest sources of uncertainty lie, but for photovoltaic system yield predictions and assessments it is the summation of absolute errors over time that carries the greatest significance.

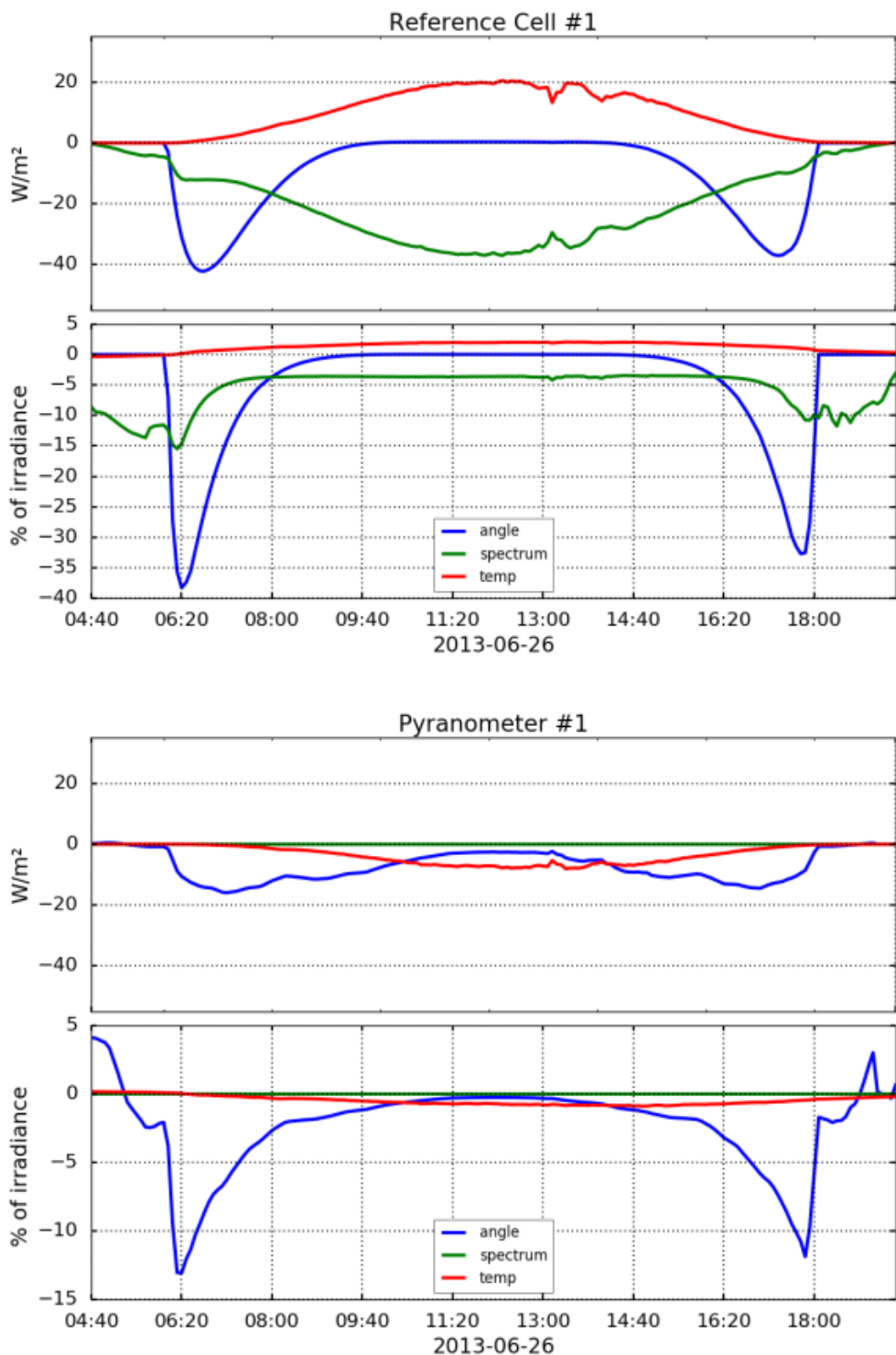


Figure 4: Daily profiles of the measurement error caused by angle-of-incidence, spectrum and temperature for a reference cell and a pyranometer located in Golden Colorado, tilted 40° South.

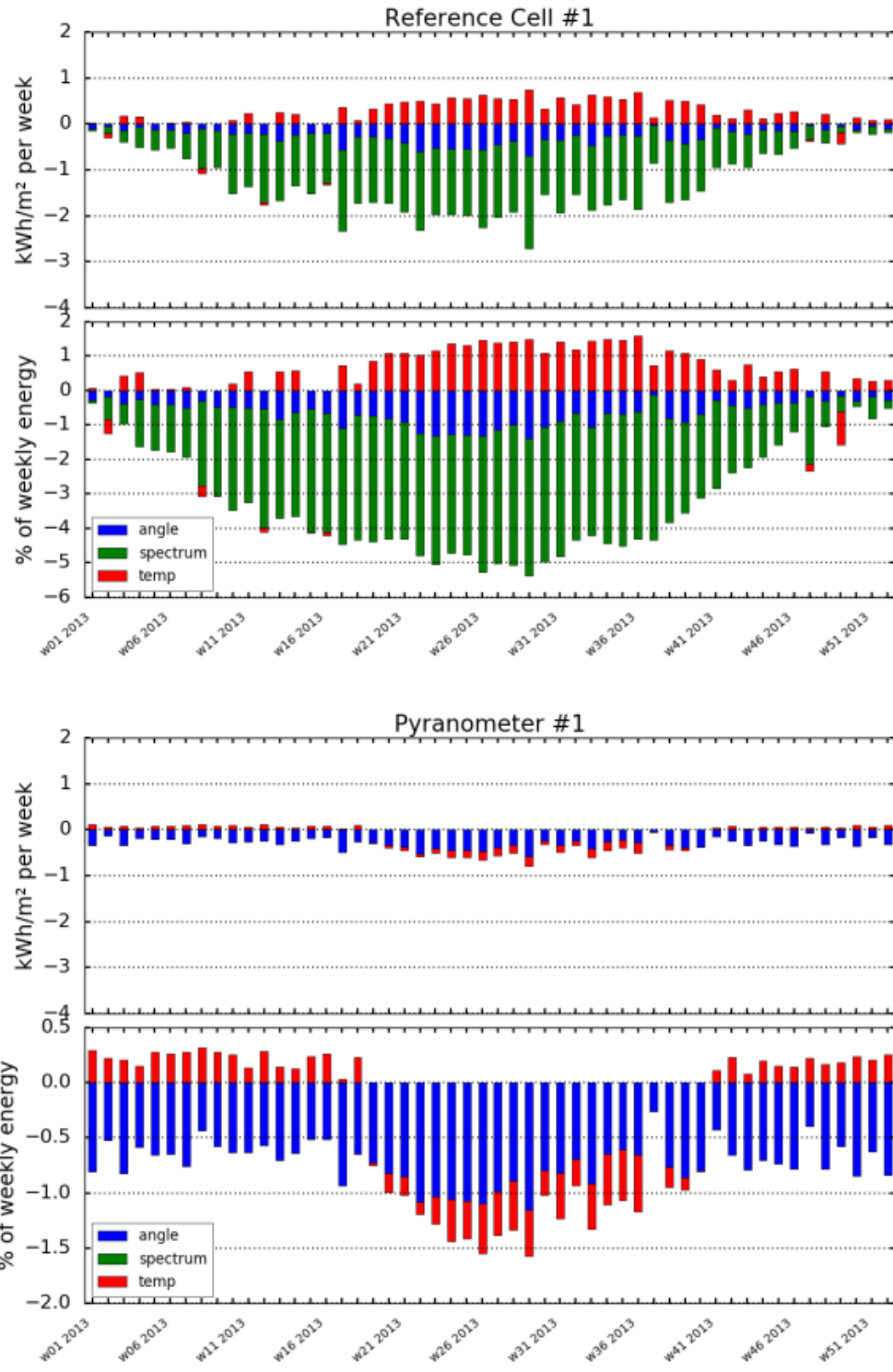


Figure 5: Annual profiles of the measurement error caused by angle-of-incidence, spectrum and temperature for a reference cells and a pyranometer located in Golden Colorado, tilted 40° South.

2.2 Laboratory (indoor) characterization of PV modules

At different steps of a PV project, laboratory testing of PV modules is valuable. Already in the design phase, confidence in the quality of the very specific batch of PV modules can be raised by means of quality benchmarking, with pre-defined quality criteria. Laboratory test can be conducted to check the power under Standard Tests Conditions (STC, i.e. 1000 W/m^2 @ 25°C and a defined spectrum), the light induced degradation of modules (LID) as well as temperature and low light behaviour. This can include the measurement of I-V curve for the power rating matrix defined in IEC 61853-1. Benchmarking PV modules can thereby help to:

- exclude systematic underperformance
- provide independent parameters for yield assessments
- compare the products to state of the art results

Additional tests may be performed to detect the sensitivity of modules to known failure mechanisms (e.g. snail trails, yellowing, potential induced degradation, ...). These testing procedures, especially for reliability testing, should be derived from the quality criteria of the customer, the experiences from the field as well as the environmental conditions (installation site, system layout, etc.).

During implementation of a PV project, an independent performance check of the modules is recommended to prevent a systematic underperformance of the purchased module lot. In this process, the flash test values should be evaluated based on a selected sample. In addition, it is essential to take into account initial effects with impact on the performance in the field. Crystalline modules lose up to 3% of their power in the first hours of operation [11], as illustrated in Figure 6. This degradation is usually completed within irradiation exposure of 10 to 20 kWh/m^2 , after which the module power has stabilized. In accordance to the European standard EN50380:2017 “Datasheet and nameplate information for photovoltaic modules” the modules must comply with rated power at STC given on the nameplate and data sheet after pre-conditioning with 20 kWh/m^2 .

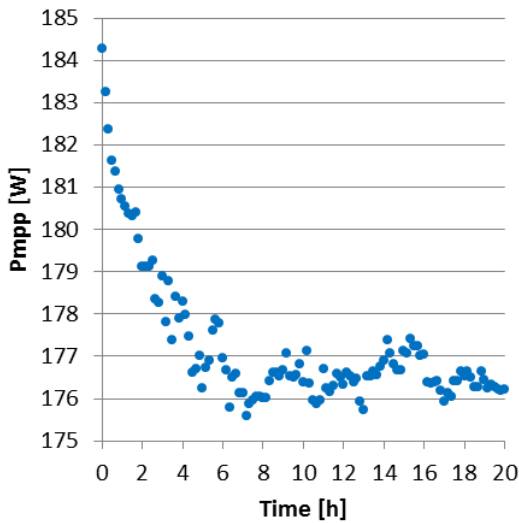


Figure 6: Power loss of a crystalline silicon PV module during the first hours of exposure to light (here: 1000 W/m^2).

2.2.1 Sample selection

Upon the arrival of the modules in the laboratory, typically a detailed visual inspection is performed. Electroluminescence images may be taken as well in order to evaluate the modules with regard to their quality of manufacture. Then, the power at STC is measured. To exclude the risk of a systematic misjudgement of the modules, the way of sample selection is of particular importance.

Often a specific number of modules is required for testing by the system integrator or the investor. To simplify matters, modules are picked randomly either before shipment or even on site. In many cases that means, if e.g. 50 modules are required, just two module palettes are sent to the laboratory. In this case, most of the modules are from the same serial number range and thus form the same time frame of production. An example is shown in Figure 7. This example shows clearly the small range of actual module power covered by the sample. Actually there is no value in measuring 25 modules out of one single palette with regard to prevent a systematic underperformance of the total quantity of purchased modules.

To exclude the risk of a systematic underperformance of the modules, the sampling needs to be done carefully and should select modules from different time serial number and power ranges as shown in Figure 8.

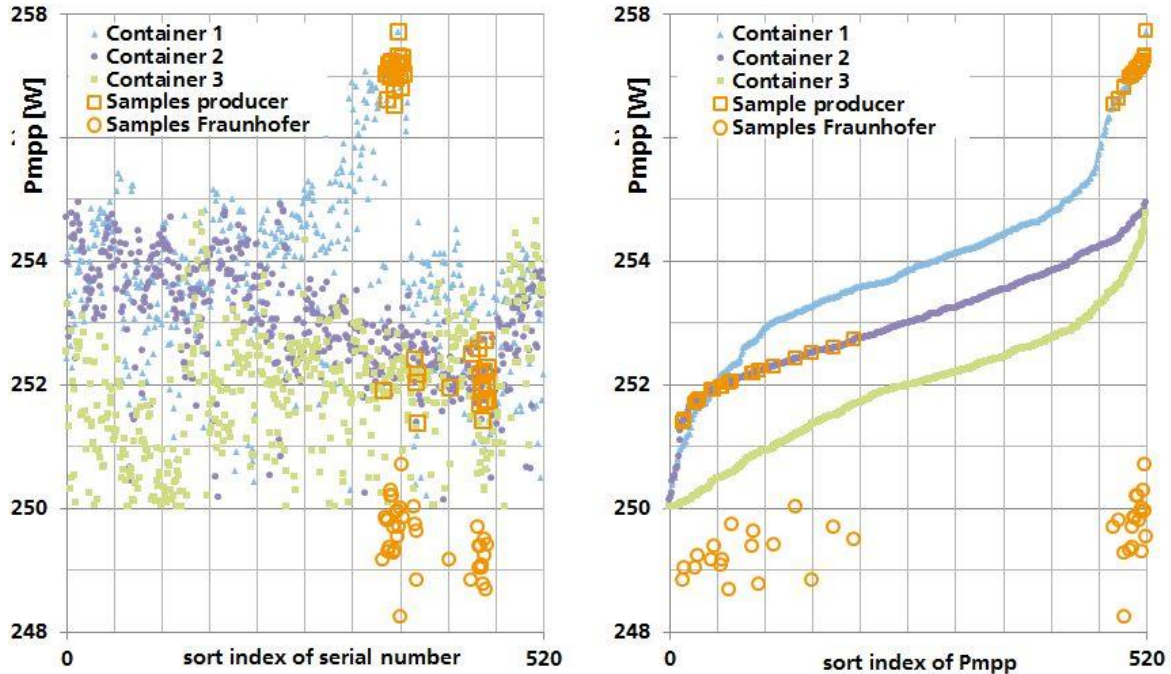


Figure 7: Two randomly selected PV module palettes (25 modules each) out of three containers (520 modules each). Small dots show STC power of all modules according to the manufacturer's flash list, squares denote manufacturer's measurements of the selected modules, circles denote Fraunhofer ISE's laboratory measurements. The two palettes cover only two small sections of serial numbers (left graph), these samples are not representative for power distribution of the entity of all modules (right graph).

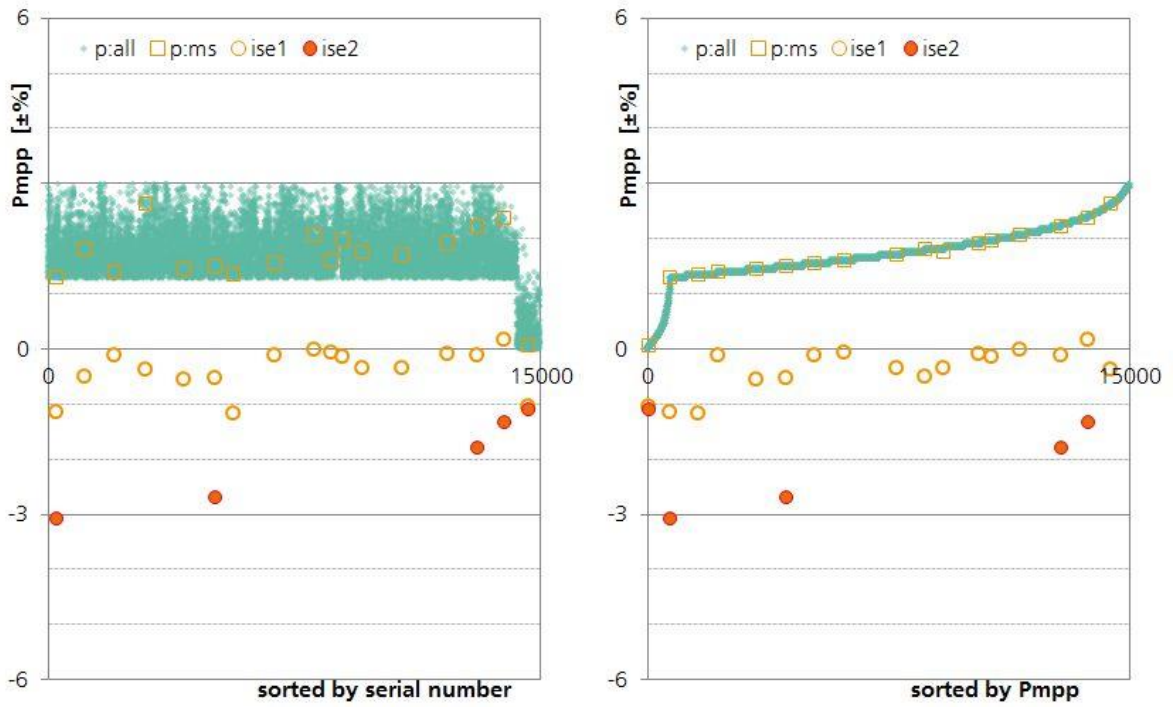


Figure 8: Proper assessment of a batch of 15,000 modules based on a small sample of 18 modules. Small dots show STC power of all modules according to the manufacturer's flash test list, squares denote manufacturer's measurements of the selected modules, empty circles denote Fraunhofer ISE's laboratory measurements, while filled circles denote measurements of the same modules after LID (after exposure to 20 kWh/m²). As the selection was based on the flash list sorted by power (instead of serial numbers), these samples are both representative for the power distribution of the entity of all modules (right graph) as well as for the full range of serial numbers (left graph).

2.2.2 Measurement uncertainties at STC

STC power measurement of PV modules and the estimation of its uncertainties is a topic that has gained attention in recent years and seen some improvements. Extensive information on this topic can be found in [12][13][14][15]. For uncertainty estimation, it is important that stability issues are considered in addition to pure measurement uncertainty: STC power is often not a constant value, but dependent on previous exposure to light and temperature. For energy rating, the STC power "representative of field operation" is essential (see [16] for detailed explanation). Briefly summarized, this means that initial stability effects like light induced degradation for c-Si and a-Si, and dark storage effects for CdTe and CIGS technologies must be taken into account.

The uncertainty of STC power as required for energy rating is composed of the measurement uncertainty, and the uncertainty due to initial or other stability effects:

$$u_{P,STC} = \sqrt{u_{\text{measurement}}^2 + u_{\text{stability}}^2}$$

This section presents results from a survey and several phone interviews with a total number of eight module test laboratories. All results are presented anonymously, i.e. the different laboratory names are not disclosed. This policy enabled us to collect more concrete data. Because of this, the reader will not be able to identify the best laboratory or to judge his current business partner, yet there is still valuable information available regarding questions like:

- Which accuracy may be achieved with best effort?
- What is the accuracy of a typical laboratory?

A main result of this survey, Figure 9, presents the measurement uncertainties achieved for STC conditions with different laboratories. The laboratories' uncertainty estimations may be interpreted like this: there are laboratories with a profound knowledge of their uncertainty budget (Labs 1 and 2), laboratories where the reference cell or reference module calibration dominates the uncertainty budget (Labs 6, 7, and 9), and laboratories where apparently uncertainties were not analysed in detail, as the complete uncertainty is attributed to a single effect only (Labs 3, 4, 5 and 8).

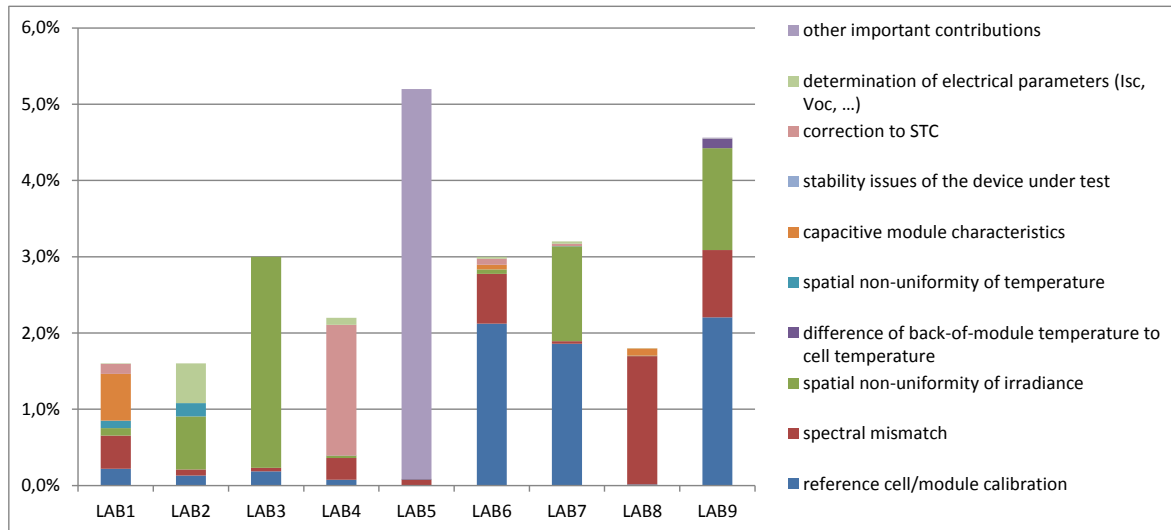


Figure 9: Contributions to overall measurement uncertainty as stated by the different laboratories. The sum of all contributions (the total column height) is normalized to the expanded uncertainty ($k=2$) of STC power measurements as stated by each laboratory.

Already in 2007, the EC Integrated Project PERFORMANCE made a suggestion on how to harmonize the calculation of uncertainty in indoor measurements [17]. Figure 10 gives an example of an uncertainty evaluation for indoor power measurements of crystalline Si modules.

The fields in yellow in the upper part are direct input fields where a user may fill in a number of single uncertainty figures (originating from estimations or specific measurements or instrument documentation). The fields in yellow in the lower part are also direct input fields concerning the type and distribution of the uncertainty. The fields in red in the lower part are reduction factors, which are dependent on the type and distribution of the uncertainties and are based on reasoned argument to each contribution's overall influence on uncertainty. They might have to be changed depending on the inputs in the yellow fields (manually, not automatic).

Such a scheme would allow for a more systematic comparison of uncertainty between different laboratories. However, often in practice, both a lack of somebody requiring such information and a lack of in-depth knowledge of some details prevent a typical laboratory from performing such an analysis.

The PERFORMANCE tool for an uncertainty evaluation of indoor module power measurements								
Created in Feb. 2007 by JRC								
Assumptions	value	unit	k					
Temperature coefficient of Isc (alpha)	500	ppm/°C						
Temperature coefficient of Voc (beta)	0,33	%/°C						
Diode coefficient D	5,3	%						
Uncertainty of Calibration of reference device	0,5	%	2					
Uncertainty of Spectral Mismatch Correction	0,54	%	2					
Uncertainty of Temperature Indicators	± 0,7	°C						
Difference between temperature during measurement and 25 °C	± 1,0	°C						
Temperature Non-Uniformity of module	± 0,3	°C						
Irradiance Non-Uniformity over module	± 1,0	%						
Off axis illumination	4	°						
Estimated misalignement between Reference and module	2	°						
Reference Cell Drift since last calibration	0,3	%						
Estimated error in Fill Factor (connections & cabling)	0,2	%						
Data acquisition error	0,2	%						
Shunts for current measurement of module	0,2	%						
Reference Cell / Trans Impedance Amplifier		%						
Standard uncertainty component	Std. uncert.	Distribution	Irradiance	Voltage	Current	Fill Factor	Value	Red. Fact.
	type (A/B)	Gauss/Rect	%	%	%	%		
Data acquisition error	B	G	± 0,08	± 0,08	± 0,11	± 0,00	0,2	2,586
Shunts for current measurement of module	A	R	± 0,00	± 0,00	± 0,12	± 0,00	0,2	1,732
Reference Cell / Trans Impedance Amplifier	A	G	± 0,00	± 0,00	± 0,00	± 0,00	0,0	2,000
Combined Standard Electrical Uncertainty			± 0,08	± 0,08	± 0,16	± 0,00		
Temperature indicators	B	R	± 0,02	± 0,13	± 0,03	± 0,00	0,7	1,732
Temperature coefficients (alpha resp. beta). Tamb: 25 °C	B	R	± 0,03	± 0,19	± 0,04	± 0,00	1,0	1,732
Non-uniformity of module temperature	B	R	± 0,00	± 0,06	± 0,01	± 0,00	0,3	1,732
Contribution of Standard Temperature Uncertainty			± 0,04	± 0,24	± 0,05	± 0,00		
Spatial Non-uniformity of irradiance	B	R	± 0,58	± 0,03	± 0,58	± 0,00	1,0	1,732
Orientaton of module and reference device	B	G	± 0,04	± 0,00	± 0,04	± 0,00	4,0	2,586
Alignment of module and reference device	B	R	± 0,02	± 0,00	± 0,02	± 0,00	2,0	1,732
Contribution of Standard Optical Uncertainty			± 0,58	± 0,03	± 0,58	± 0,00		
Calibration of reference device	A	G	± 0,25	± 0,01	± 0,25	± 0,00	0,5	2,000
Determination of Spectral Mismatch correction factor	B	G	± 0,00	± 0,00	± 0,27	± 0,00	0,5	2,000
Reference Cell Drift	B	R	± 0,17	± 0,01	± 0,17	± 0,00	0,3	1,732
Contribution of Standard Reference Device Uncertainty			± 0,30	± 0,02	± 0,41	± 0,00		
Estimated error in Fill Factor (connections & cabling)	A	G	± 0,00	± 0,00	± 0,00	± 0,20	0,2	1,000
Combined Standard Uncertainty			± 0,66	± 0,26	± 0,73	± 0,20		
Expanded Combined Uncertainty (k=2)			± 1,32	± 0,52	± 1,46	± 0,40		
			Isc ± 1,5 %					
			Voc ± 0,52 %					
			Fill Factor ± 0,40 %					
			Pmax ± 1,6 %					
Expanded Combined Uncertainty (k=2)								

Figure 10: Example of a filled PERFORMANCE tool for the uncertainty evaluation of indoor module power measurements. The tool was created in Feb. 2007 by the JRC [17].

2.2.3 Non-STC conditions

Up to now, there is only rudimentary information on individual measurement uncertainties of different laboratories achieved for power measurements at conditions different from STC. This is partly caused by a lack of demand of such measurements – a typical PV module data sheet contained 2 or 3 power specifications (for STC and for 200 W/m² @ 25 °C, sometimes for 800 W/m² @ NOCT) and the temperature coefficient of output power only.

Today, with higher demands on product characterization and the availability of the IEC 61853 standards on PV module energy rating, more and more laboratories offer comprehensive power rating measurements, covering a full matrix of irradiance and temperature conditions. Nevertheless, the uncertainty of these non-STC measurements is still more or less unknown. A few laboratories provided some information on the maximum uncertainty of power measurements at the related conditions:

Table 2: Uncertainty levels for non-STC conditions (first survey).

Uncertainty	Conditions
Lab 1	some 5%
Lab 2	3.6%
Lab 4	3.2%
Lab 7	3.5%
Lab 8	2.2%
	for extreme temperature/irradiance combinations with matrix measurements at low irradiance values at 200 W/m ² and 65 °C at 1000 W/m ² and 70 °C at 100 W/m ² and 75 °C

2.2.4 Comparison of indoor and outdoor power rating

Outdoor measurements of PV module performance may be performed for several reasons:

- an outdoor setup extends the range of ambient conditions even for short term measurements (real solar spectrum, continuous illumination instead of pulsed light)
- outdoor testing on a longer period is closer to commercial operation of PV modules—up to a realistic benchmark of different module types in side-by-side operation

The extraction of module characteristics (especially STC power) from outdoor measurements is sometimes considered an alternative, or seen as complementary, to indoor testing. Depending on the site of the test, the duration of an outdoor test may vary, and the normalization to STC (or other reporting conditions) imposes additional uncertainty on the results. The following example depicts some of the challenges when comparing outdoor to indoor data.

2.2.4.1 Definitions

The (initial) module performance is commonly determined under Standard Tests Conditions (STC, i.e. 1000 W/m² @ 25 °C and a defined spectrum). However, the initial performance can still deliver a wide range of values (the values below in parentheses are extracted from a commercial multi-crystalline module, and are shown as well in Figure 11 c):

- the module power class labelled (in the case of this module: 250 Wp)
- the module flash-test value from the factory (258.4 Wp)
- the module flash-test value from a reference laboratory (253.0 Wp)
- the on-site Standard Irradiance and Temperature (SIT) conditions, measured around 1000 W/m² and corrected to 25 °C, meaning the equivalent of STC through an outdoor IV bench

The SIT power itself may be derived from different sets of measurements:

- extracted from the 1st suitable outdoor measurement (253.4 Wp)
- extracted from the 1st day of outdoor measurements (252.3 Wp)
- extracted from the 1st month of outdoor measurements (251.6 Wp)
- extracted from 1 year of outdoor measurements (247.7 Wp), which can be considered as a seasonal corrected value
- extracted from 1 year of outdoor measurements comprising a linear degradation correction (248.0 Wp)
- extracted from several years of outdoor measurements and with a non-linear degradation correction (248.3 Wp)

This list is not extensive, and for technologies like amorphous silicon, with an important initial degradation, the initial performance is even more difficult to handle. For instance, the STC value given by the manufacturer is much lower than the initial measured value.

2.2.4.2 Data comparisons

In this test of a commercial polycrystalline module considered here, the module is facing south, the fixed tilt is 25°, and the temperature is measured with a thermocouple glued on the middle of rear side (on the middle of a cell). I-V curves are taken every 5 minutes, while the MPP is tracked between the I-V curve acquisitions. The modules were mounted in December. The reference flash-test, called “STC INES” was performed at CEA-INES.

With the frequency of 12 I-V curves per hour, the $1000 \pm 20 \text{ W/m}^2$ irradiance is reached around 5 times per summer day (average value) and 150 times per month.

Figure 11 a) represents the power data filtered at the irradiance $700 \text{ W/m}^2 \pm 30 \text{ W/m}^2$ and corrected to 700 W/m^2 . This representation allows to see the evolution of the module even in winter conditions.

Figure 11 b) shows the filtering at $1000 \text{ W/m}^2 \pm 20 \text{ W/m}^2$ that allows the SIT values extraction. In this graph, the data are corrected to 1000 W/m^2 and to 25°C . This representation shows missing values in the winter, indeed, with the 25° tilt, the 1000 W/m^2 value is never reached in this period. So the very initial performance is not extractable for this module.

Figure 11 c) is a zoom on the data corrected at 1000 W/m^2 . It allows one to see the dispersion of the initial performance values based on the different possible definitions.

In Figure 12, we see the result for another crystalline commercial module placed on another test bench. Oriented at 163° (17° off south), tilted at 30°, monitored with a flat Pt100, the module has been mounted in June, and 1000 W/m^2 is reached during the first days.

Figure 11 c) and Figure 12 show the gaps between the initial values within their possible definitions. Other kinds of deviations are observed on other modules, and it is difficult to observe systematic deviations.

It is important to note that most of these values fall within the expected uncertainties limits: considering the results of the previous European Commission projects, Performance Europe and SOPHIA, STC uncertainties are known to stand between 2% and 4% while SIT uncertainties stand between 4% and 6%.

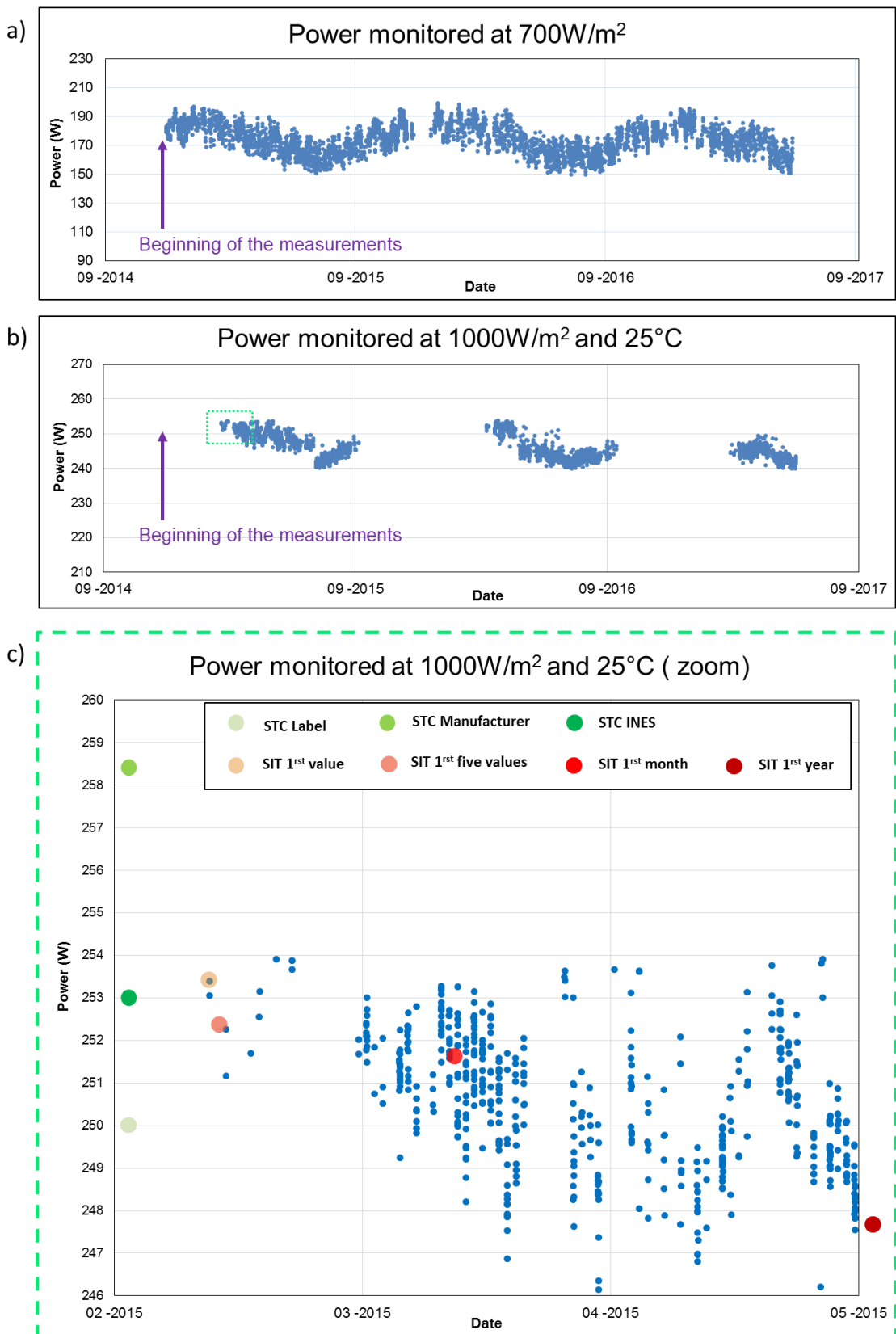


Figure 11: a) Power data filtered at the irradiance $700\text{W/m}^2 \pm 30\text{W/m}^2$ and corrected to 700W/m^2 ; b) Power data filtered at the irradiance $1000\text{W/m}^2 \pm 20\text{W/m}^2$ and corrected to 1000W/m^2 and to 25°C ; c) Zoom on the power data filtered at the irradiance $1000\text{W/m}^2 \pm 20\text{W/m}^2$ and corrected to 1000W/m^2 and to 25°C . All relevant initial performance values are plotted. STC = Standard Test Conditions. SIT = Standard Irradiance and Temperature conditions, it is an equivalent of STC in outdoor conditions.

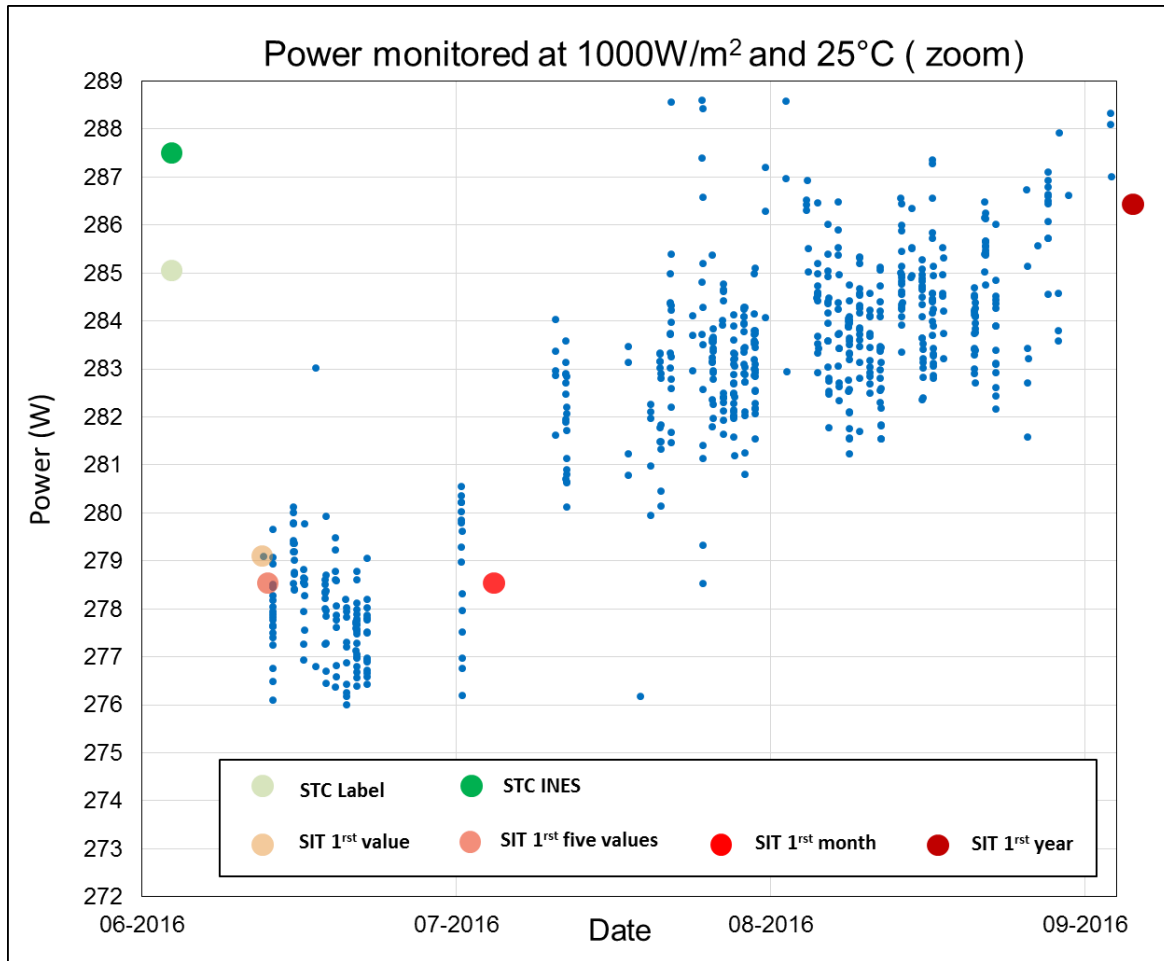


Figure 12: Power data of another crystalline module filtered at the irradiance $1000 \text{ W/m}^2 \pm 20 \text{ W/m}^2$ and corrected to 1000 W/m^2 and to 25°C . All relevant initial performance values are plotted. STC = Standard Test Conditions. SIT = Standard Irradiance and Temperature conditions, it is an equivalent of STC in outdoor conditions.

Although the spectrum of the direct sunlight is often closer to the AM1.5 than a simulator light, the outdoor operating conditions of the module are much more variable than the indoor ones. The main deviations between indoor measurements and outdoor measurement are:

- the temperature correction deviation, due to:
 - the difference of temperature between the module's cells average and the temperature sensor
 - the propagation of the temperature coefficient uncertainty
- the mismatch between the reflection of the reference cell and the module under test
- the mismatch between the spectral response of the indoor and the outdoor reference cells
- the mismatch between the indoor and the outdoor irradiation spectrum
- the early degradation, when the beginning of the measurement setup is not done at 1000 W/m^2 , because of the time, the weather, or the season (cf. Figure 11 b)
- the measurement uncertainty, especially for modules comprising a low number of cells

Considering these sources of deviation, filters may be tested in order to look for systematic deviations.

2.2.4.3 Systematic deviations search

The study concerns 191 modules data from the CEA test benches on the rooftop of the INES site. These are oriented at 163°, tilted at 30°, and temperature monitored by a flat Pt100. Although Figure 11 c) shows a high number of different initial values definition, this section will focus on the deviation between the “STC INES” and the “SIT 1st month” (150 first values around 1000 W/m²). The filters applied are:

- Early degradation influence: modules installed in “winter” (1st October to 31st March) are excluded
- Weather influence: modules that do not have at least 30 days of available data are excluded. This filter is relevant but does not take into account any LID (Light Induced Degradation) effects.
- Flash-testers and their reference devices influence: only STC values originating from the same flash-tester (INES flash-tester) are used.
- Other influences: aberrant data are also excluded (improper temperature data, unreported amorphous module preconditioning, extreme discarded data, bifacial modules with a monofacial STC).

After these four restrictive filters, 41 modules could be analysed. The selection is mostly composed of standard multi and mono crystalline silicon modules, and also comprises other technologies: 8 heterojunction, 5 N-type, 2 CIGS, and 1 IBC module.

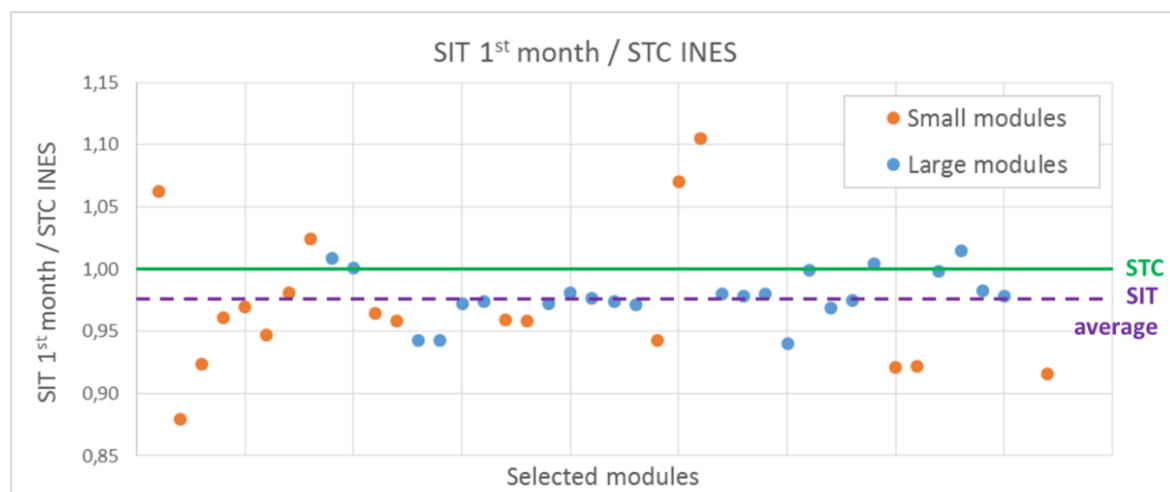


Figure 13: SIT/STC plot for the filtered modules, namely the average of the 150 first power values under an irradiance of $1000 \pm 20 \text{ W/m}^2$ corrected at 1000 W/m^2 and at 25°C , divided by the STC power value measured at INES. Small modules ($P < 10 \text{ Wp}$) have been coloured differently as their standard deviation has been observed higher than large modules ($P > 150 \text{ Wp}$). STC = Standard Test Conditions. SIT = Standard Irradiance and Temperature conditions.

The result of the study is (within 2σ):

- For all selected modules: $P_{\text{SIT}} = P_{\text{STC}} - 2.5\% \pm 8.3\%$
- For the small selected modules: $P_{\text{SIT}} = P_{\text{STC}} - 3.0\% \pm 11.9\%$
- For the large selected modules: $P_{\text{SIT}} = P_{\text{STC}} - 2.1\% \pm 3.9\%$

Large modules have a lower standard deviation than the small ones. A systematic deviation seems to be found between 2% and 3%, but the associated standard deviation weakens this conclusion.

2.3 System testing

System testing looks at the performance of the complete conversion chain of a PV system. This conversion chain includes many steps, from PV module DC output to inverter and transformer efficiencies, adds mismatch and ohmic losses and also losses due to poor system design or poor workmanship. Nevertheless the most important test, whether a PV systems meets its expected performance, needs only two precise measurements: the amount of solar irradiation received in a certain period of time, and the amount of electric energy delivered at the billing meter in the same period of time. The numerical ratio of both amounts (when given in kWh/m^2 and kWh/kW_P) is identical with the system Performance Ratio (PR).

Therefore, the measurement of the PR is rather easy, including an assessment of its uncertainty: the uncertainty of irradiance measurement is discussed in Section 2.1, the uncertainty of AC billing meters is rather small (0.5% or 0.2%) and well documented. The determination of the expected PR (as a quality requirement) is the major issue, as the PR depends on the system design and changes with the system's operating conditions. The uncertainties related to PR determination are dealt with in Section 3. Despite this potential weakness, a PR test can form a valuable tool during the commissioning of a PV system.

Most of the acceptance testing, initial performance and safety evaluation or plant certification takes place in the commissioning phase of a project. Beside a visual inspection, safety and component testing, actual PR of the system should therefore be validated. By comparing actual (measured) and expected (simulated) PR, one can obtain valuable information on whether the system performs as expected. Important input data for the calculation of PR are the actual irradiance and the system output. Thus, both values have to be measured accurately during operation. It has been observed that in many cases, however, unreliable and inaccurate measurement equipment is used.

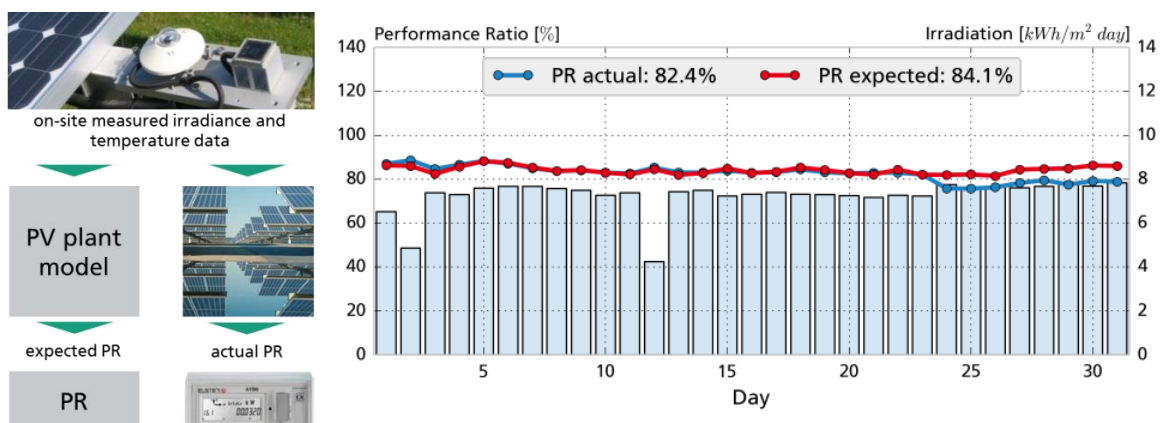


Figure 14: Schematic process of performance verification (left pane) and exemplary results for July 2013 of a utility scale PV system in southern Spain (right pane). Note a failure in the system caused a drop of PR by almost 10% can discerned for day 24.

Available monitoring data can be validated with data from calibrated and high-quality measurement equipment, temporally installed at the site for a defined time period. If required, monitoring data is corrected to the calibrated instruments. After validation and correction, existing monitoring can be used to determine the actual Performance Ratio (PR measured). For comparison with expected PR (PR modelled), the measured weather data (irradiance, temperature) are used to simulate the PR with an established procedure and the system model and parameters from the original yield prediction. Over the last years, this procedure for performance verification has been applied successfully for utility scale PV plants worldwide. It has been shown, that the performance

can be accurately evaluated within just a few weeks and as the plants monitoring system is validated, third party evaluation of existing and future yield data is possible.

2.4 Degradation and uncertainties related to long-term stability

Long term changes in system performance—often called degradation—are still among the most unexplored effects with PV systems. From a survey regarding degradation effects in LTYP carried out among PVPS Task 13 experts, a large variety of assumptions is documented:

- A participant uses variable degradation rate for the first 5 years, then fixed from years 5–30. Generally they assume a 1% to 2% drop in the first year, 0.7% to 0.5% to year 5, then 0.3% to 0.5% up to year 30
- Another participant affirms that they also include an initial degradation (LID) of 0.3% to 1.0%, depending on module technology and location (increased degradation caused by unfavourable environmental conditions)
- Another participant uses 0.25%/year for crystalline Silicon based PV
- The last participant uses constant degradation over the years with the exception of the first year where technology specific behaviour is considered. Values are based on extensive (publicly available) literature review

The calculation of the performance loss rate (PLR) from field data, usually expressed in percentage of power loss per year, requires:

- the adoption of a performance metric, i.e. an index describing the behaviour of the PV system during a specific time range (e.g. the weekly, monthly, yearly etc. values of performance ratio)
- the adoption of a statistical technique, i.e. how the trend of the performance loss is extracted from the time series of the adopted performance metric. For example, the most common technique is to derive the PLR from a linear regression of monthly values of the performance metric.

The overall uncertainty associated to PLR is therefore a combination of the uncertainty related to the performance metric, which is a result of the uncertainty of the field measurements, and to the application of the statistical technique.

2.4.1 Uncertainty of the estimation of the performance metric

The performance metric calculated for a specific time range bears an uncertainty that propagates from the measurement uncertainties of the electrical and meteorological parameters involved in the calculation of its value.

Let us consider for example the Performance Ratio metric on a monthly level, calculated from 15-minute interval time-series measurements of power and plane-of-array irradiance:

$$PR = \frac{\sum_{i=1}^N P_i * 0.25 G_{STC}}{\sum_{i=1}^N G_i * 0.25 P_n}$$

where N is the total number of records within a month, P_i is the i -th record of power (DC or AC) output of the PV system, G_i is the i -th record of plane-of-array irradiance, P_n is the nominal power of the PV system and G_{STC} is the plane-of-array irradiance at Standard Test Conditions, equal to 1000 W/m².

The uncertainty affecting P_i , G_i and P_n depends on the quality of the sensors and procedures used to measure these quantities. For example, the absolute uncertainties listed in Table 3 are considered for the specific case of seven different PV systems installed in Bolzano (North-East of Italy):

Table 3: Uncertainty values associated to the measurement of plane-of-array irradiance, DC-Power, and to the PV system nominal power.

Parameter	Uncertainty value (k=1)	Measurement device
G_i	2% of the reading	Pyranometer
P_i (DC)	3% of the max readable current and voltage	Commercial inverter
P_n	1% of P_n	

The uncertainty of the monthly values of PR is calculated by applying the procedure proposed by the Guide to the Expression of Uncertainty in Measurement (Joint Committee for Guides in Metrology 2008a):

$$U(y)^2 = \sum_i^N \left(\frac{\partial f}{\partial x_i} \right)^2 * U(x_1)^2$$

where $y = f(x_1, \dots, x_N)$ is a generic linear equation. By applying this to the PR definition above, the absolute uncertainty of PR is found to be

$$U_{PR} = \sqrt{ \left(\frac{1000}{Pn + \sum Gi * 0.25} \right)^2 * \left(\sqrt{\sum (0.25 * U(P_{DCI}))^2} \right)^2 + \left(\frac{-1}{Pn^2} * \frac{(\sum P_{DCI} * 0.25) * 1000}{\sum Gi * 0.25} \right)^2 * (U(Pn) * Pn)^2 + \left(\frac{-1}{(\sum Gi * 0.25)^2} * \frac{(\sum P_{DCI} * 0.25) * 1000}{Pn} \right)^2 * (\sqrt{\sum (0.25 * U(Gi) * Gi)^2})^2 }$$

Figure 15 shows the monthly values of PR, of the absolute uncertainty and of the relative uncertainty on a time range of 5 years for seven investigated PV systems installed in Bolzano, Italy.

The absolute uncertainty of monthly PR is higher in winter than in summer, due to the lower values of both irradiance and power measurements. This is also true for the relative uncertainty, i.e. the ratio of absolute uncertainty of PR and PR itself.

Once the monthly values of PR are known, it is possible to perform a linear regression. However, each value of PR is affected by an error that is supposed to be distributed in a certain way (e.g., normally). Therefore, the uncertainty of every single monthly value of PR propagates to the slope of the linear regression, and to the PLR itself.

Another uncertainty contribution comes from the statistical technique adopted for extracting the power loss trend. For example, if we consider linear regression, the associated uncertainty corresponds to how well a regression line is able to fit the time series of the performance metric. If, for example, all the values of the performance metric were perfectly distributed on a line, this uncertainty component would be equal to zero.

In the case of the linear regression technique, the associated uncertainty depends on:

- the dimension of the time series: the longer is the number of the available points, the lower is the uncertainty. Makrides et al. [18] and Jordan et al. [19] indicate 3 years as the minimum period to achieve reasonable values of uncertainty with this analysis.
- the seasonality of the time series: the lower is the seasonality, the lower is the uncertainty because the time series will resemble more to a line.

For the latter reason, other metrics than the PR might be more suitable. Belluardo et al. have carried out an analysis of the linear regression uncertainty using three different metrics. Results may be found in [20].

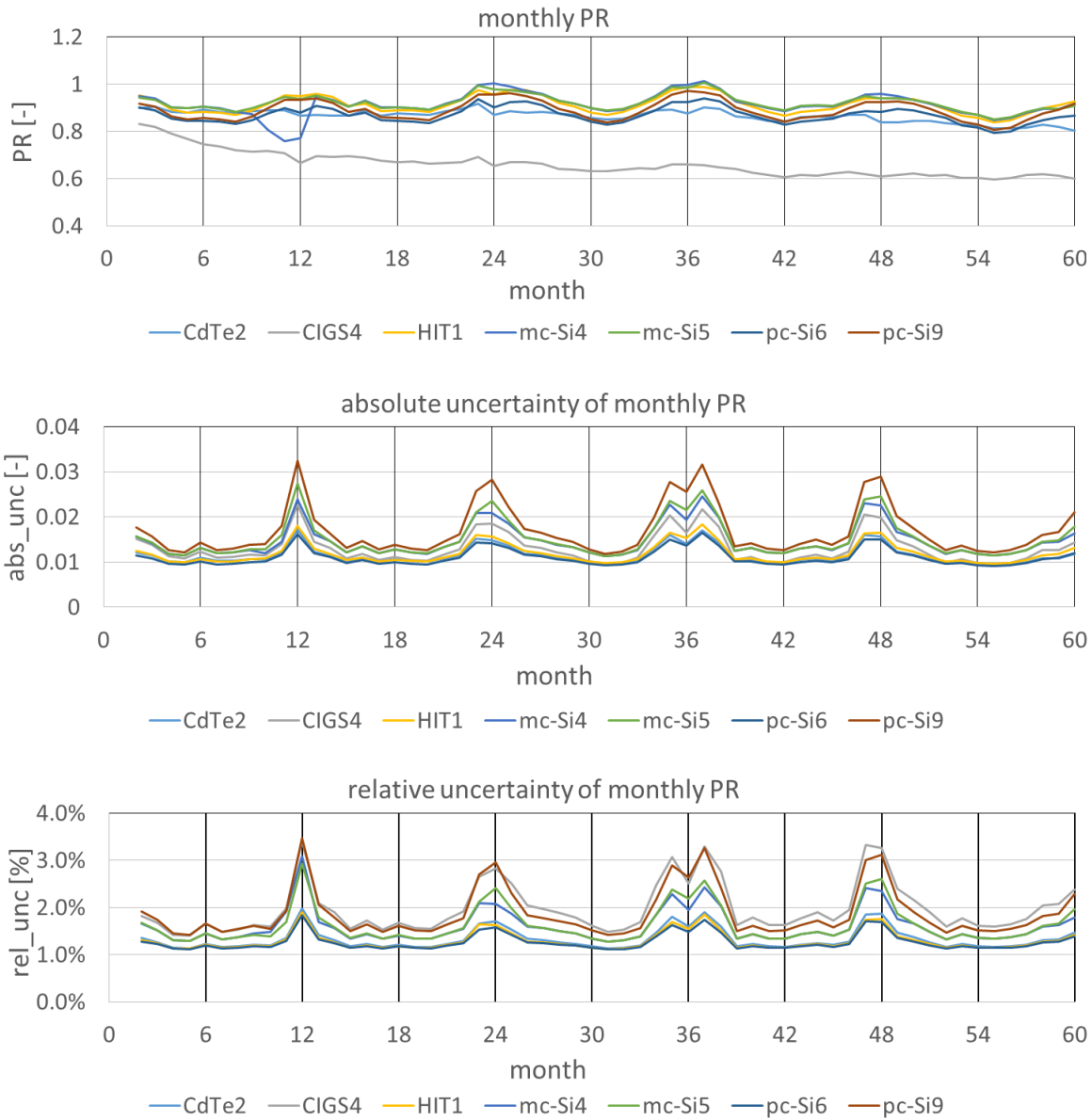


Figure 15: 2011–2015 monthly series of (top) performance ratio, (centre) absolute uncertainty of performance ratio and (bottom) relative uncertainty of performance ratio, calculated for seven different photovoltaic systems installed in Bolzano. (1=January 2011; 60=December 2015).

2.4.2 Overall uncertainty of the performance loss ratio

In this section the calculation of the contributions to the overall uncertainty of PLR is performed on five years of data from seven different PV systems installed in Bolzano, Italy, using the Monte Carlo technique. The uncertainty of records of P_i , G_i , and of P_n are assumed as in Table 3. For each month, the value of PR is calculated. The associated error is supposed to be distributed normally, and the absolute uncertainty is calculated as explained above. By associating a normal distribution to the error of each monthly PR, with a mean equal to the value of PR calculated from field data (Figure 15, top), and with a standard deviation equal to the calculated absolute uncertainty (Figure 15, centre), a number N of possible values of PR is generated using the software *Statistics101*. This number of “draws” is supposed to be high enough to be statistically significant, as demonstrated below in this section. This way, by combining the N different values of PR for each month, a total number of N possible time series of PR is generated. These combinations are shown as grey lines in Figure 16. In the same figure also the 25th, 50th and 75th percentiles are shown.

For each of the N time-series of PR, a linear regression is performed. This way, N values of PLR are retrieved, as well as N values of uncertainty associated to the linear regression. In particular, the distributions of both PLR and the associated linear regression resembles a Gaussian distribution, as shown in Figure 17 and Figure 18.

The standard deviation of the N values of PLR correspond to the absolute uncertainty related to the estimation of the performance metric, while the average of the N values of uncertainty associated to the linear regression represents the uncertainty related to the application of this statistical technique. These values are reported in Table 4 for each of the seven module types under consideration. The combined uncertainty of the two contributions, calculated with the rule of squares, is also reported.

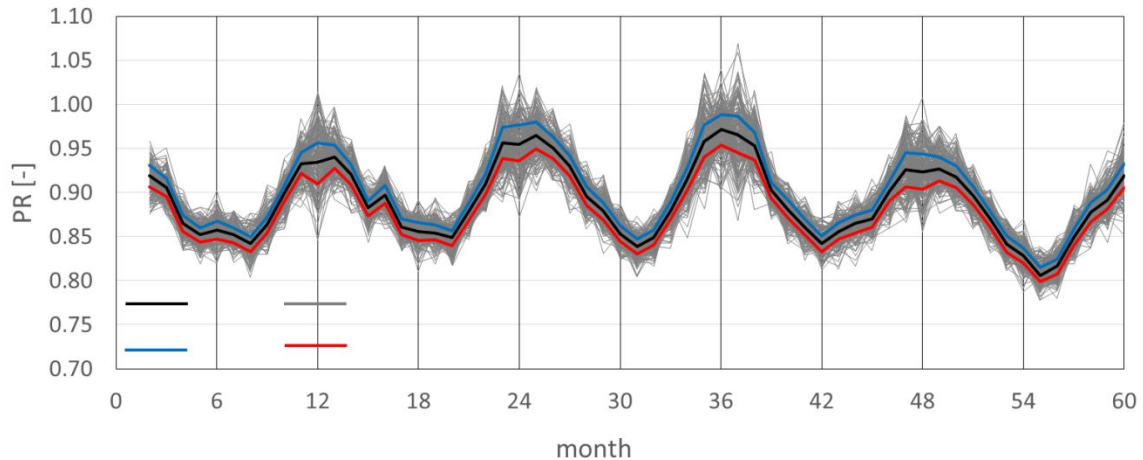


Figure 16: N time series of PR for a PV system (pc-Si6) installed in Bolzano. The values are obtained for each month by a generation of N values of PR according to the value of the associated uncertainty and assuming a normal distribution of the error. Time series related to specific percentiles are also displayed.

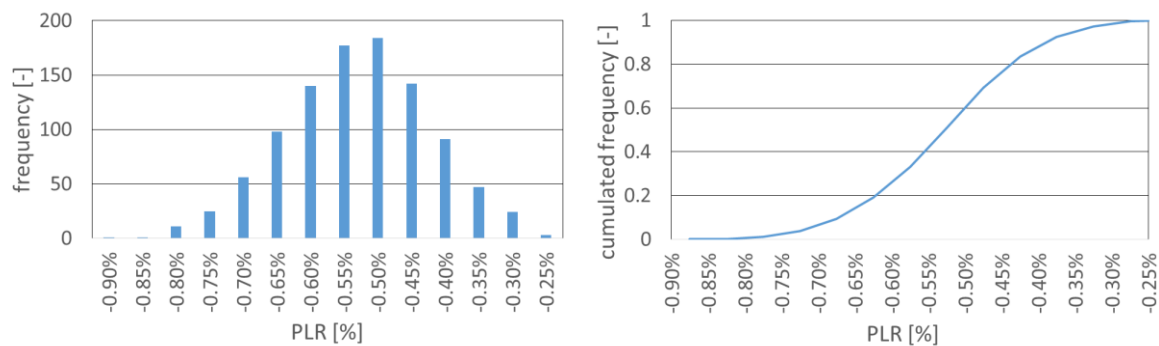


Figure 17: Frequency distribution and cumulated frequency distribution of N values of PLR calculated from the N time series of monthly values as in Figure 16, for a PV system (pc-Si6) installed in Bolzano.

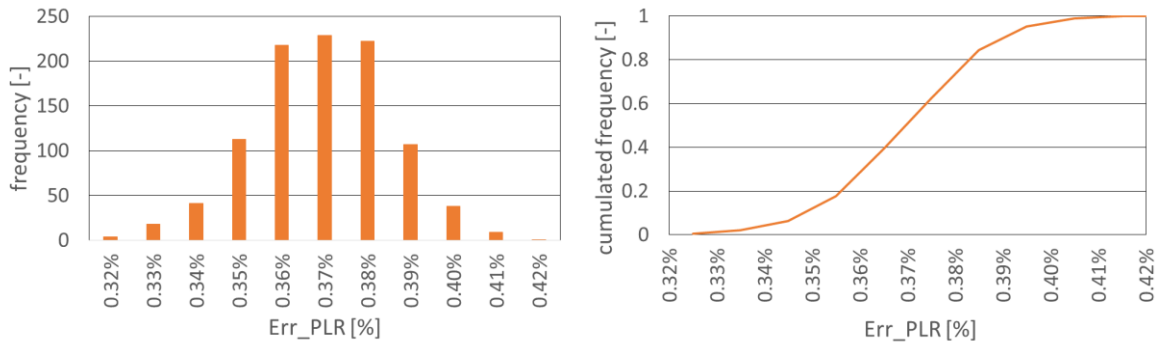


Figure 18: Frequency distribution and cumulated frequency distribution of N values of uncertainty of the linear regression calculated from the N time series of monthly values as in Figure 16, for a PV system (pc-Si6) installed in Bolzano.

The displayed results have been calculated with a Monte Carlo technique using $N=1000$ generated values of PR. This number is considered statistically significant in the sense that the obtained values of PLR, the absolute and the relative uncertainty of PLR can be considered stabilized, as shown in Figure 19.

By comparing Table 4 and Figure 15, it is clear that the technology with the highest absolute uncertainty in PLR (pc-Si9) has also the highest values of the absolute uncertainty of monthly PR. At the same time, the technology with the highest absolute uncertainty in regression uncertainty (mc-Si4) has a strong seasonality coupled with an anomalous loss of performance due to a failure occurred during a short period at the end of 2011, that made PR deviate from the performance trend.

Both uncertainties (performance metric and statistical technique) add up to values between 15% and 140% for all modules without real failures. In this light, the assumption cited at the beginning of this section (“among the most unexplored effects”) looks more understandable.

Table 4: Values of average PLR, absolute and relative uncertainty of PLR, absolute and relative uncertainty of the linear regression, and combined uncertainty for seven technologies installed in Bolzano.

technology	average PLR	Uncertainty related to the performance metric		Uncertainty related to the statistical technique		
		absolute uncertainty PLR (k=1)	relative uncertainty PLR (k=1)	absolute uncertainty Lin. Regres- sion (k=1)	relative uncertainty Lin. Regres- sion (k=1)	Combined uncertainty (k=1)
		(%/year)	(%/year)	(%)	(%)	(%)
CdTe2	-1.5	0.11	7.2	0.21	13.5	15.2
pc-Si6	-0.5	0.11	20.3	0.37	69.7	72.6
HIT1	-0.5	0.12	25.5	0.39	85.6	89.3
mc-Si4	+0.3	0.14	56.5	0.52	204.4	212.1
mc-Si5	-0.4	0.15	34.2	0.36	85.1	91.7
pc-Si9	-0.4	0.17	47.2	0.46	131.7	139.9
CIGS4	-4.5	0.14	3.2	0.36	7.9	8.6

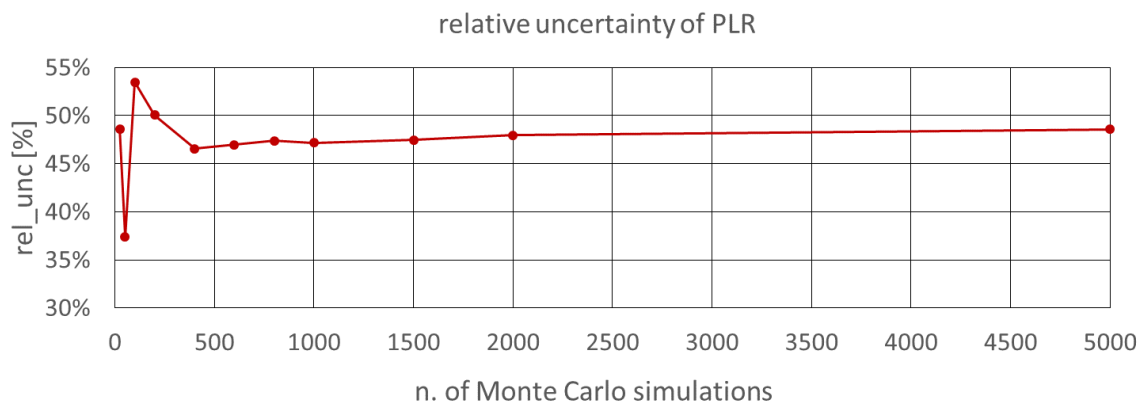


Figure 19: values of relative uncertainty of PLR calculated with the above-described methodology for a PV system (pc-Si6) installed in Bolzano by considering different number N of values of monthly PR generated according to the value of associated uncertainty and assuming a normal distribution of the error.

3 Modelling & uncertainties

Modelling the future behaviour of a PV system is an essential part of any yield prediction. Beside, system modelling is needed for PR assessments, or, more generally, for an analytical understanding of PV system operation. Starting from the needs of a Long Term Yield Prediction, this section examines the most important contributions to modelling uncertainty.

3.1 Long-term energy yield predictions

A Long-Term Yield Prediction (LTYP) refers to the estimate of the accumulated total energy production of a defined PV system at a specified location for a specified period (the prediction period). The sequence of creating LTYP reports can be broken down into three main steps [21]:

1. Determination of the solar resource potential in the reference period: Selection or creation of time series data, which provides information as accurate as possible for direct and horizontal global and diffuse solar irradiation at the particular location in a historical reference period. Calculated solar irradiation incident onto the plane-of-array is added to this time series together with other meteorological parameters (e.g. ambient temperature, wind speed and direction).
2. Determination of the energy yield in the reference period: Simulation of the PV energy yield on the basis of irradiation and meteorological time series as determined in step 1 using mathematical models for the PV system.
3. Determination of the energy yield in the prediction period: Projection of the annual PV energy yields in the reference period onto the individual years of the prediction period as well as the determination and consideration of parameters affecting PV energy yield in the prediction period. These include estimation of inter-annual variability in irradiance and degradation assumed for the PV modules and other system components.

Analogous to this sequence of steps, sources of uncertainty can be distinguished and related to each of the three steps individually.

Uncertainties related to the solar resource potential in the reference period can be differentiated into three separate causes. First, deviations between assumed and actual horizontal solar irradiation in the reference period result from using imperfect models to derive horizontal irradiation from satellite images. Although these techniques and subsequent modelling are greatly advanced, uncertainty in the order of 3% constitutes a major part to overall uncertainty. Secondly, subsequent modelling applied to global horizontal irradiation (GHI) time series to calculate irradiation onto the plane-of-array causes additional deviations, which depends on the models used, the accuracy of underlying meteorological input data such as the direct-diffuse ratio of solar irradiation, the temporal resolution of the time series, as well as the albedo of the ground surface, which contributes to ground reflected irradiance on the array surface. The accuracy of this irradiation transposition depends heavily on both the particular location concerned and the particular transposition model used. Finally, the long-term average of the solar resource may exhibit multi-decadal trends, dubbed “global dimming and brightening” (see e.g. [22][23]). Therefore, the chosen time period to be used as the reference period can affect uncertainty [24].

Uncertainty of PV energy yield in the reference period stems from actual modelling of the PV energy yield, based upon chosen input data of step one. Consequently, in this category uncertainty is added due to inaccuracies of chosen models and simulation tools. Most simulation tools, such as e.g. *PVsyst*, calculate PV energy yield by a chain of subsequent models, comprising various energy gain and energy loss mechanisms within the PV system. The PV energy yield of the reference period is calculated using calibrated or best-guess values of model parameters for the various

models used in the model chain. In other words, parameters perceived as most likely to be true within a given parameter space are chosen, inherently introducing uncertainty.

Uncertainty of PV energy yield for the prediction period is related to potential differences of the PV energy yield caused by reference and prediction periods being different. Although this may lead to significantly different PV energy yield, this third consideration that may affect uncertainty is sometimes disregarded in typical LTYP reports.

Long-term changes in PV system characteristics are usually considered by including a simple linear model of module degradation. Uncertainty related to module degradation and other aspects affecting PV system performance in the long term is usually not considered, although recent publications that focus on economic aspects started to address these aspects [25][26]. Effects relating to long term trends in solar resource are usually omitted or rarely regarded as significant (see e.g. [27][28][29][30]). Consequently, the effect of uncertainties related to long-term changes are not addressed. Expected deviations of PV energy yield of individual years are often given as relative standard deviation with respect to the average overall yield in the reference period.

3.2 Estimation of overall uncertainty in modelling

Uncertainty analyses can be defined as a systematic process involving two dedicated steps in order to propagate the uncertainty of a model or its input values to the modelling results [31]. These two steps are:

- Quantification of uncertainties of all inputs, modelling steps and respective parameter
- Combination of uncertainties to determine overall uncertainty of the final result

The uncertainty quantification for long-term PV energy yield predictions in a fully complete and mathematically defined way would need to consider individual uncertainties of meteorological input data as well as individual uncertainties of each parameter used as input in each model. Furthermore, correlations and interdependencies of the uncertainties of individual models themselves and each meteorological input parameter would need to be excluded, as to allow for conducting error propagation accurately. This is of relevance for the overall uncertainty, since overall uncertainty implies the entire model chain and their related interdependencies are relevant. Uncertainty associated with meteorological input values and with some individual models is not constant but varies. Daily and seasonal fluctuations cause constantly changing ambient conditions (e.g. temperature and irradiation levels, incident angles and direct-diffuse ratios) and imply the need for conditional uncertainties. This is highly complex in itself, and the high number of individual models and model parameters further add to the difficulty [31][32]. Therefore, uncertainty quantifications are currently not performed the way outlined in this paragraph.

Alternatively, we describe a simplified approach here to quantify overall uncertainty. Calculating predicted yield Y of year n is thereby simplified to [33]:

$$Y_n = GHI_{mean} \Delta_{GPOA} \eta_{STC} A_{Generator} \prod_{i=1}^M (1 - \Delta_{i,n})$$

with GHI_{mean} the best estimate of mean annual GHI in the reference period, Δ_{GPOA} mean annual gain or loss of irradiance transposition to plane-of array (GPOA), η_{STC} the initial module conversion efficiency under STC, $A_{generator}$ the area of the PV modules of the system, $\Delta_{i,n}$ the relative gain or loss of modelling step i in year n , and M the number of all iterative model steps for the prediction of overall yield. Introducing index n allows a simplified (annual) consideration of long term (annual) changes that affect predicted yield.

Uncertainties of individual factors can be derived by model validations and comparisons of measured with modelled data. Such comparisons show residuals that can be related to each model and can be quantified. For the analysis of residuals it is relevant to consider their dependency on envi-

ronmental conditions as well as the overall duration of the comparison of measured with modelled data that provides the dataset of residuals. It is recommended to at least consider one year of data as to include seasonal effects.

An alternative to the “classical” approach is the use of Monte-Carlo techniques, which have been greatly facilitated by both increasing computational power and decreasing costs of computers. The next subsections will deal with the isolated uncertainties of the most important modelling steps, while a Monte-Carlo approach will be presented in Section 4.2.

3.3 Uncertainties associated with irradiation data

From a survey on LTYP best practises among PVPS Task 13 experts, a variety of answers is documented:

- A variety of solar resource database are used such as SolarGIS, PVGIS, Meteonorm, etc. One of the organizations highlights the preference towards ground data when available.
- In general, one database is preferred against others and it is used as benchmark for various sites. Site adaptation techniques are also adopted as routine by some but it does not seem to be common practice.
- Typically, a time resolution of 1 h is taken.
- A deviation larger than 3% (1 answer) or 5% (3 answers) is considered as “very different”.
- Weighted average is used by the majority of the participants to the survey.

3.3.1 Comparing different data sources of satellite-derived irradiation time series

Irradiation data derived from satellite images are increasingly used as input for long-term yield estimations and as reference yield for monitoring and business reporting. Asset managers and O&M contractors rely on irradiation data for the calculation of key performance indicators (KPIs). Therefore, the fidelity of these data has to be confirmed independently and with scientific rigour. Several authors have evaluated the quality of satellite-based irradiance data in the past and some comprehensive overviews for further reading can be found in [34][35]. Typical normalized root mean square errors for satellite-based irradiation reported in literature are situated between 4 to 8% for monthly and 2 to 6% for yearly irradiation values.

Recently, several new or improved satellite-based irradiance services have become available. In several of these services, the underlying cloud models increasingly take into account the physical properties of the clouds. The Solar Bankability project (www.solarbankability.eu) has recently published a large-scale evaluation of the precision of different methods and services available for the practical use of satellite-based irradiation as reference yield [1][36]. This validation study compared the satellite-based irradiance data from seven satellite-based irradiance data services (Table 5) with data from meteorological stations for the years 2011 to 2015.

The reference data covers measurements from 203 meteorological stations maintained by the national public weather services of France, Belgium and the Netherlands. The available reference data sets are listed in Table 6 with the spatial distribution of the stations illustrated in Figure 20.

Table 5: Satellite derived irradiance models under evaluation

Model (abbreviation)	Available through
MACC-RAD (maccrad)	CAMS Radiation service, through SoDa
HelioClim-3 v3 (hc3_v3)	SoDa
HelioClim-3 v4 (hc3_v4)	SoDa
HelioClim-3 v5 (hc3_v5)	SoDa
MSG-CPP (cpp)	KNMI
GSIP (gsip)	NOAA (since 3/2014)
EnMetSOL (enmetsol)	University of Oldenburg

Table 6: Reference data set of global horizontal irradiation and minimum aggregation period available for the evaluation

Provider	Sites	Aggregation	Coverage
Météo France (FR)	160	daily	2012–2013
RMI (BE)	12	daily	2012–2013
KNMI (NL)	31	hourly	2011–2015

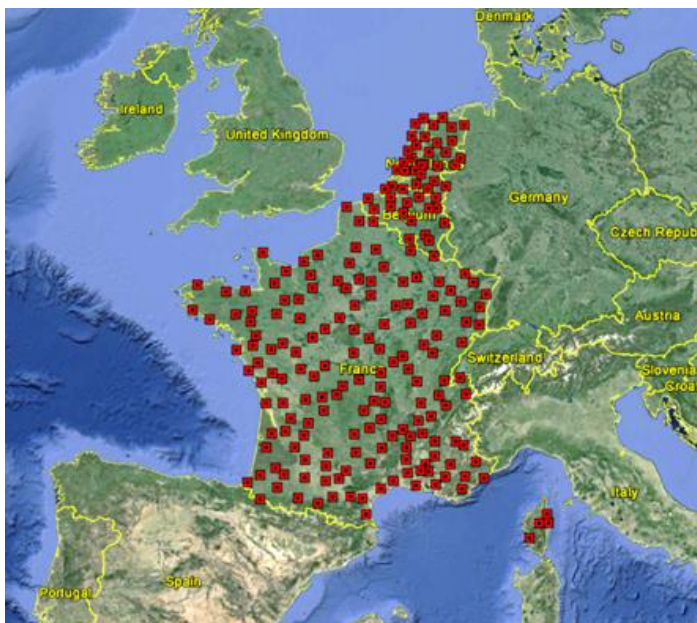


Figure 20: Meteorological stations used as reference dataset for the evaluation.

The satellite derived irradiation data have been evaluated against the reference data by their root mean square error (RMSE):

$$\text{RMSE}^2 = \text{SDE}^2 + \text{Bias}^2$$

This equation describes a circle and allows one to split the RMSE into a random error, i.e. standard deviation of error (SDE) and a systematic error (Bias). When setting out SDE against Bias in Cartesian coordinates, the RMSE is the distance from the origin. The principle is illustrated in Figure 21. In practice, when computing irradiation by integrating irradiance over long times, random errors are averaged out while the bias will remain the same.

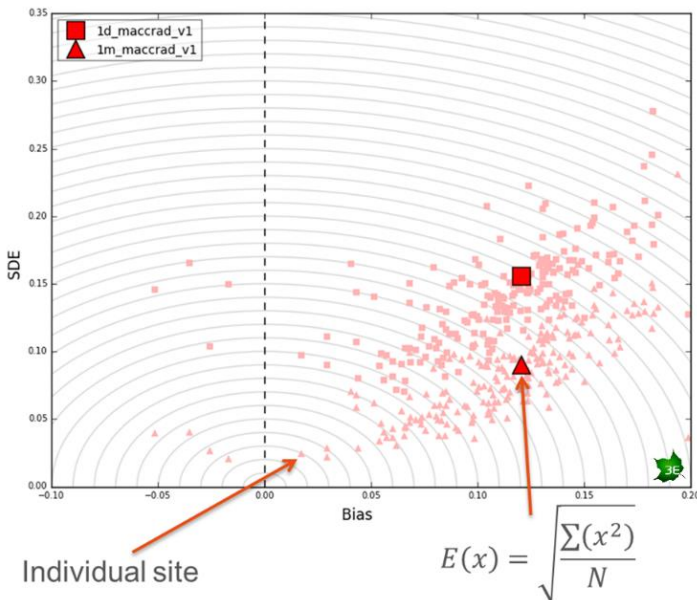


Figure 21: Exemplary distribution of the error measures RMSE, SDE and Bias for data with daily (square) and monthly (triangle) aggregation.

The three error measures were computed separately for each station and year. Moreover, the three error measures were evaluated for monthly, daily, and in the Netherlands also hourly resolution. Finally, the expected error values $E(x)$ for each service, year and time aggregation from the geometric mean of error x over all stations has been calculated. These values can be interpreted as mean error values for each service over the region.

The results for daily and monthly data are shown in Figure 22 (a) for 2012 and Figure 22 (c) for 2013. The results are consistent for both years. A relatively high Bias for MACC-RAD is observed. Notably, no default bias correction is applied to the results of the MACC-RAD model by Copernicus or SoDa. Being the direct outcome of an R&D project, the idea is that users of the model results would correct for the bias themselves and depending on their particular situation. Furthermore, results show that the HelioClim model improves with each version and the best performing models for monthly irradiation are HelioClim-3 v4 and v5, EnMetSOL and MSG-CPP.

For hourly data, EnMetSOL and MSG-CPP perform a little bit better than the HelioClim models. The results for hourly, daily and monthly data for the Netherlands are shown in Figure 22 (b), (d), (e) and (f) for different years. The results for data covering 11 months running from April 2014 to February 2015 rather than from January to December 2014 are shown in Figure 22 (f) as this allowed to include the results from the GSIP model. Data from GSIP for Western Europe have only been fully available since April 2014.

Overall results show that the bias of most data services lies consistently between 3% and 5%. However, for individual sites, the bias rather ranges between -5% and 10%. The SDE can be as low as 2% for monthly irradiation values from the MSG-CPP method. For daily and hourly irradiation, the SDE and, hence, also the RMSE are much higher. The average SDE for daily values lies above 10% for all services and for hourly value it lies even above 20%. Accordingly, the RMSE values for the best performing models (EnMetSol, HelioClim-3 v5, MSG-CPP and GSIP) are of 3% to 6% for monthly and 9% to 11% for daily irradiation. The RMSE for hourly irradiation for the better performing models is much worse, in the range of 19% to 23%.

Finally, the average bias values of the different models over all stations in the Netherlands are compared in Figure 23.

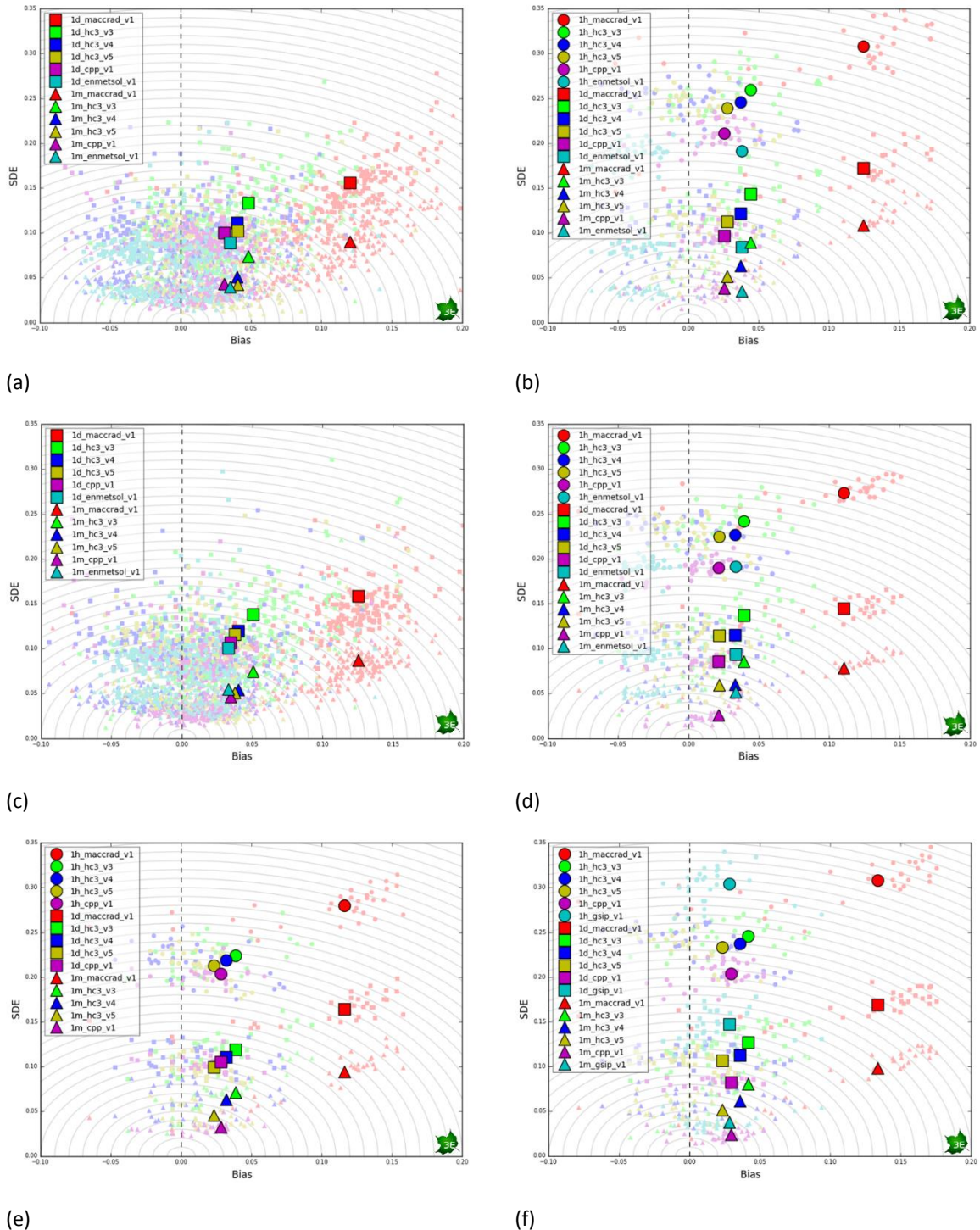


Figure 22: Error measures for the different models for hourly (circles), daily (squares) and monthly (triangles) irradiation in (a) 2012 all sites, (b) 2012 Netherlands only, (c) 2013 all sites, (d) 2013 Netherlands only, (e) 2011 Netherlands only and (f) 11 months from April 2014 to February 2015, Netherlands only.

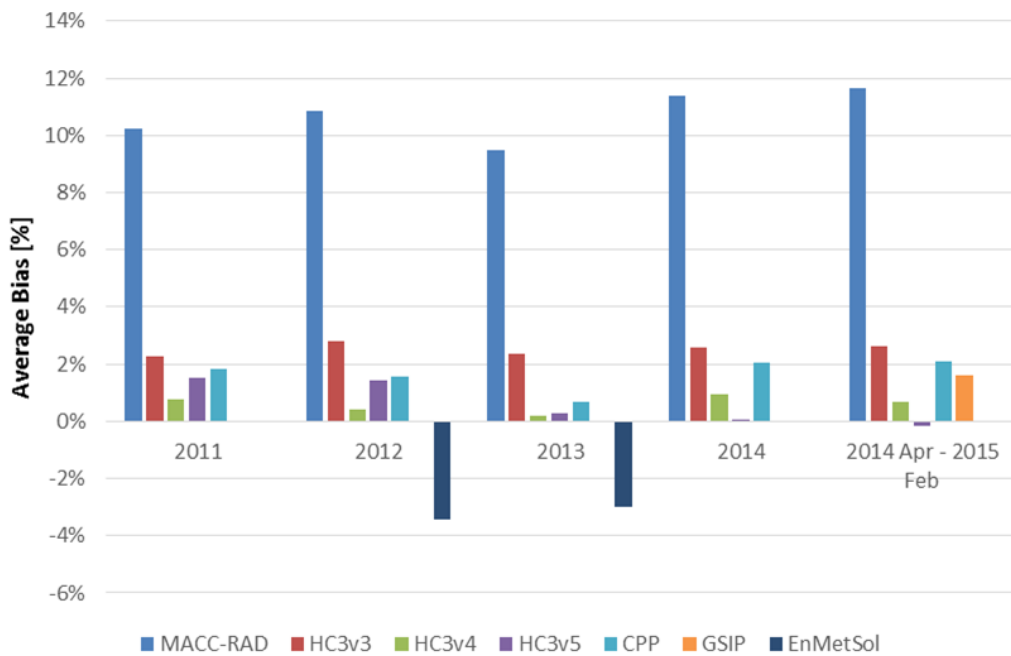


Figure 23: Arithmetic average bias over all stations in the Netherlands (31 meteorological stations) for the different models and years.

When comparing the results to on-site measurements, it is clear that on-site measurements with calibrated and well-maintained instruments will be much more precise than the satellite-based data. However, for first and second class pyranometers (ISO 9060 classification) as well as for silicon irradiance sensors as often used in small to medium size PV plants, the precision of the satellite services is generally comparable and sometimes even better than that of the on-site measurement.

The conclusions of this study highlight that satellite-based irradiation data are a valid and reliable reference for long-term yield estimates as computed by investors, installers and consultants during the design phase of a PV plant. Moreover, satellite-based irradiation data can also be used today as an alternative to on-site measurements for monthly and quarterly performance reporting for small to medium-size PV plants. In case of doubt, it is recommended to always evaluate the quality of the satellite data with ideally one or two years of data from a well-maintained meteorological station in the neighbourhood. For fault detection during PV plant operation hourly or daily resolution is required. Therefore, on-site sensors are the first choice as satellite data are less precise in this time scale. However, satellite-based irradiation data may be considered as back-up when the sensors fail or appear to be poorly maintained. Finally, satellite data may also serve to validate the proper calibration and configuration of irradiance sensors in case of doubt. Particularly for large deviations, cleaning needs or shadowed sensors, the satellite may spare the operator a site visit and can already indicate what is wrong.

3.3.2 Long-term trends of global horizontal irradiation

Solar resource assessments use solar irradiation data from past observations to estimate the average annual solar irradiation over the expected lifetime for a solar energy system. These assessments are typically based on the assumption that the long-term average annual solar irradiation from the past is not significantly different from the “true” climatological value and can therefore be used as an estimator for the availability of solar resources in the future (see e.g. [30][29]). Consequently, related uncertainties are considered to be negligible compared to other modelling uncertainties (e.g. [28]). However, solar irradiation at the Earth’s surface is not stable over time

for all locations on earth but may undergo significant long-term variations for particular regions, which is referred to as “global dimming and brightening”.

Evidence that solar irradiation incident on the Earth’s surface is not stable over time but is subject to long-term trends spanning multiple decades has been reported in numerous studies. A general decrease (“global dimming”) in surface solar irradiation at many observation sites from the beginning of widespread measurements in the 1950s up to the 1980s was followed by a partial recovery in surface solar irradiation at many of the sites since the mid-1980s, a phenomenon referred to as “brightening” [22][37]. Increasing and decreasing air pollution and associated aerosol loads, as well as their effects on clouds, are considered as major contributors to the dimming and brightening, respectively.

The selected period of historical data becomes highly relevant given these trends of irradiation, as illustrated in Figure 24 prepared by Müller et al. and also discussed more in depth in [24], where long-term irradiation measurement time-series made available by Germany’s meteorological institution Deutscher Wetterdienst (DWD) were analysed regarding dimming and brightening.

In Germany, the period 1951–2010 is clearly divided into a period of dimming, where the annual average global horizontal irradiance decreased, and a period of brightening, where the GHI increased. The turning point lies in the early 1980s. For the stations analysed, the calculated trend for the dimming period is $(-1.7 \pm 1.3) \text{ \%}/\text{decade}$, and the trend for the brightening period is $(3.3 \pm 1.6) \text{ \%}/\text{decade}$. The observed brightening trend is composed of an increase in the amount of direct irradiation, and a decrease in diffuse irradiation of smaller magnitude, as seen in data from 1991 to 2010. As the fraction of direct irradiance increases, the trends are amplified for tilted or tracked planes.

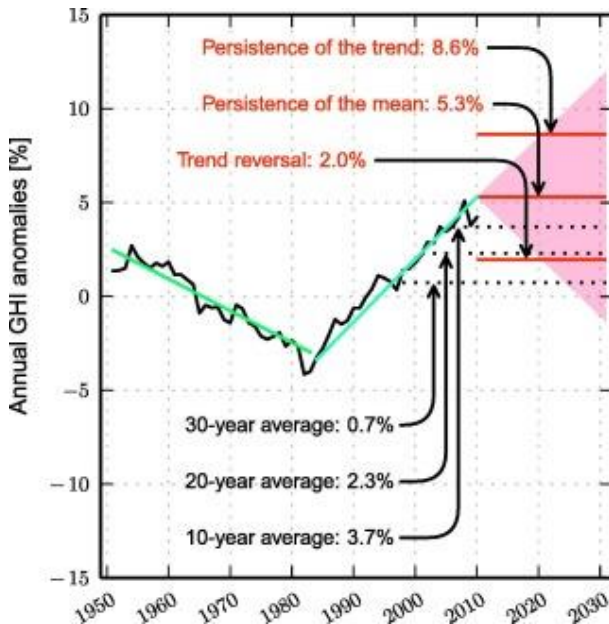


Figure 24: Different possibilities to estimate future solar resources as published in [24]. The moving average of the mean GHI anomalies (black) and the trend lines (green for the dimming period and blue for the brightening period) are shown together with the possible irradiance in the future. Future irradiance is indicated by the red plane, the mean values for the three scenarios are given as red lines. The trend of the mean anomalies used to derive scenarios 1 and 3 is 3.3% per decade (see text).

Figure 25 showcases an analysis that suggests the reported brightening effect to be of relevance for solar PV projects also at locations outside of Germany [37].

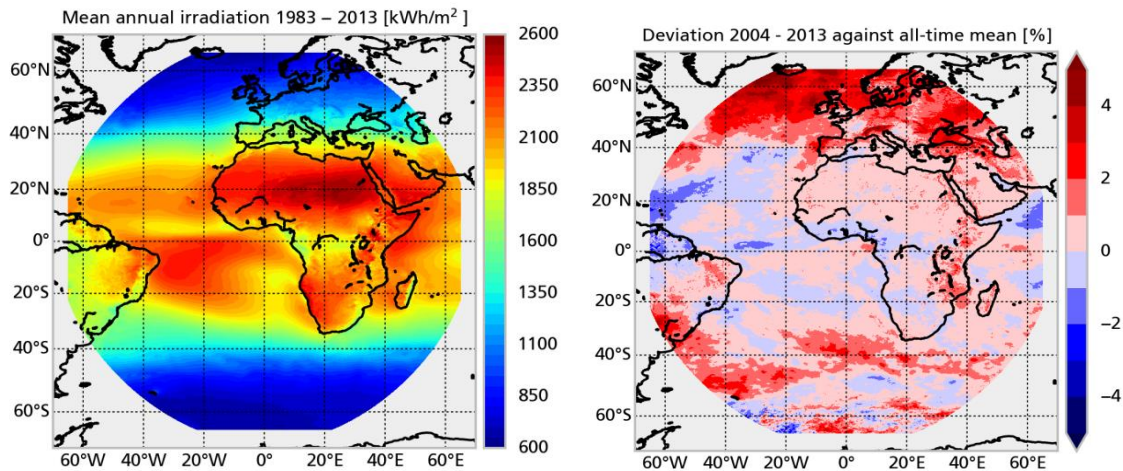


Figure 25: Visualization of potential irradiation trends using the openly available CM SAF SARAH data set of global horizontal irradiation [37].

These trends make it difficult to establish a representative or “true” long-term average value that could be used to predict future solar energy availability. In fact, historical data from Germany show that using the average global horizontal irradiance from the past to predict the average of the subsequent 20 years the dimming and brightening trends create an additional uncertainty of about 3%. This trend-related uncertainty is estimated to 4% to 5% for global irradiance in a 30° tilted, south facing plane, about 6% to 7% for global normal irradiance and to 15% for direct normal irradiance. These values represent significant additional uncertainties for solar resource assessments.

In the presence of these long-term trends, the question for solar resource assessments is no longer, what is the “true” climatological value, but what is the best predictor for the next 20 years. A suitable estimator should be a recent time period, that is long enough to filter the influence of single years with high anomalies, but which is short enough, to minimize the influence of past trends. Müller et al. propose to use the solar irradiance data of the 10 most recent years as a good compromise to fulfil these conditions [24].

Applying this methodology to current solar resource assessments in Germany today, we project about 3% higher global horizontal irradiance values and up to 5% higher irradiance in tilted planes compared to a 30-year average. For tracked planes or direct normal irradiance the differences are even higher. While we recognize the importance of avoiding overly optimistic solar resource assessments, we believe that this new approach will provide more appropriate predictions in general. While Müller et al. [24] focused on Germany, the conclusions should also apply in other parts of the world where substantial long-term variations have been observed, see Figure 25.

3.4 Conversion to tilted plane

The calculation to the plane of array irradiation for tilted and sun-tracking surfaces requires the availability of diffuse and direct irradiation values. However, these components are not always measured. Therefore, algorithms to split the global horizontal irradiation (GHI) into its components are often used. So, the conversion of GHI to the plane of array irradiance (GPOA) requires two major steps: first, the GHI is split into its components, i.e. horizontal diffuse irradiance and horizontal direct irradiance, by the use of a decomposition model; subsequently the diffuse, direct

and ground reflected irradiance components are transformed to the plane of array and recombined again in order to obtain GPOA.

Different combinations of decomposition methods and algorithms for the horizontal to plane of array conversion were evaluated using more than two years of five minutes data measurements from two well-maintained secondary standard pyranometers at a site in France. The first pyranometer is placed in the horizontal plane and the second pyranometer is facing south with an inclination of 25°. The evaluated decomposition models (from global to components) are: Erbs [38], Ruiz (G0 and G2 variations) [39] and Skartveit [40]. The evaluated algorithms for the horizontal to the plane-of-array conversion are: Isotropic [41], Hay [42], Muneer [43] and Perez [44]. Table 7 shows the validation results for the different algorithm combinations. For all combinations, an albedo of 0.2 and a turbidity of 2.0 are considered. Finally, the effective irradiance on the PV panel GPOA is calculated by applying the incidence angle modifier (IAM) to the plane of array irradiance as described in [45] and [46].

The validation shows that, for the analysed case, the highest overall accuracy was obtained using the Skartveit decomposition algorithm in combination with the Hay conversion algorithm (Table 7). The resulting normalized root mean square error (nrmse) is 4.8% for hourly resolution (Figure 26). Similar values are reported in literature as e.g. in [47] where 4.5% for the Perez model is reported and 5.4% for the Hay model. In [48], the authors highlight that the Hay and the Perez models have a very similar behaviour and that different results published in the literature may be influenced by, among others, the reflected component.

Table 7: Validation of the different algorithm combinations (analysed period: May 2010 to January 2013).

		Hay	Isotropic	Muneer	Perez
nrmse	Erbs	28.8%	28.8%	28.9%	18.7%
	Ruiz_G0	5.1%	5.8%	5.3%	6.3%
	Ruiz_G2	5.4%	5.4%	5.6%	6.4%
	Skartveit	4.8%	6.6%	4.8%	5.2%
nmbe	Erbs	-14.7%	-14.8%	-14.7%	-9.7%
	Ruiz_G0	1.1%	-1.3%	1.5%	2.7%
	Ruiz_G2	1.3%	-1.0%	1.7%	2.8%
	Skartveit	0.0%	-2.5%	0.4%	1.4%
nmae	Erbs	17.3%	17.3%	17.3%	11.3%
	Ruiz_G0	3.4%	3.8%	3.5%	4.3%
	Ruiz_G2	3.5%	3.6%	3.6%	4.3%
	Skartveit	3.0%	4.2%	3.1%	3.5%

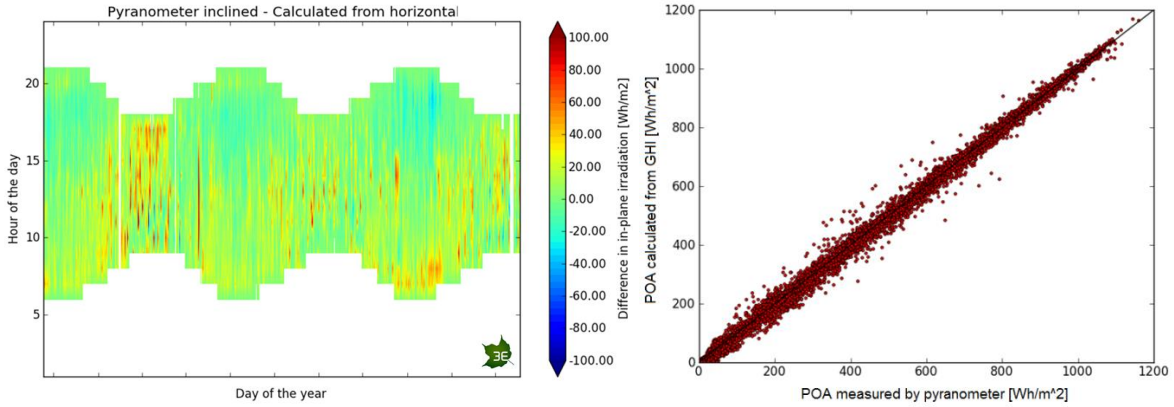


Figure 26: Carpet plot and scatter plot of the difference between the measured inclined irradiation and the irradiation calculated from the horizontal measurements using the selected model combination.

The Hay model is simpler than the Perez model and requires less input parameters. Therefore, it is often recommended in the literature to use the Perez model only when high quality weather files are available, as unreliable input data may potentially distort the output of the model. The newest version of the PVsyst software proposes to use the Perez conversion model as default. However, the users are informed that the Perez model usually gives yearly averages higher than the Hay model (up to 2% higher depending on the climate and the plane orientation).

3.5 Soiling

Energetic losses caused by soiling are currently among the most difficult ones to be quantified in PV energy yield predictions. This is reflected by the fact that no established physical model of PV soiling mechanisms currently exists, i.e., no specific model is applied in PV energy yield prediction studies judging the bankability of a project by any of the respondents of the LTYP reporting questionnaire, but only estimated monthly gross averages are used.

In addition to the current lack of effective soiling modelling methods, the global PV market has transitioned from being localized in the seasonally very rainy region of central Europe to more arid regions, with consequently much higher potential energy losses caused by soiling, unless soiling-limiting designs and/or module cleaning is appropriately implemented.

One part of the challenge to model PV soiling losses is attributable to the broad variety of parameters and effects that play a role in mechanisms governing soiling and de-soiling rates, respectively. On top of the sheer amount of influential parameters, some of the basic environmental input variables that affect soiling exhibit apparent contradictions in their influence on (de-)soiling rates, and also the time sequence of events is of relevance, as illustrated in the following.

One descriptive example of a contradictory influence is for the effects of wind speed; with high wind speeds being capable of cleaning soiled PV modules off dry dust, thus lowering soiling losses. Yet, high wind speeds can also lead to additional deposition of dirt and/or dust onto PV modules, since wind can transport dust and soil from nearby (or far away) locations, thus increasing soiling losses. Wind speed is therefore a poor predictor for soiling and de-soiling rates.

Also the time sequence of events are of importance: Whereas heavy rain events may effectively clean soiled PV modules, light rain or high humidity (e.g. morning dew) can lead to relatively wet and tenacious soiling compounds on the glass surface of PV modules. When such an effect is subsequently followed by a clear-sky day, the soiling compounds literally get cemented onto the glass substrate. This cemented soiling of PV modules is hardly to be cleaned by any wind. Also larger rain events are less likely to clean glass surfaces of this cemented soiling. From the modelling per-

spective, time sequences are even more complicated because pro-active cleaning of PV modules as an O&M activity will reset the soiling condition of a PV array artificially, which is also time-dependent and last but not least highly project-specific. It is clear from these examples that accurate predictions of energy losses associated with soiling of PV modules for time periods covering multiple decades can bring along significant uncertainty.

From a survey on LTYP best practises among PVPS Task 13 experts, a variety of answers is documented:

- The answers varied from the use of empirical values of soiling with a fixed derating factor to more comprehensive analysis including the combination of rainfall information, tilt angle, site specific information (e.g. pollution level) and cleaning practices.
- Differentiated climatic zones are not used by all participants to the survey. However assessment of local rainfall is performed by all.
- Generally only monthly factors based on rainfall and average humidity are used in the calculation.

As an example, Fraunhofer ISE has developed a simplified procedure to estimate overall energy losses associated with soiling in a deterministic and consistent manner. It has to be noted that the underlying assumption of this fairly simplistic procedure, outlined in Table 8, is that appropriate O&M cleaning schedules limit energy losses caused by soiling to acceptable levels.

Assuming appropriate O&M cleaning schedules, soiling losses are currently estimated by Fraunhofer ISE for lifetime PV yield predictions as outlined in Table 8 and uncertainties as stated in LTYP of Fraunhofer ISE are listed in Table 9. As listed, overall 9 climate regions of the Köppen-Geiger climate classification systems are distinguished in order to select, from a lookup table that is differentiated into three module tilt classes, the average annual energetic loss to be attributed to soiling. If project specific contractual obligations are in effect, the (maximum) soiling losses defined there will be used instead of the “default values” given in Table 8.

Table 8: Annually averaged soiling losses to be used as de-rate factors in LTYP simulations at Fraunhofer ISE as of 2016.

Climate classification (Köppen-Geiger)		Module tilt angle		
		below 5°	5° to 15°	above 15°
		Overall annual soiling loss [%]		
Tropics	A	1.0	0.5	0.5
Arid	B	4.0	4.0	4.0
Warm moderate	Cf	2.0	1.0	0.5
	Cs	2.5	1.5	1.0
	Cw	2.5	1.5	1.0
Snow	Df	2.0	1.0	0.5
	Ds	3.0	2.0	1.5
	Dw	3.0	2.0	1.5
Polar	E	—	—	—
Exceptional soiling sources		Decision on a by-case basis		

Table 9: Uncertainty attributed to annually averaged soiling loss to be included in the overall uncertainty calculation in LTYP at Fraunhofer ISE as of 2016.

	Estimated uncertainties for soiling losses [%] (assuming normal distribution)		
	below 5°	5° to 15°	above 15°
Module tilt angle			
Germany	1.0	1.0	0.5
Outside of Germany	2.0	2.0	2.0

3.6 Module efficiency

The DC energy yield of a PV module (Y_{DC}) depends on module characteristics as well as operating conditions. The principle for calculation used here is given below and works as follows: first, global broadband irradiation in plane of array (as measured by a pyranometer) is multiplied with the module STC efficiency to calculate the energy that would be produced at constant module efficiency. Then, the actual operating conditions are taken into account by multiplying a specifically determined factor representing the change of module efficiency at realistic compared to STC conditions.

$$Y_{DC} = \sum_{i=1}^N G_{POA,i} \eta_{STC} A_{\text{module}} f_i(AOI, \text{spectrum}, T, \text{module characteristics})$$

where N is the number of available time steps, G_{POA} is the irradiance in module plan, η_{STC} the module efficiency at STC, A_{module} the module area in m^2 , and f the factor for efficiency at operating conditions.

The efficiency change at time i represented by factor f_i depends on the combination of module characteristics and operating conditions. In practice, it is very difficult to determine the complete influence as a total, so that the different influencing effects (irradiance, temperature, etc.) are typically represented by one individual factor per effect. The influences are assumed to be independent. Furthermore, it is often useful to use the factors in integrated form, e.g. over one year. These assumptions lead to the following expression used for the calculation of DC yield in this section:

$$Y_{DC} = H_{POA} \eta_{STC} A_{\text{module}} f_{AOI} f_{\text{spectral}} f_G f_T$$

where H_{POA} is the irradiation (integrated irradiance over one year) in module plane in kWh/m^2 , η_{STC} the module efficiency at STC, A_{module} the module area in m^2 , f_{AOI} the relative influence due to angle-of-incidence (AOI) effects, f_{spectral} the relative influence due to the varying spectral irradiance, f_G the relative influence due to low light behavior, and f_T the relative temperature influence. Note that $\eta_{STC} A_{\text{module}} = \frac{P_{STC}}{1\text{W}/\text{m}^2}$, therefore the terms power and efficiency may be used redundantly in this section.

DC energy Y_{DC} depends on module size, and is thus of limited significance when it comes to comparing different module types. Other indicators like the module performance ratio (MPR) are more useful for this task. MPR is derived from the definition of the PV system performance ratio (PR), the only difference being that the DC power produced by a module constantly operated at its maximum power point is used instead of the final AC yield of the system.

$$MPR = \frac{Y_{DC}/P_{STC}}{H_{POA}/1\text{W}/\text{m}^2} = f_{AOI} f_{\text{spectral}} f_G f_T$$

MPR basically indicates how much of the energy that could be produced by a module with given nominal power at permanent STC conditions is actually produced. As MPR is not dependent on

total H_{POA} (just on the distribution of irradiance and temperature levels), it allows for comparison of modules at different locations. For this reason, *MPR* will be used for discussing results in this section.

In order to evaluate the significance of calculated MPR results, their uncertainty must be considered in the interpretation. Basic rules for the estimation of uncertainty are described in the ‘Guide to the expression of uncertainty in measurement’ GUM [49][50]. As the measurement equation used here is of simple structure, it is easy to calculate the combined uncertainty for MPR:

$$u_{\text{MPR}} = \sqrt{u_{f_{\text{AOI}}}^2 + u_{f_{\text{spectral}}}^2 + u_{f_{\text{G}}}^2 + u_{f_{\text{T}}}^2}$$

where u is the relative standard uncertainty for each influencing factor.

The calculation of the influencing factors and the uncertainty estimation in detail is described and discussed in the following subsections. All models and approaches that were used were chosen because they were readily implemented at Fraunhofer ISE, and partly have been used for many years. We point out that the focus of this section is to demonstrate general uncertainties in energy rating, not to compare or benchmark different models.

3.6.1 Angle of incidence effects

In general, the angle of incidence (AOI) factor f_{AOI} accounts for losses that occur due to reflection at AOI different from perpendicular irradiance. The magnitude depends on the AOI—and thus on the sun positions for the location under consideration and the selected tilt angle/orientation—as well as on the ratio of direct and diffuse irradiance at the location, and on module reflection characteristics. Measurement of module-specific reflection behaviour for full size modules is only now becoming a typical, readily available characterization. Results from literature show that there can be relatively large differences if modules with antireflective coating or structured glass are compared to standard-glass modules [51][52]. However, the modules looked at here all use standard glass for PV applications. Therefore, their reflection characteristics were not measured, as suggested by the IEC 61853-2 standard, but assumed to be equal and approximated by the characteristics of low-iron standard glass. These characteristics correspond to an “air–glass” configuration without soiling for the commonly used Martin and Ruiz model [53].

The module reflection losses are calculated with respect to this reflection characteristic separately for direct and diffuse irradiation. For losses in direct irradiation, the AOI on the plane of array and the module reflection behaviour are combined for each time step. Losses in diffuse irradiance are estimated to be 3.5% for all time steps which assumes that the diffuse part is isotropic, but can be approximated by using an average AOI between 50° and 60°.

Uncertainties in estimation of f_{AOI} are on the one hand due to the module characteristics: in the case here, the actual reflection characteristics can differ from the assumed standard behaviour, and in case the characteristics were measured, measurement uncertainty would have to be accounted for. On the other hand, the uncertainty is due to the assumption of an isotropic distribution of diffuse irradiance, which will mostly add to the overall uncertainty at locations with high shares of diffuse irradiance. The uncertainty for f_{AOI} is roughly estimated to be 1% for all locations and modules, which should be analysed in more detail in the future.

3.6.2 Spectral effects

Spectral effects correspond to gains or losses in the performance of a photovoltaic module or system due to the solar spectrum shape impinging on the active surface. In particular, this effect increases when the spectral shape of the incident solar irradiance differs from the standard spectrum called ASTM G173-03 AM 1.5. Spectral effects play a minor role with respect to temperature and irradiance effects, but should not be neglected. In fact, several authors have studied this topic

in recent years and quantified gains or losses in several locations on a monthly or annual time basis. Just to cite some results and with no aim to fully cover this topic, Alonso-Abella et al. [54] quantified spectral effects on amorphous silicon-based PV systems to vary between -16% and $+4\%$ and between -3% and $+6\%$ on a monthly basis for, respectively, Stuttgart (Germany) and Tamanrasset (Algeria). On a yearly basis, this turns into -0.35% and $+2\%$ for the two locations.

Different indexes are used to quantify spectral effects on photovoltaic systems, like the Average Photon Energy *APE*, the average wavelength λ_{ave} and the spectral mismatch factor *MM*. The latter is defined as:

$$MM = \frac{\int_c^d G_{ref}(\lambda) SR_{ref}(\lambda) d\lambda}{\int_c^d G_{in}(\lambda) SR_{ref}(\lambda) d\lambda} \cdot \frac{\int_a^b G_{in}(\lambda) SR_{dut}(\lambda) d\lambda}{\int_a^b G_{ref}(\lambda) SR_{dut}(\lambda) d\lambda}$$

where $G_{in}(\lambda)$ is the incoming solar spectrum (either measured or simulated), $G_{ref}(\lambda)$ is the ASTM G173-03 AM 1.5 standard spectrum, $SR_{dut}(\lambda)$ is the spectral response of the PV device being tested and $SR_{ref}(\lambda)$ is the reference spectral response, i.e. the spectral response of the device measuring the reference spectrum. If this is a pyranometer, with spectral response curve compared to quartz glass, $SR_{ref}(\lambda)$ is assumed equal to 1 for every wavelength and the previous becomes:

$$MM = \frac{\int_c^d G_{ref}(\lambda) d\lambda}{\int_c^d G_{in}(\lambda) d\lambda} \cdot \frac{\int_a^b G_{in}(\lambda) SR_{dut}(\lambda) d\lambda}{\int_a^b G_{ref}(\lambda) SR_{dut}(\lambda) d\lambda}$$

Integration limits c and d must include the reference spectral response, while a and b are integration limits that must include the spectral response of the PV device. MM higher than 1 corresponds to spectral gain compared to STC, while MM lower than 1 corresponds to spectral loss.

The study of Belluardo et al. [55] focuses on the calculation of the uncertainty of the spectral mismatch factor on seven different photovoltaic technologies: monocrystalline (mc-Si) and polycrystalline (pc-Si) Silicon, double junction amorphous Silicon (a-Si), Copper Indium Gallium Selenide (CIGS), Cadmium Telluride (CdTe), organic cell (organic) and Copper Zinc Tin Sulfide (CZTS). The spectral response SR of the investigated technologies has been measured in laboratory and is shown in Figure 27.

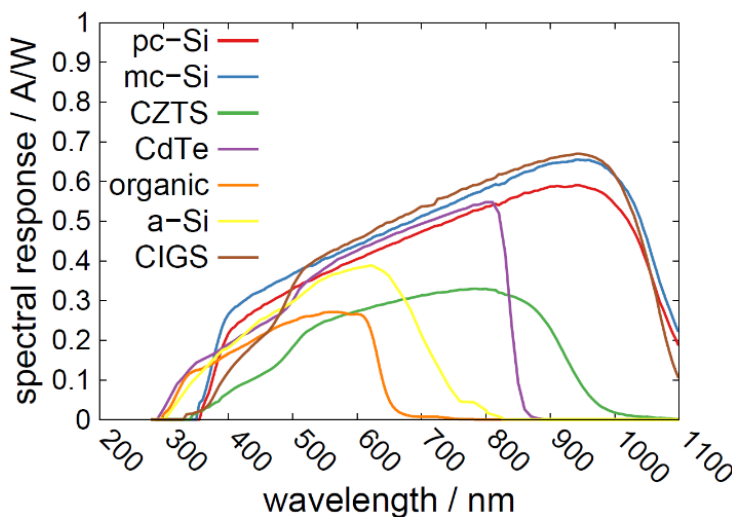


Figure 27: Spectral response of the seven investigated technologies [55].

According to the last equation for MM, and under the hypothesis of neglecting the uncertainty of the measurement of SR, only the contribution of the uncertainty of the incoming spectrum $G_{in}(\lambda)$ affects the uncertainty of MM. The uncertainty of MM has been calculated using the Monte Carlo technique. First, a statistically significant number of spectra (in this case, 500) has been simulated using the tool *SDISORT*. Each of the spectra has been generated using a set of input parameters,

i.e. atmospheric and geometric parameters, randomly retrieved according to the specific Probability Density Distribution of their error and a reference set of value, both set by the authors. In particular, the reference set corresponded to the atmospheric conditions recorded at Kanzelhöhe observatory (Austria) at 10 AM (UTC) on April 25th, 2013. Once the 500 spectra have been obtained, the corresponding values of MM have been calculated. The pool of values has been therefore analysed in a statistical way in order to calculate its standard deviation, its mean value and the ratio of the two, which corresponds to the relative uncertainty of MM.

Table 10: Values of relative uncertainty for seven different PV technologies, for the reference case, and for the cases ensuring the minimum and maximum levels of uncertainty.

	Relative uncertainty of MM (values in %)		
	Reference	Min	Max
mc-Si	0.08	0.01	2.13
pc-Si	0.08	0.01	2.16
a-Si	0.19	0.03	7.16
CIGS	0.08	0.01	2.14
CdTe	0.15	0.01	4.61
Organic	0.23	0.04	9.45
CZTS	0.11	0.01	3.56

An extension of the analysis to all the possible sets of atmospheric conditions which are different from the reference ones defined above requires that different values and combinations of input parameters have been considered in order to define minimum and maximum levels of uncertainty. Results are shown in Table 10. In general, the uncertainty of MM strictly depends on the technology. The reference case is much closer to the minimum limit than to the maximum limit. In general, technologies with a narrower spectral response (e.g. organic and a-Si) are affected by a higher level of relative uncertainty that might theoretically reach 9%. On the other hand, technologies with a broader spectral response show lower levels of relative uncertainty, with a limit around 2% for monocrystalline- and polycrystalline silicon, and CIGS.

3.6.3 Irradiance level

For modelling the module performance at irradiance (and temperatures) different from STC various models are available. For the simulations within this section, the efficiency model developed by Heydenreich [56] was used:

$$\eta(G, T_{\text{STC}}) = a G + b \ln(G + 1) + c \left(\frac{\ln^2(G+e)}{G+1} - 1 \right)$$

where G is the irradiance, T_{STC} is 25 °C, η the module efficiency at specific conditions, and a , b , c are free or fitting parameters, describing among others the low light behaviour.

This model is a simple efficiency model, which is capable of reproducing the low light behaviour for all relevant PV technologies sufficiently well based on data sheet values or measured module efficiencies. The parameters a , b and c are determined from measured module characteristics by a least square fitting procedure. Modelled and measured efficiencies show good agreements, with slightly higher deviations up to 2% to 3% at irradiance levels below 200 W/m² (see Figure 28). These deviations at very low irradiance levels are however not considered to be energetically relevant for calculations of annual influencing factors.

The influence on produced energy is calculated for each time step, using the irradiance after reflection losses, in order to obtain the factor f_G :

$$f_G = 1 - \frac{\sum_{i=0}^N G_i (\eta_{STC} - \eta(G_i, T_{STC}))}{\sum_{i=0}^N G_i \eta_{STC}}$$

where G is the irradiance, η the module efficiency at specific conditions, and N is the number of available time steps.

An important contribution to the uncertainty of irradiance related influences is the measurement uncertainty inherent in PV module low light behaviour determination. It must be considered that measurement uncertainties depend on the target conditions for the measurement, as simulators generally are optimized for measurements at STC. How measurement uncertainties propagate to f_G was estimated using the approach described in [57]. As shown in Figure 28 for two examples, the sensitivity of f_G on the input low light behavior was evaluated by calculating f_G using a set of different low light curves as follows: the originally measured data, and modified data to express the worst-case effects of measurement uncertainty. For simplification, only 3 data points were actually used for the modified sets: the 1000 W/m² value for reference, the 600 W/m² and the 200 W/m² value. The relative measurement uncertainty for the latter two was estimated specific to the PV technology being studied, resulting in 0.5% at 600 W/m² and 1% at 200 W/m² for crystalline silicon modules. For thin film modules, the uncertainty is 1% and 2% respectively. Note that the absolute uncertainty at 1000 W/m² is not relevant as the 1000 W/m² value is used for normalizing the low light curves. The variability between modules of one type is usually smaller than the measurement uncertainty, so that it is not included as an extra contribution here (whenever high variability is observed in a specific case, however, it should be included).

The irradiance factor uncertainty was assumed conservatively to have a rectangular distribution, with a width equal to the difference between highest and smallest influence calculated from the different cases as mentioned above. It was found that the uncertainty of the factor f_G does not significantly vary between the different module types, but with the site-specific conditions: the larger the share of low light conditions, the higher the uncertainty. The most important influence is the relative measurement uncertainty, which is directly proportional to the factor's uncertainty.

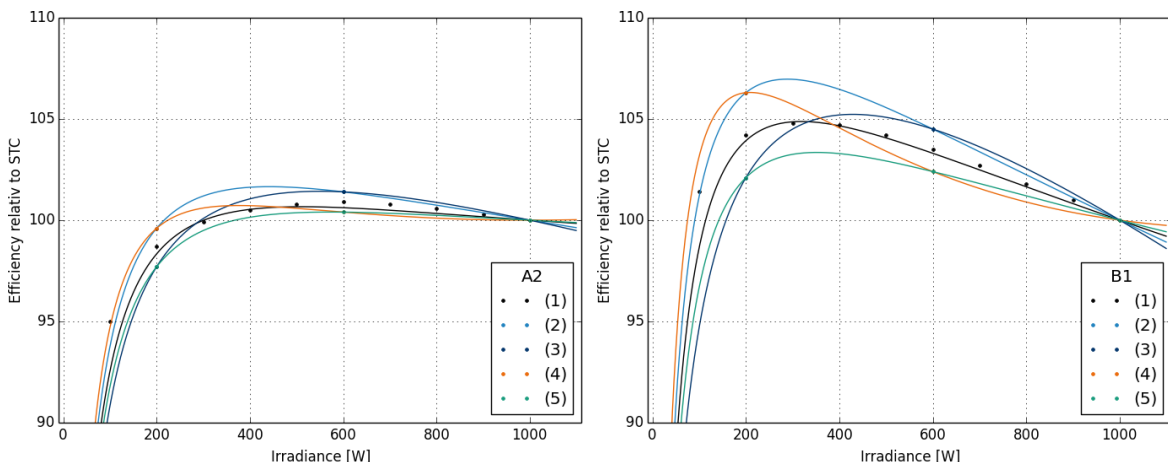


Figure 28: Example for the different curves for uncertainty estimation (left: c-Si with uncertainty u of efficiency at 600 W/m² and 200 W/m² of 0.5% and 1%, respectively, right: CdTe, uncertainty 1% and 2% respectively). The five curves are: (1) as measured, (2) $(1+u) \eta_{200}$ and $(1+u) \eta_{600}$, (3) $(1-u) \eta_{200}$ and $(1+u) \eta_{600}$, (4) $(1+u) \eta_{200}$ and $(1-u) \eta_{600}$ (5) $(1-u) \eta_{200}$ and $(1-u) \eta_{600}$.

3.6.4 Temperature

For modelling the module performance at temperatures different from STC, often a simple linear dependency is used:

$$\eta(G, T_{\text{mod}}) = \eta(G, T_{\text{STC}}) (1 + \gamma(T_{\text{mod}} - T_{\text{STC}}))$$

where T_{mod} is the module temperature, T_{STC} is 25 °C, and γ the temperature coefficient of module efficiency (or power). Accordingly, the factor f_T is calculated as follows:

$$f_T = 1 - \frac{\sum_{i=0}^N G_i (\eta(G_i, T_{\text{STC}}) - \eta(G_i, T_{\text{mod},i}))}{\sum_{i=0}^N G_i \eta(G_i, T_{\text{STC}})}$$

As with the irradiance dependency, an important contribution to uncertainty of temperature related influences is the measurement uncertainty of the temperature coefficient (TC) determination. For temperature influence f_T the calculation was performed using the temperature coefficient as measured and multiplied with 0.9, 0.95, 1.05 and 1.1 (corresponding to a measurement uncertainty of 5% and 10%). As was to be expected, the uncertainty propagates linearly to f_T , so that the relative TC uncertainty is equal to the relative f_T uncertainty. We assume TC uncertainty to be 10% for all technologies for simplicity.

4 Effects of uncertainty

After a discussion of uncertainties in measurements (Section 2) and in modelling (Section 3), the combination of the knowledge gained shall be demonstrated with two examples.

One example deals with the uncertainty of PV module energy rating, i.e. the question, whether the expected differences in performance between two module types are bigger than the associated error margins. This is a direct continuation of the investigation in Section 3.6, the full work is documented in [58].

In a second step, a framework for the calculation of uncertainty for a complete Long Term Yield Prediction is presented. As the simplified error propagation approach of the first example is not suitable for a complex LTYP, a Monte-Carlo simulation is used here instead.

4.1 Uncertainty in module energy rating

PV modules are rated and sold according to their STC power, even though the energy they produce during their lifetime is decisive for the return on investment. Consequently, scientists have worked on procedures to rate PV modules according to their output energy (or energy yield) rather than STC power for several decades (see e.g. [59][60]). These procedures are usually referred to as “energy rating”. The aim of energy rating in general is to enable a significant differentiation between PV modules according to their yield for typical locations, so that users have better information for selecting the optimal module type for their purposes.

These past efforts are now integrated in the series of standards IEC 61853, which aims to establish “IEC requirements for evaluating PV module performance based on power (watts), energy (watt-hours) and performance ratio”. Part 1, which deals with power rating measurements, i.e. *I-V* curve measurements for PV modules at different irradiance and temperature levels, is already a valid standard. Part 2 for determination of angle of incidence (AOI) effects, spectral response and operating temperature is in press. Part 3 for energy rating calculation methods and part 4 for standard weather data sets covering different climatic regions are in earlier stages of development.

The parts of the standard are consistent with the basic steps of energy rating, which can be very briefly summarized as follows:

- Obtain module characteristics – first of all STC power, then irradiance dependency, temperature coefficients and sometimes also spectral response, angular response and typical operating temperature. As energy rating is aimed at differentiating modules, the module characteristics are the most important input data.
- Obtain reference weather data – In energy rating, weather data plays the same role as standard conditions for module power measurement, even though for energy rating, the reference conditions are much larger data sets. The reference weather data must be comprised of first the weather of specific climates, and second assumption regarding the operating situation, such as module tilt and orientation. As predefined and standardized reference weather data sets are not yet available, alternatively ground-measured data, typical meteorological years (TMY) or location-specific data from one of many weather data bases can be used. Weather data should at least contain irradiance and temperature; spectral irradiance, wind or humidity are rarely available. Suggestions for development of reference data sets for energy rating are given in [61].
- Simulate the energy that the module type under scrutiny will produce under the conditions described by the selected weather data set.

These steps are also part of yield predictions for PV systems, which however cover system-related influences like shading or electrical losses additionally. Yield predictions aim at giving a very realistic indication of the energy yield over the expected system lifetime, and thus also include assumptions for degradation. Therefore, the predicted specific yield for a module will always be larger than that for a PV system.

The uncertainties inherent in yield predictions and module energy rating are consequently of different nature: solar resource assessment is a major contribution to uncertainty for yield predictions, see Section 3.3 for more details and Section 4.2 for a complete assessment. In energy rating, the dominating uncertainties come with module characterisation, and the results of Section 3.6 are used here in an exemplary manner.

4.1.1 Module characteristics

In order to illustrate the range of different module characteristics and implications on energy rating uncertainty, a data set representing eight module types was selected from real-life measurements performed in Fraunhofer ISE's module calibration laboratory CalLab PV Modules. The data are shown in Table 11, Figure 29 (irradiance and temperature dependence) and Figure 30 (spectral response). The number of modules measured per type varied from 1 to 5. The variability of module characteristics within one type generally depends on the module type, and is, according to the author's experience, often smaller than associated measurement uncertainties. Therefore, we do not include variability quantitatively in the calculations and uncertainty analysis in this investigation. The shown examples are realistic, but do not represent a specific technology or module type in general – especially for thin film technologies, variety in behaviour can be observed even within one technology (e.g. CdTe, CIGS, ...).

Also, a so called reference data set was derived from measurements in CalLab PV Modules in 2013. The reference is the median of about 100 measurements of irradiance dependency and 100 measurements of temperature dependency.

4.1.2 Meteorological data

For the calculations in this investigation, *SolarGIS* time series data were used for three locations. Basic requirements for energy rating data sets as established by Huld et al. were followed [61]. The time series includes global and diffuse horizontal irradiance and ambient temperature data in a 15 minute resolution. 10 years of input data are used to compute the mean annual DC energy, instead of using a TMY. The locations correspond to the regions defined in [61] as given in Table 12 along with other details.

Irradiation in the plane of array can be calculated straightforward using geometrical relations for the direct part. Diffuse in-plane irradiance is calculated using the model by Perez et al. [62]. The albedo of the surrounding was selected to be a fixed value of 0.2, a usual simplification whenever the local albedo is not known or measured. We furthermore assumed that the modules are oriented due south at an inclination angle of 25°.

Module temperature, which is the crucial influencing factor for calculation of temperature influence, was estimated from the ambient temperature given in the *SolarGIS* time series using an irradiance-dependent offset of 25 K at STC irradiance:

$$T_{\text{mod}} = T_{\text{amb}} + 25K \frac{G}{1000 \text{W/m}^2}$$

where T_{mod} is module temperature, T_{amb} is ambient temperature, and G is irradiance in module plane.

Table 11: Module types used in this investigation.

ID	Technology	ID	Technology
A1	c-Si	B2	CdTe
A2	c-Si	C1	CIGS
A3	c-Si / high efficiency	C2	CIGS
B1	CdTe	D	a-Si

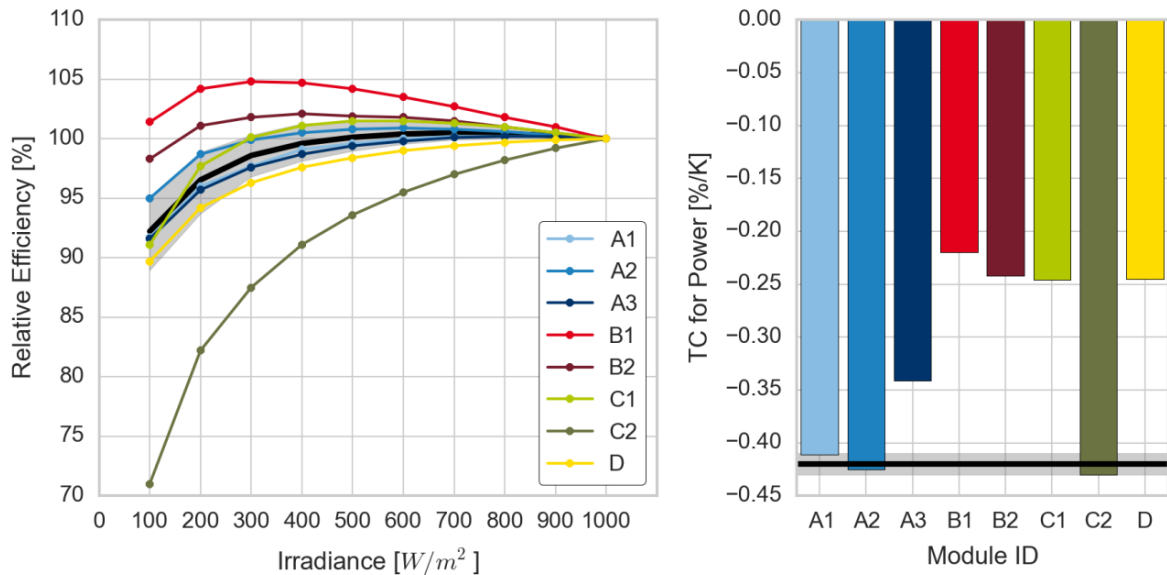


Figure 29: Irradiance dependency and temperature coefficient of the efficiency for eight selected module types. The black line shows the median value for crystalline silicon modules measured at Fraunhofer ISE's CalLab PV Modules in 2013 (~100 measurements for temperature dependency and ~100 for irradiance dependency); the grey area indicates the typical range (5th to 95th percentile).

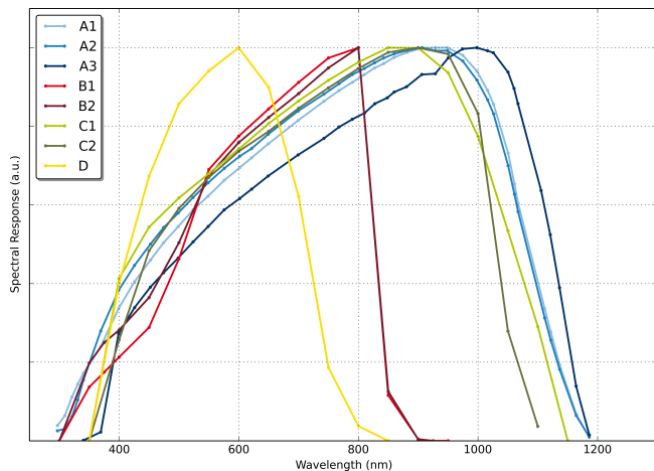


Figure 30: Spectral response of the selected module types (350 nm data point for C1, C2 and D is extrapolated).

Table 12: Selected locations and relevant information characterizing their climate.

Location	Lat.	Lon.	Elev. m.a.s.l.	G_{HOR} kWh/m ²	T_{AMB} avg.	Region in [61]
1 Norwich, UK	52.7	1.1	54.0	978	10.3	2
2 Breisach, Germany	48.0	7.6	188.0	1216	9.8	3
3 Rafah, Egypt	31.2	34.3	87.0	1876	20.7	~ 5

4.1.3 Module performance ratio and uncertainty

Detailed results for calculated influencing factors, *MPR* and uncertainties are presented in Table 13 and Table 14. Figure 31 presents results for the *MPR*, including error bars that represent the associated uncertainties. For location 1, the *MPR* values range from 88% to 101%, with a reference value of 95.5%. With increasing temperature, they drop to roughly 87.6% to 98% for location 3 (91.0% for the reference). The results correspond to what can be expected from module characteristics: the module types B1 and B2, which have both good low light behaviour and low temperature coefficients perform well at all locations. Module type C2 with worst low light behaviour and largest (but still average) TC performs worst at all locations. The example of C2 also shows that at a high-irradiance and high-temperature location, the low light behaviour is not irrelevant: C2 has a significantly lower performance compared to A1 and A2, which have a similar temperature coefficient but better low light behaviour. On the other hand, at a low-irradiance location like location 1, good low light behaviour is essential, but the temperature coefficient does hardly make a difference (compare A1, A3, D at location 1). The positive effect of low temperature coefficient on *MPR* is visible for module type D with about average low light behaviour: it performs level with the c-Si types for location 1 and 2, but outperforms them at location 3.

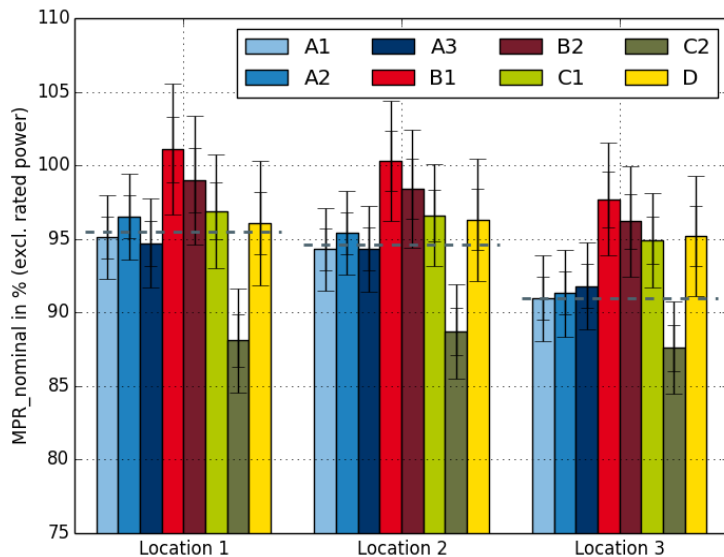


Figure 31: Module Performance Ratio (*MPR*) for eight different module types and three locations from different climates (broad caps of error bars indicate expanded uncertainty, narrow lines in the middle of the error bars indicate standard uncertainty).

Table 13: Energy Rating input data, results and uncertainty for all locations.

Norwich	A1	A2	A3	B1	B2	C1	C2	D	Ref.
$f_{AOI} [\%]$	-3.1	-3.1	-3.1	-3.1	-3.1	-3.1	-3.1	-3.1	-3.1
$f_{\text{spectrum}} [\%]$	1.4	1.4	1.1	2.4	2.4	1.4	1.5	3.4	1.4
$f_G [\%]$	-2.6	-1.2	-2.8	2.2	0.1	-1.0	-9.6	-3.7	-2.2
$f_T [\%]$	-0.7	-0.6	-0.6	-0.3	-0.4	-0.4	-0.9	-0.4	-0.7
MPR [%]	95.1	96.5	94.7	101.1	99.0	96.9	88.1	96.1	95.5
Exp. Uncert. [%]	3.0	3.0	3.2	4.4	4.4	4.0	4.0	4.4	
Breisach	A1	A2	A3	B1	B2	C1	C2	D	Ref.
$f_{AOI} [\%]$	-2.7	-2.7	-2.7	-2.7	-2.7	-2.7	-2.7	-2.7	-2.7
$f_{\text{spectrum}} [\%]$	1.4	1.4	1.1	2.4	2.4	1.4	1.5	3.4	1.4
$f_G [\%]$	-2.0	-0.8	-2.1	1.9	0.2	-0.6	-7.5	-2.9	-1.6
$f_T [\%]$	-2.5	-2.5	-2.0	-1.3	-1.4	-1.5	-2.8	-1.5	-2.5
MPR [%]	94.3	95.4	94.3	100.3	98.4	96.6	88.7	96.3	94.6
Exp. Uncert. [%]	3.0	3.0	3.1	4.1	4.1	3.6	3.6	4.3	
Rafah	A1	A2	A3	B1	B2	C1	C2	D	Ref.
$f_{AOI} [\%]$	-2.3	-2.3	-2.3	-2.3	-2.3	-2.3	-2.3	-2.3	-2.3
$f_{\text{spectrum}} [\%]$	1.4	1.4	1.1	2.4	2.4	1.4	1.5	3.4	1.4
$f_G [\%]$	-0.7	-0.1	-0.9	1.7	0.6	0.3	-4.0	-1.3	-0.5
$f_T [\%]$	-7.5	-7.8	-6.2	-4.0	-4.4	-4.5	-8.0	-4.5	-7.7
MPR [%]	91.0	91.3	91.8	97.7	96.2	94.9	87.6	95.2	91.0
Exp. Uncert. [%]	3.2	3.2	3.2	3.9	3.9	3.4	3.6	4.3	

Table 14: Uncertainty of influencing factors depending on module type and location (standard uncertainty, $k=1$).

Norwich	A1	A2	A3	B1	B2	C1	C2	D
$u_{f_AOI} [\%]$	1.0	1.0	1.0	1.0	1.0	1.0	1.0	1.0
$u_{f_spectral} [\%]$	0.9	0.9	1.0	1.4	1.4	1.0	1.0	1.8
$u_{f_G} [\%]$	0.7	0.7	0.7	1.4	1.4	1.4	1.4	0.7
$u_{f_T} [\%]$	0.1	0.1	0.1	0.0	0.0	0.0	0.1	0.0
$u_{MPR} [\%]$	1.5	1.5	1.6	2.2	2.2	2.0	2.0	2.2
Breisach	A1	A2	A3	B1	B2	C1	C2	D
$u_{f_AOI} [\%]$	1.0	1.0	1.0	1.0	1.0	1.0	1.0	1.0
$u_{f_spectral} [\%]$	0.9	0.9	1.0	1.4	1.4	1.0	1.0	1.8
$u_{f_G} [\%]$	0.6	0.6	0.6	1.1	1.1	1.1	1.1	0.6
$u_{f_T} [\%]$	0.2	0.3	0.2	0.1	0.1	0.1	0.3	0.1
$u_{MPR} [\%]$	1.5	1.5	1.5	2.0	2.0	1.8	1.8	2.1
Rafah	A1	A2	A3	B1	B2	C1	C2	D
$u_{f_AOI} [\%]$	1.0	1.0	1.0	1.0	1.0	1.0	1.0	1.0
$u_{f_spectral} [\%]$	0.9	0.9	1.0	1.4	1.4	1.0	1.0	1.8
$u_{f_G} [\%]$	0.4	0.4	0.4	0.8	0.8	0.8	0.8	0.4
$u_{f_T} [\%]$	0.8	0.8	0.6	0.4	0.4	0.4	0.8	0.4
$u_{MPR} [\%]$	1.6	1.6	1.6	1.9	1.9	1.7	1.8	2.1

Amongst the relative influences, there are two aspects worth discussing: on the one hand, which influencing factors are largest, i.e. have the highest impact on absolute *MPR*, and on the other hand, which factors vary most between different modules, i.e. have the highest impact on the rating. Note that only irradiance and temperature dependence and in part spectral impact (location-independent values were used) can be evaluated here. AOI losses were calculated using a generic reflection characteristic for all modules, so that they do not contribute to the difference.

With a magnitude of 2% to 3%, AOI losses are usually the largest or second-largest influence on *MPR* for the locations analysed here. This demonstrates that further research aimed at reducing AOI losses and improving the simulation of these losses is useful. Spectral influences are moderate in magnitude, and contribute moderately to the difference between modules. Irradiance-related influences are the larger when the share of low irradiance levels at a location is large; and/or when the low light efficiency is low. Therefore, their absolute influence on *MPR* highly depends on location and module type. However, in terms of contribution to the differences between the module types, irradiance influences are most important with disregard of location. Temperature influences are largest and contribute stronger to the difference at a hotter location.

The standard and expanded uncertainty is indicated in Figure 31 for each result by error bars with narrow caps in the middle, and broad caps at the ends, respectively; and the further is given in numbers for each factor in Table 14 (expanded uncertainty is calculated here by multiplying standard uncertainty with a coverage factor $k=2$). Expanded uncertainty means that the true value of the measurand lies within the range indicated by result and uncertainty limits (e.g. Figure 31, right side: *MPR* of A1 at location 1: $93.5 \pm 3.7\%$) with a probability of 95%. For the standard uncertainty range, the probability is 68%.

4.1.4 Energy rating under consideration of uncertainty

The results presented above give important insights in energy production of PV modules, but are too comprehensive to allow for quickly capturing them—especially for more or less unexperienced customers like residential home owners. Therefore, we suggest establishing a simple module classification based on the deviation of each module type's performance from the reference value.

For interpretation of the *MPR* values including uncertainty information, a procedure similar to the one in [15] is used. Each individual result is compared to the reference value, and the difference is divided by the individual result's uncertainty to calculate a 'z-score':

$$z = (MPR_i - MPR_{ref}) / u_{MPR_i}$$

where *MPR* is the module performance ratio of the module type under scrutiny, u_{MPR} the associated uncertainty, and MPR_{ref} the module performance ratio obtained with the reference characteristics.

If the z-score is larger than 2, the deviation of predicted energy/performance ratio per module is larger than the expanded uncertainty, which means there is a significant difference and we can be sure the module type outperforms the reference data set. In Figure 31, this is easily visible from the error bar not crossing the indicated reference value. If the z-score is smaller than 1, this means the difference is smaller than the standard uncertainty and thus not significant. The modules can be looked at as essentially equal regarding their performance at the specific location (in the figures: the error bar crosses the average line within half its length).

If the z-score is in between 1 and 2, the situation is not clear, and there is a certain probability for the modules being equal or different in their actual performance (the error bar crosses the average in the outer quarters of its length).

Following this approach, five qualitative ranking levels can be defined: ++ or -- for module types that differ significantly from the reference performance ($|z| > 2$); (+) or (-) for modules with a slight

trend to differ from the reference ($2 > |z| > 1$), and ‘o’ for modules that do not significantly differ from reference performance ($|z| < 1$).

A limitation of this approach is that the rating as suggested above does not give continuous results, which may seem arbitrary in places. This objection could be met by displaying the result graphically, as shown exemplarily for two module types in Figure 32. The y-axis represents the calculated z-score, but does explicitly name only the rating result, while the markers indicate the exact z-score numbers. MPR values and uncertainties were used as given in Table 13.

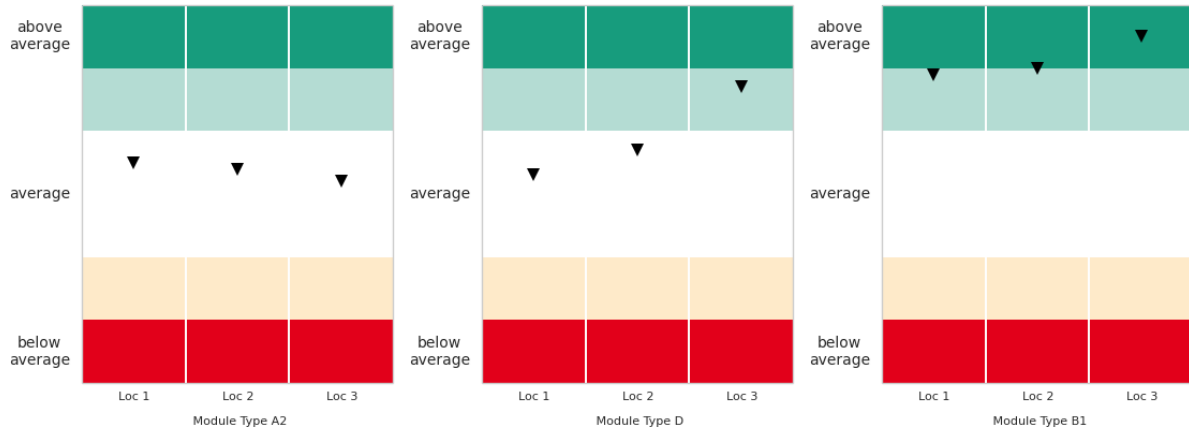


Figure 32: Exemplary energy rating result as it could be included on a data sheet as qualitative information of the module type in question. Location 1, 2, and 3 correspond to England, Southern Germany and Egypt. Module type A2 is a typical crystalline silicon module type, module type D has a lower-than-average temperature coefficient and average low light behaviour, module type B1 has both above-average temperature coefficient and low light behaviour. The vertical axis represents the z-score calculated with MPR and uncertainties as presented above.

The results show that significant energy rating is possible already today, at least if a module reference data set is available, if the modules show typical degradation, and the difference from reference energy yield is evaluated for the rating. In summary, energy rating can already be useful for a number of reasons, but its full opportunities will only come to life after the IEC 61853 standard is finalized. The work presented here can be helpful in this process and includes a method suitable for being used as part of the standard.

4.2 A framework to calculate yield prediction uncertainties

4.2.1 Introduction

Up to now, there is no standardized uncertainty framework for lifetime energy yield predictions available. Furthermore, there is a lack of definitions in this field, so as to make sure, we are talking about the same concepts. For this reason it is difficult for financers, investors and other stakeholders to compare uncertainty assessments for yield predictions.

Furthermore, up to now often just an initial yield and the P90 of the initial yield as well as the average yield over the assumed lifetime of the system and the P90 of the average yield are given. These numbers may not be adequate to feed financial models taking effects of degradation and dimming and brightening trends including their uncertainties into account. The same applies to influences from inter-annual variations and the time they need to cancel out.

The aim of this section is to develop a method to “handle” all sources of uncertainties influencing lifetime energy yield predictions and to present the information needed to feed financial models with time dependent yield estimates and exceedance probabilities as desired by investors or

stakeholders. This method can be seen as a part of “a common framework that can assess the impact of technical risks on the economic performance of a PV project” [63].

4.2.2 Definitions

To be clear in this discussion, we should define some terms in advance. First of all, yield is used as synonym for energy production.

Lifetime Energy Yield Prediction

A lifetime energy yield prediction is an estimate of the total energy production for a PV system at a specific site. The primary aim is to predict the energy production for the Prediction Period. State of the art yield predictions can be partitioned in three main parts (see Section 3.1) and should comprise an analysis of uncertainties for the Predicted Yield:

1. Assessment of the solar resource and other meteorological quantities for the Reference Period as well as the generation or selection of the best possible time series to describe meteorological conditions for this period
2. Simulation of the PV system energy output based on modelling and parametrization of the actual PV system and using the meteorological time series from 1) (calculation of Predicted Reference Yield)
3. Estimation of long-term changes in energy yield over the Prediction Period and application of these changes to Predicted Reference Yield from 2) to determine the Predicted Yield

Predicted Reference Yield

The best estimate of the mean annual yield for the PV system under consideration within a reference period in the past. This yield is calculated using a simulation program, best estimates of the parameters for the simulation program (in other words the most likely values of all possible uncertain parameters) and the best source of meteorological data for the reference period. It is usually given as absolute value [kWh] or specific value [kWh/kWp].

Predicted Yield

The predicted yield is derived from predicted reference yield by applying best estimates of expected changes of the yield within the assumed lifetime of the PV system (the prediction period). These changes could be changes in system behaviour (e.g. degradation) or climate changes (e.g. dimming and brightening).

Predicted Yield can be given for individual years (predicted yield in year x) and / or as mean annual yield over the prediction period (predicted mean annual lifetime yield). It can be given as absolute value [kWh], specific value [kWh/kWp] or as percentage of Predicted Reference Yield.

4.2.3 Uncertainty sources

According to Hansen et al. [31], an uncertainty analysis is “a systematic process to propagate uncertainty in a model or its inputs to uncertainty in the model’s output” that involves two primary steps: uncertainty quantification and uncertainty propagation. A full quantification of uncertainties includes both, the quantification of uncertainties for all parameters and all models of the modelling chain. These uncertainties are then propagated through the whole modelling chain.

However, as for the prediction of lifetime energy yields of PV systems this approach is difficult to apply (e.g. the number of models and parameters is high, each uncertainty vary with daily as well as seasonal cycles and actual site of the PV system..., see e.g. [31] for more details), it is not implemented in state of the art yield predictions. Instead for recent yield predictions the uncertainty

is quantified by assigning an uncertainty distribution to the output of each modelling step to derive Predicted Yield.

A first category of uncertainty is resulting from modelling the Predicted Reference Yield. In practice it is usually considered by assigning uncertainty distributions to the annual losses or gains for each modelling step calculated by the yield simulation program. For a number of modelling steps losses or gains are close to zero, while their uncertainty may be quite high. Furthermore it is physically not meaningful for some modelling steps to show positive results (e.g. it is only meaningful that soiling, shading... cause losses, not gains). In these situations it may be more appropriate to assign asymmetric uncertainty distributions to losses or gains that include only physically meaningful results.

To include uncertainties from the conversion of Predicted Reference Yield to Predicted Yield, uncertainty distributions for the estimated change rates have to be quantified as well. Note that the uncertainties of Predicted Yield for individual years will increase with time when an uncertainty for linear change rates is included in the uncertainty quantification: while the effect of e.g. an actual 0.5%/year deviation from the expected change rate for system behaviour will be small for the first year of operation, the system will generate 5% less energy in year 10. For consideration of uncertainty of change rate for system behaviour again an asymmetric uncertainty distribution may be more appropriate, as observations of degradation rates tend to be asymmetric and positive degradation rates are physically not meaningful.

As a third category of uncertainty inter-annual variation of the Predicted Yield has to be considered. The background for the consideration of inter-annual variation as an uncertainty is the fact, that Predicted Reference Yield and as a follow up Predicted Yield is calculated as an annual value (it is the yield in a “typical year”). However solar irradiation (as the main influencing factor for yield variations) and other meteorological quantities will vary from year to year and influence annual yields. As long as this variation is interpreted as a variation around a possible trend of meteorological quantities whose effects on yield are considered when calculating Predicted Yields, this variation may not influence cumulated Predicted Yields to a high extent but may have a high impact on annual Predicted Yields.

4.2.4 Uncertainty propagation

After quantifying all uncertainties they are propagated to derive the final uncertainty of Predicted Yields for all individual years in the Prediction Period. At least two possible approaches for the propagation of uncertainties can be defined: the law on propagation of uncertainties (see e.g. [49]) and the propagation of probability distributions using a Monte Carlo method (see e.g. [28][31][50]). While this is a simplification, usually independence of all losses and gains is assumed for both methods. Also, for the law on propagation of uncertainties, normality is assumed and therefore normal distributions are used.

If asymmetric uncertainty distributions are applied to some of the modelling steps, the law on propagation of uncertainties may not be applicable. There are other circumstances and conditions under which the results of a Monte Carlo approach may be preferable (see e.g. [31][50]).

Probability exceedance values are used to deliver information on the uncertainty distribution of the Predicted Yield. P_{xx} is the value that is exceeded with the probability $xx\%$. E.g. P50 for Predicted Yield in year 1 may be 1000 kWh/kWp, which means that 1000 kWh/kWp is the Predicted Yield that is exceeded with a probability of 50%. If the law of propagation of uncertainties is applied to propagate uncertainties, P_{xx} values can be calculated based on the quantile of a normal distribution. In the case a Monte Carlo approach is used they can be derived from the quantile of the empirical distribution of all Z realizations of Predicted Yield, where Z is the sample size of the Monte Carlo approach.

P_{xx} values can be given as absolute value [kWh], specific value [kWh/kWp] or as percentage of Predicted Reference Yield. They can be given for individual years (P_{xx} in Year n), for mean annual yield over the Prediction Period (P_{xx} of Predicted Mean Annual Lifetime Yield) and/or for cumulative yield over the Prediction Period (P_{xx} for Predicted Lifetime Yield).

4.2.5 Results

The implementation of a Monte-Carlo simulation technique into PV energy yield simulation software means that not only one single simulation is performed, but a large number of simulations with inputs being randomly chosen from pre-defined probability distributions.

The practical implementation into the software code introduces the drawing of Z realizations from a pre-defined probability distribution of GHI, which can be denoted u_{GHI} . The probability distribution of energetic gains related to irradiation transposition can be denoted u_{GPOA} , and similarly other probability distributions that are deemed necessary to be included.

Similarly, the uncertainty related to predicted PV energy yield is included by drawing Z realizations reflecting Z possible long-term rates of change in system behaviour (i.e., drawing Z realizations from predefined probability distribution of degradation rates).

Using appropriate equations for each gain or loss mechanism, the PV energy yield is calculated for each individual year of assumed PV system lifetime, with the effect of Z realizations that reflect long-term changes being considered separately for each subsequent year. Next – and independent from other uncertainty categories – different overall irradiation of each individual year can be included to reflect the effects of uncertainty related to inter-annual variation of irradiation. This leads to the incorporation of all described uncertainties for each individual uncertainty category for each individual year n throughout the assumed PV system lifetime simulated by this Monte-Carlo approach. Since this procedure can be implemented in simple loops regarding software coding, it is straightforward to numerically determine the cumulative yields of years 1 through n for all Z realizations.

Figure 33 depicts example results for this simulation procedure for an assumed PV system lifetime of 20 years. All values in Figure 33 were normalized to the best estimate of predicted reference yield. Our assumptions of probability distributions leading to the determination of uncertainties of individual models are summarized in Table 15.

Due to the incorporation of non-normal uncertainty distributions, one can denote a qualitative difference between yield predicted deterministically and the P50 yield (Figure 33a). The difference between these yields increases over time (Figure 33b), since the uncertainty associated with changing system output over time also exhibits a non-normal probability distribution. Figure 33b also shows the general increase of uncertainty in the prediction period.

Including uncertainties of inter-annual variation of meteorological conditions leads to a stark increase of uncertainties related to individual yields (Figure 33c). However, these uncertainties are substantially reduced for cumulative yields within only few years, as shown in Figure 33d.

In a final step, we compared observed annual yield values to the uncertainty range as expected from the Monte-Carlo simulations. We used the performance data of 26 individual PV systems as described in [21] for this comparison. The parameters given for a single system in Table 15 were adapted to the specific systems and sites, and subsequently a number of realizations were calculated for the set of 26 systems. Figure 34 presents both the Monte-Carlo results and the measured values in a similar presentation as in the lower section of Figure 33. The measured values fit quite well into the uncertainty range as expected from the Monte-Carlo simulations.

4.2.6 Conclusion

A method to calculate uncertainties and the Pxx values for year by year and life-time energy yield predictions of PV systems is presented. The method is based on a Monte-Carlo simulation which uses Gaussian or triangular distributions for individual modelling steps, including the solar resource data and long term changes of system behaviour. The parameters may be adjusted to individual sites and system layouts. A comparison of expected uncertainty and observed variability showed a good agreement.

The proposed approach is an effort to standardize the procedure of uncertainty calculation of predicted energy yields of PV systems in order to properly estimate financial investment risk. Similar efforts have been carried out by Belluardo et al. on a fleet of around 2000 PV plants [64].

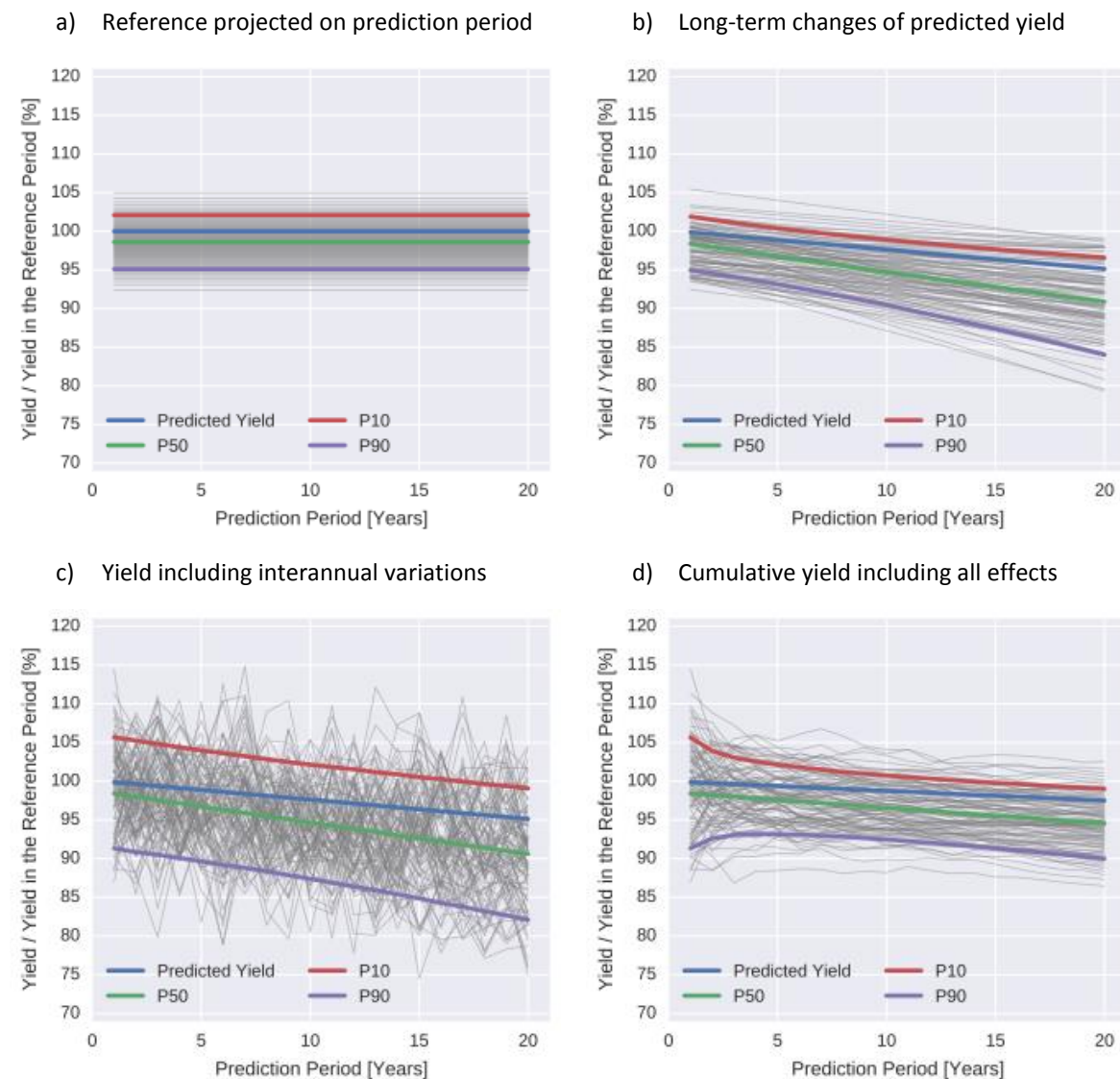
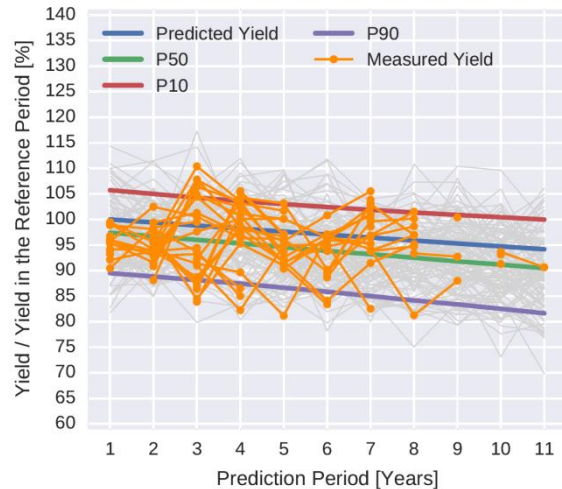


Figure 33: Ratio of simulated PV energy yield in the prediction period over PV energy yield in the reference period for various stages in a Monte-Carlo simulation, notably a) yield in the reference projected onto prediction period (GHI and irradiation transposition); b) long-term changes (degradation and irradiation trends); c) inter-annual variations of meteorological conditions and d) the cumulative predicted PV energy yield as an expanded annual average value.

Table 15: Uncertainties of individual modelling steps used in the exemplary yield simulation. A normal (Gaussian) distribution is characterized by mean value μ and standard deviation σ , while a triangular distribution is characterized by minimum a , maximum b , and modus c .

Calculation step	Symmetric (assuming normal distributions for all parameters)			Asymmetric (individually selecting normal and triangular distributions)		
	Parameter		Distribution	Parameter		
	μ	σ		μ	σ	a
<i>Solar resource potential in the reference period</i>						
GPOA	11.4	2.5	normal	11.4	2.5	
<i>Yield in the reference period</i>						
Horizon shading	0	0.5	triangular	-1.0	0	0
Row-shading	-1.0	2.0	triangular	-5.0	0	-1.0
Soiling	-0.5	0.5	triangular	-1.5	0	-0.5
Reflection	-3.1	0.5	triangular	-4.1	-2.6	-3.1
STC power	0	2.0	normal	0	2.0	
Spectrum	-1.0	0.5	normal	-1.0	0.5	
Irradiation level	-3.9	1.9	normal	-3.9	1.9	
Temperature	-2.4	1.0	normal	-2.4	1.0	
Mismatch	-0.8	0.5	triangular	-1.8	0	-0.8
DC cabling	-1.5	0.5	triangular	-2.5	-1.0	-1.5
Inverter	-2.7	1.5	triangular	-5.7	0	-2.7
Power limitation	0	0.5	triangular	-1.0	0	0
Transformer	-1.0	0.5	triangular	-2.0	-0.5	-1.0
<i>Yield in the prediction period</i>						
System behavior	-0.6	0.5	triangular	-1.6	0	-0.6
Solar irradiation	0	0.3	normal	0	0.3	
Annual variation	0	4.9	normal	0	4.9	

a) Predicted yield and observed values for 26 systems



b) Cumulative yield and observed values for 26 systems

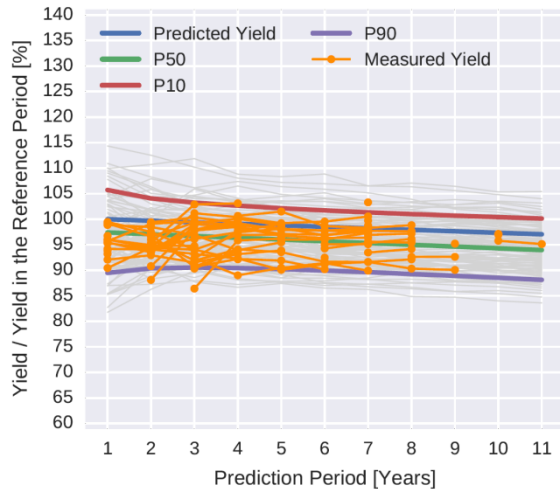


Figure 34: Predicted yield and observed annual yield values for 26 PV systems located in Germany and Spain [21]. The Monte-Carlo calculations for a single system as shown in Figure 33c and Figure 33d were adapted to the specific systems and sites. The measured values fit quite well into the uncertainty range as expected from the Monte-Carlo simulations.

References

- [1] Richter, Mauricio; Vedde, Jan; Frearson, Lyndon; Stridh, Bengt; Herteleer, Bert; Jahn, Ulrike et al.: Technical Assumptions Used in PV Financial Models - Review of Current Practices and Recommendations. IEA PVPS Task 13, Report IEA-PVPS T13-08:2017.
- [2] WMO Guide to Meteorological Instruments and Methods of Observation: WMO No. 8. 7th edition. Geneva, Switzerland, 2008.
- [3] McArthur L. J. B.: Baseline Surface Radiation Network (BSRN). Operations Manual. Version 2.1. WCRP-121, WMO/TD-No. 1274, 2005
- [4] Sengupta, M; et al: Best Practices Handbook for the Collection and Use of Solar Resource Data for Solar Energy Applications. NREL/TP-5D00-63112. Golden, CO: National Renewable Energy Laboratory, 2015.
- [5] Driesse, A.; Zaaiman, W.; Riley, D.; Taylor, N.; and Stein, J.S.: Indoor and Outdoor Evaluation of Global Irradiance Sensors. Proc. 31st European Photovoltaic Solar Energy Conference, 14-18 September 2015, Hamburg, Germany.
- [6] Reda, I.: Method to Calculate Uncertainties in Measuring Shortwave Solar Irradiance Using Thermopile and Semiconductor Solar Radiometers, National Renewable Energy Laboratory, Golden, CO, 2011.
- [7] Vuilleumier, L., M. Hauser, C. Félix, F. Vignola, P. Blanc, A. Kazantzidis, and B. Calpini (2014): Accuracy of ground surface broadband shortwave radiation monitoring, *J. Geophys. Res. Atmos.* 119 (2014), 13,838–13,860, doi:10.1002/2014JD022335.
- [8] Habte, A., Sengupta, M., Reda, I., Andreas, A., Konings, J.: Calibration and Measurement Uncertainty Estimation of Radiometric Data, NREL/CP-5D00-62214. National Renewable Energy Laboratory, Golden, CO, p. 9, Preprint 2014.
- [9] Riches, M.R.; Stoffel, T.L. and Wells, C.V. editors: Proceedings of the International Energy Agency Conference on Pyranometer Measurements 1982. SERI/TR-642-1156R, Golden, CO.
- [10] Wardle, D.I. et al: Improved Measurements of Solar Irradiance by Means of Detailed Pyranometer Characterization. Report IEA-SHCP-9C-2, IEA Solar Heating and Cooling Programme 1996.
- [11] Gostein, M.; L. Dunn: Light soaking effects on photovoltaic modules: Overview and literature review. In Proc. 37th IEEE Photovoltaic Specialists Conference 2011, S. 3126–3131.
- [12] Müllejans H, Zaaiman W, Galleano R.: Analysis and mitigation of measurement uncertainties in the traceability chain for the calibration of photovoltaic devices. *Measurement Science and Technology* Jul 2009; 20: 1–12.
- [13] Emery K.: Uncertainty analysis of certified photovoltaic measurements at the National Renewable Energy Laboratory. National Renewable Energy Laboratory (NREL), Golden, CO. NREL/TP-520-45299, Aug 2009.
- [14] Dirnberger D.: Uncertainty in PV module measurement—part I: calibration of crystalline and thin film modules. *IEEE Journal of Photovoltaics* 2013; 3: 1016–1026.

- [15] Dirnberger D, Kräling U, Müllejans H, Salis E, Emery K, Hishikawa Y, Kiefer K.: Progress in photovoltaic module calibration: results of a worldwide intercomparison between four reference laboratories. *Measurement Science and Technology* Sep 2014; 25: 105005.
- [16] Dirnberger, Daniela: Uncertainty in PV Module Measurement---Part II: Verification of Rated Power and Stability Problems. In: *IEEE J. Photovoltaics* 4 (3) 2014, S. 991–1007. DOI: 10.1109/JPHOTOV.2014.2307158.
- [17] PERFORMANCE – A science base on photovoltaics performance for increased market transparency and customer confidence: Report D1.4.2 “Principles of uncertainty analyses and evaluation of the traceability chain” by JRC, Ispra, 2007.
- [18] Makrides, G., Zinsser, B., Schubert, M., Georghiou, G.E.: Performance loss rate of twelve photovoltaic technologies under field conditions using statistical techniques. *Sol. Energy* 103 (2014), 28–42.
- [19] Jordan, D., Smith, R., Osterwald, C., Gelak, E., Kurtz, S.: Outdoor PV degradation comparison. In Proc. 35th IEEE Photovoltaic Specialists Conference, Honolulu, Hawaii 2010, pp. 2694–2697.
- [20] Belluardo, Giorgio; Philip Ingenhoven, Wolfram Sparber, Jochen Wagner, Philipp Weihs, David Moser: Novel method for the improvement in the evaluation of outdoor performance loss rate in different PV technologies and comparison with two other methods. *Solar Energy* 117 (2015) 139–152
- [21] Müller, Björn; Hardt, Laura; Armbruster, Alfons; Kiefer, Klaus; Reise, Christian: Yield predictions for photovoltaic power plants: empirical validation, recent advances and remaining uncertainties. In: *Prog. Photovolt: Res. Appl.* 24 (4), S. 570–583, 2015. DOI: 10.1002/pip.2616.
- [22] Wild, Martin: Global dimming and brightening: A review. In: *Journal of geophysical research* 114 (D10) 2009, S. D00D16. DOI: 10.1029/2008JD011470.
- [23] Wild, Martin: How well do IPCC-AR4/CMIP3 climate models simulate global dimming/brightening and twentieth-century daytime and nighttime warming? In: *J. Geophys. Res.* 114 (D10) 2009. DOI: 10.1029/2008JD011372.
- [24] Müller, B.; Wild, M.; Driesse, A.; Behrens, K.: Rethinking solar resource assessments in the context of global dimming and brightening. In: *Sol. Energy* 99 (2014), S. 272–282. DOI: 10.1016/j.solener.2013.11.013.
- [25] Del Fabbro, Borut; Valentinčič, Aljoša; Gubina, Andrej F.: An adequate required rate of return for grid-connected PV systems. In: *Solar Energy* 132 (2016), S. 73–83. DOI: 10.1016/j.solener.2016.03.006.
- [26] Leicester, Philip A.; Goodier, Chris I.; Rowley, Paul: Probabilistic evaluation of solar photovoltaic systems using Bayesian networks: a discounted cash flow assessment. In: *Progress in Photovoltaics: Research and Applications*, 2016, DOI: 10.1002/pip.2754.
- [27] Stoffel, Tom: Terms and Definitions. In: Jan Kleissl (Hg.): *Solar Energy Forecasting and Resource Assessment*. Boston: Academic Press, pp 1–19, 2013.
- [28] Thevenard, Didier; Pelland, Sophie: Estimating the uncertainty in long-term photovoltaic yield predictions. In: *Sol Energy* 91 (2013), S. 432–445. DOI: 10.1016/j.solener.2011.05.006.

- [29] Vignola, F.; Grover, C.; Lemon, N.; McMahan, A.: Building a bankable solar radiation dataset. In: Sol. Energy 86 (8) 2012, pp 2218–2229. DOI: 10.1016/j.solener.2012.05.013.
- [30] Gueymard, C. A.; Wilcox, S. M.: Assessment of spatial and temporal variability in the US solar resource from radiometric measurements and predictions from models using ground-based or satellite data. In: Sol. Energy 85 (5) 2011, S. 1068–1084. DOI: 10.1016/j.solener.2011.02.030.
- [31] Hansen, Clifford W.; Martin, Curtis E.: Photovoltaic System Modeling: Uncertainty and Sensitivity Analyses. Sandia National Laboratories, Report SAND2015-6700, 2015.
- [32] Strobel, M. B.; Betts, T. R.; Friesen, Gabi; Beyer, Hans Georg; Gottschalg, R.: Uncertainty in Photovoltaic performance parameters – dependence on location and material. In: Solar Energy Materials and Solar Cells 93 (6-7) 2009, pp 1124–1128. DOI: 10.1016/j.solmat.2009.02.003.
- [33] Dirnberger, Daniela: Uncertainties in Energy Rating for Thin-film PV Modules. Dissertation. Carl von Ossietzky Universität, Oldenburg, 2015.
- [34] Ineichen, Pierre: Five satellite products deriving beam and global irradiance validation on data from 23 ground stations. University of Geneva, 2011. <http://archiveouverte.unige.ch/unige:23669>.
- [35] Ineichen, Pierre: Long Term Satellite Global, Beam and Diffuse Irradiance Validation. In: Proceedings of the 2nd International Conference on Solar Heating and Cooling for Buildings and Industry, Freiburg, 2013. (Energy Procedia, 48), S. 1586–1596.
- [36] Tjengdrawira, Caroline; Richter, Mauricio: Review and Gap Analysis of Technical Assumptions in PV Electricity Costs. Public Report of the Solar Bankability Project, WP3 D3.1, 2016.
- [37] Wild, Martin; Folini, Doris; Henschel, Florian; Fischer, Natalie; Müller, Björn: Projections of long-term changes in solar radiation based on CMIP5 climate models and their influence on energy yields of photovoltaic systems. In: Solar Energy 116 (2015), S. 12–24. DOI: 10.1016/j.solener.2015.03.039.
- [38] Erbs, D.G., S. A. Klein, and J. A. Duffie, “Estimation of the diffuse radiation fraction for hourly, daily and monthly-average global radiation,” Sol. Energy, vol. 28, no. 4, pp. 293–302, 1982.
- [39] Ruiz-Arias, J. A., H. Alsamamra, J. Tovar-Pescador, and D. Pozo-Vázquez, “Proposal of a Regressive Model for the Hourly Diffuse Solar Radiation Under All Sky Conditions,” Energy Convers. Manag., vol. 51, no. 5, pp. 881–893, 2010.
- [40] Skartveit, A., J. A. Olseth, and M. E. Tuft, “An Hourly Diffuse Fraction Model with Correction for Variability and Surface Albedo,” Sol. Energy, vol. 63, no. 3, pp. 173–183, 1998.
- [41] Liu, B. Y. H., and R. C. Jordan, “The Interrelationship and Characteristic Distribution of Direct, Diffuse and Total Solar Radiation,” Sol. Energy, vol. 4, no. 3, pp. 1–19, Jul. 1960.
- [42] Hay, J. E., and J. A. Davies, “Calculation of the Solar Radiation Incident on an Inclined Surface,” in Proceedings First Canadian Solar Radiation Workshop, 1980, pp. 59–72.
- [43] Muneer, T., Hourly Slope Irradiation and Illuminance, in Solar Radiation and Daylight Models (Second Edition), Oxford: Butterworth-Heinemann, 2004, pp. 143–220.

- [44] Perez, R., P. Ineichen, R. Seals, J. Michalsky, and R. Stewart, "Modeling Daylight Availability and Irradiance Components from Direct and Global Irradiance," *Sol. Energy*, vol. 44, no. 5, pp. 271–289, 1990.
- [45] Soto, W. D., S. A. Klein, and W. A. Beckman, "Improvement and validation of a model for photovoltaic array performance," *Sol. Energy*, vol. 80, no. 1, pp. 78–88, 2006.
- [46] Sjerps-Koomen, E. A., E. A. Alsema, and W. C. Turkenburg, "A Simple Model for PV Module Reflection Losses Under Field Conditions," *Sol. Energy*, vol. 57, no. 6, pp. 421–432, 1996.
- [47] Cameron, Christopher P., William E. Boyson, and Daniel M. Riley, "Comparison of PV system performance-model predictions with measured PV system performance," in Photovoltaic Specialists Conference, 2008. PVSC'08. 33rd IEEE, 2008, pp. 1–6.
- [48] Ineichen, Pierre.: Global irradiance on tilted and oriented planes: model validations, 2011.
- [49] Joint Committee for Guides in Metrology: Evaluation of measurement data - Guide to the expression of uncertainty in measurement. JCGM 100:2008: Bureau International des Poids et Mesures (BIPM).
http://www.bipm.org/utils/common/documents/jcgm/JCGM_100_2008_E.pdf.
- [50] Joint Committee for Guides in Metrology: Evaluation of measurement data - Supplement 1 to the "Guide to the expression of uncertainty in measurement" - Propagation of distributions using a Monte Carlo method. JCGM 101:2008: Bureau International des Poids et Mesures (BIPM).
http://www.bipm.org/utils/common/documents/jcgm/JCGM_101_2008_E.pdf.
- [51] Williams SR, Betts TR, Gottschalg R, Neumann D, Prast MO, Nositschka A.: Evaluating the outdoor performance of PV modules with different glass textures. In Proc. 26th European Photovoltaic Solar Energy Conference and Exhibition, Hamburg, Germany, 2011, 3152–3156.
- [52] Herrmann W, Rimmelspacher L, Reuter M.: Optical characteristics of PV module front glasses—incidence angle effects of various glass types and impact on annual energy yield. In 28th European Photovoltaic Solar Energy Conference and Exhibition, Paris, France, 2013, 2882–2886.
- [53] Martin N, Ruiz JM.: Calculation of the PV modules angular losses under field conditions by means of an analytical model. *Solar Energy Mat Solar C* 2001; 70: 25–38.
- [54] Alonso-Abella, M, Chenlo, F, Nofuentes, G, Torres-Ramírez, M.: Analysis of spectral effects on the energy yield of different PV (photovoltaic) technologies: The case of four specific sites. *Energy* 67 (2014) 435–443
- [55] Belluardo et al.: Uncertainty analysis of a radiative transfer model using Monte Carlo method: impact on PV device. In Proc. PV-Symposium Bad Staffelstein 2016
- [56] Heydenreich W, Müller B, Reise Ch.: Describing the world with three parameters: a new approach to PV module power modelling. In Proc. 23rd European Photovoltaic Solar Energy Conference and Exhibition, Valencia, Spain, 2008, 2786–2789.
- [57] Dirnberger D, Müller B, Kräling U, Dittmann S.: Uncertainties of laboratory measurements for energy rating. In 27th European Photovoltaic Solar Energy Conference and Exhibition, Frankfurt, Germany, 2012, 3294–3301.
- [58] Dirnberger D, Müller B, Reise Ch.: PV module energy rating: opportunities and limitations. *Prog. Photovolt: Res. Appl.* 2015; 23(12): 1754–70, DOI: 10.1002/pip.2618.

- [59] Kroposki, B, D. Myers, K. Emery, L. Mrig, C. Whitaker, and J. Newmiller (1996): Photovoltaic module energy rating methodology development, Proc. 25th IEEE Photovoltaic Specialists Conference, Anaheim, 1996, pp. 1311-1314.
- [60] Kenny, R.P., G. Friesen, D. Chianese, A. Bernasconi, and E. D. Dunlop: Energy rating of PV modules: Comparison of methods and approach," in Proceedings of 3rd World Conference on Photovoltaic Energy Conversion, Vols a-C, Osaka, Japan, 2003, pp. 2015-2018.
- [61] Huld T, Dunlop E, Beyer HG, Gottschalg R.: Data sets for energy rating of photovoltaic modules. *Solar Energy* 2013; 93(0): 267–79, DOI: 10.1016/j.solener.2013.04.014.
- [62] Perez, R., R. Seals, J. Michalsky, and P. Ineichen, "Geostatistical properties and modeling of random cloud patterns for real skies," *Sol Energy*, vol. 51, pp. 7-18, Jul 1993.
- [63] Moser D, Del Buono M, Jahn U, Herz M, Richter M, Brabandere K de. Identification of technical risks in the photovoltaic value chain and quantification of the economic impact. *Prog. Photovolt: Res. Appl.* 2017;25 (7), 592-604, DOI: 10.1002/pip.2857.
- [64] Belluardo G, Pierro M, Ingenhoven P, Cornaro C, Moser D, Statistical Analysis of the Performance Loss Rate of PV Plants Distributed in a Region: A Real-Case Study in South Tyrol. *Proc. 33rd European Photovoltaic Solar Energy Conference and Exhibition*, 1904 – 1908, 2017

For further information about the IEA Photovoltaic Power Systems Programme and Task 13 publications, please visit www.iea-pvps.org.



ISBN 978-3-906042-51-0

A standard linear barcode representing the ISBN number 978-3-906042-51-0.

9 783906 042510 >